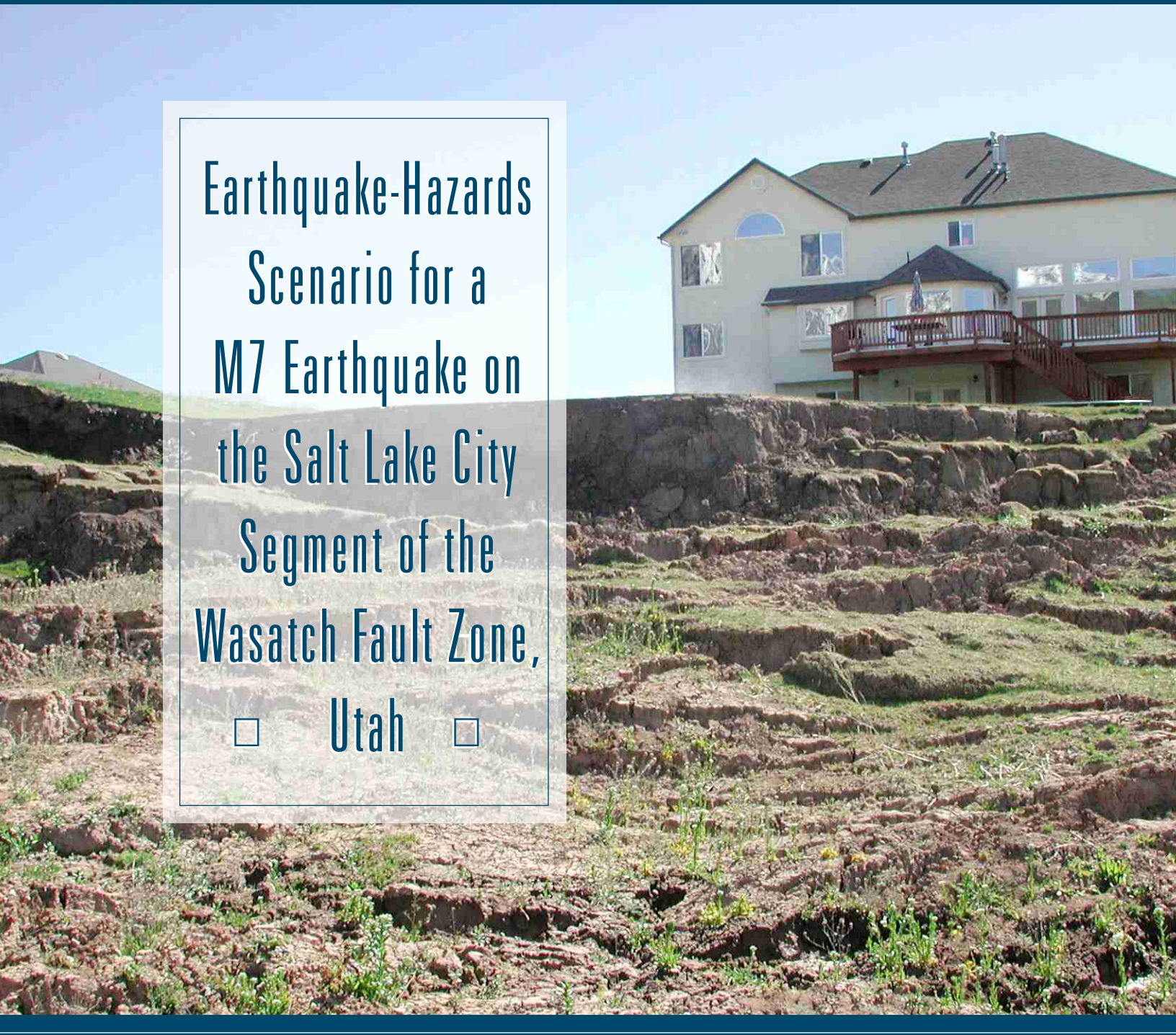

Earthquake-Hazards Scenario for a M7 Earthquake on the Salt Lake City Segment of the Wasatch Fault Zone, Utah

by Barry J. Solomon, Neil Storey, Ivan Wong, Walter Silva, Nick Gregor, Douglas Wright, and Greg McDonald

Utah Geological Survey 2004

Special Study 111DM

STATE OF UTAH

Olene S. Walker, Governor

DEPARTMENT OF NATURAL RESOURCES

Robert L. Morgan, Executive Director

UTAH GEOLOGICAL SURVEY

Richard G. Allis, Director

PUBLICATIONS

contact
Natural Resources Map/Bookstore
1594 W. North Temple
telephone: 801-537-3320
toll-free: 1-888-UTAH MAP
website: http://mapstore.utah.gov
email: geostore@utah.gov

THE UTAH GEOLOGICAL SURVEY

contact
1594 W. North Temple, Suite 3110
Salt Lake City, UT 84116
telephone: 801-537-3300
website: http://geology.utah.gov

1/04

EARTHQUAKE-HAZARDS SCENARIO FOR A M 7 EARTHQUAKE ON THE SALT LAKE CITY SEGMENT OF THE WASATCH FAULT ZONE, UTAH

by

Barry J. Solomon[1], Neil Storey[2], Ivan Wong[3], Walter Silva[4], Nick Gregor[4], Douglas Wright[3], and Greg McDonald[1]

[1] Utah Geological Survey (UGS), 1594 West North Temple, Salt Lake City, Utah 84114-6100
Phone: (801) 537-3388, Fax: (801) 537-3400, e-mail: barrysolomon@utah.gov

[2] formerly with UGS, now with CH2M Hill, 215 South State Street, Salt Lake City, Utah 84111
Phone: (801) 350-5258, Fax: (801) 355-2301, e-mail: nstorey@ch2m.com

[3] Seismic Hazards Group, URS Corp., 500 12th Street, Suite 200, Oakland, California 94607
Phone: (510) 874-3014, Fax: (510) 874-3628, e-mail: Ivan_Wong@urscorp.com

[4] Pacific Engineering & Analysis, 311 Pomona Avenue, El Cerrito, California 94530
Phone: (510) 528-2821, Fax: (510) 528-2135, e-mail: pacificengineering@juno.com

ISBN 1-55791-704-3

Special Study 111 2004
Utah Geological Survey
A division of
Utah Department of Natural Resources

Research supported by the U.S. Geological Survey (USGS), Department of the Interior, under USGS award number 99HQGR0091. The views and conclusions contained in this document are those of the authors and should not be interpreted as necessarily representing the official policies, either expressed or implied, of the U.S. Government.

CONTENTS

FIGURES

TABLES

PLATES

EARTHQUAKE-HAZARDS SCENARIO FOR A M7 EARTHQUAKE ON THE SALT LAKE CITY SEGMENT OF THE WASATCH FAULT ZONE, UTAH

by

Barry J. Solomon[1], Neil Storey[2], Ivan Wong[3], Walter Silva[4], Nick Gregor[4], Douglas Wright[3], and Greg McDonald[1]

ABSTRACT

We mapped geologic hazards posed by a moment magnitude 7 earthquake on the Salt Lake City segment of the Wasatch fault zone, a major active zone of normal faulting. This event is characteristic of surface-faulting earthquakes in the central Wasatch Front region of northern Utah, which has a population of about 1.7 million centered upon the Salt Lake City metropolitan area. We modeled the scenario earthquake with a rupture plane 29 miles (46 km) long, 12 miles (19 km) wide, and dipping 55 degrees to the west.

Peak ground accelerations (PGAs) from our scenario earthquake exceed 1.0 *g*, with the highest PGA in stiff gravels and sands on the east side of Salt Lake Valley. Potentially damaging ground motions of 0.1 *g* and greater extend along the Wasatch Front from Provo to Ogden at distances of about 30 to 40 miles (50-60 km) from Salt Lake City. The pattern of ground shaking for short-period (0.2 second) spectral accelerations resembles that for PGA, but long-period (1.0 second) spectral accelerations are greatest in the deeper central portions of the basin.

Our scenario earthquake results in surface faulting with a maximum displacement of 6.1 feet (1.9 m) and is accompanied by liquefaction, landsliding, and tectonic subsidence. These hazards place densely populated and developed areas at risk. Liquefaction is most likely to occur in saturated fine sandy soils in central and eastern Salt Lake Valley, where lateral spread displacements may exceed 1 foot (30 cm) and settlement displacements may exceed 8 inches (20 cm). Although some earthquake-induced landsliding occurs on mountain slopes near the Salt Lake City segment, where Newmark displacements may exceed 4 inches (10 cm) on range-front spurs, deposits susceptible to slope failure are more common in areas of more moderate ground shaking to the north and south. Tectonic subsidence could displace the shoreline of Great Salt Lake, when near its historical maximum elevation, as much as 3 miles (4.8 km) into areas around Salt Lake City, although shoreline displacement at the long-term average lake elevation will be significantly less. Ponding of shallow ground water may occur locally in the subsidence trough on the east side of the valley in a zone about 4 miles (6.4 km) wide. Seiche hazards due to ground shaking appear to be negligible in Great Salt Lake, and current programs to modify large, high-hazard dams are designed to provide satisfactory performance with no uncontrolled releases during an earthquake similar to our scenario.

[1] Utah Geological Survey (UGS), 1594 West North Temple, Salt Lake City, Utah 84114-6100
[2] CH2M Hill, 215 South State Street, Salt Lake City, Utah 84111
[3] Seismic Hazards Group, URS Corporation, 500 12th Street, Suite 200, Oakland, California 94607
[4] Pacific Engineering & Analysis, 311 Pomona Avenue, El Cerrito, California 94530

Emergency-response planners will use our 1:250,000-scale hazard maps with software such as HAZUS to estimate the consequences of the scenario earthquake. This estimate may describe the extent of damage and disruption, approximate number of casualties, repair and replacement costs, losses of function for critical facilities, and extent of induced hazards, providing an important tool for emergency-response planning and preparedness.

INTRODUCTION

Large earthquakes can disrupt lives with devastating effects on communities and individuals. An important step in characterizing the risk posed by a large earthquake is to map accompanying geologic hazards. Hazard maps can provide the geologic basis for a comprehensive loss estimate using computer software such as HAZUS (which stands for Hazards U.S.), developed for the Federal Emergency Management Agency (FEMA) by the National Institute of Building Sciences (1999). The estimate, including losses from geologic effects, may describe the scale and extent of damage and disruption, with quantitative estimates of the casualties and costs for repair and replacement of damaged buildings and facilities, losses of function for critical facilities, and the extent of induced hazards such as fire, flood, or contamination by hazardous materials. The estimate and hazard maps can then be used to increase awareness and improve emergency-response planning and preparedness.

The purpose of this report is to discuss and map (at a scale of 1:250,000) geologic hazards that may result from a scenario earthquake of moment magnitude (**M**) 7 on the Salt Lake City segment of the Wasatch fault zone. Our mapping procedures, using Geographic Information System (GIS) software, modify default methods included with HAZUS. Our modifications include recently published relationships based on the effects of historical earthquakes worldwide and techniques allowing the use of existing surficial geologic data in a regional study. Our analysis begins with calculating ground motions associated with the scenario earthquake, a key factor for mapping geologic hazards induced by strong ground shaking. The resultant earthquake-hazard maps can be used to estimate the consequences of our scenario earthquake to the central Wasatch Front.

The Study Area and its Geologic Setting

We mapped geologic effects of a scenario earthquake in the populous region of the central Wasatch Front, Utah, centered upon the Salt Lake City metropolitan area (figure 1). The study area, with a population of 1.7 million (2000 census), also includes the Ogden and Provo metropolitan areas and numerous smaller communities. The area extends 100 miles (160 km) from north to south and 75 miles (120 km) from east to west, encompassing 7,500 square miles (19,400 km^2).

The Wasatch fault zone, a major active zone of normal faulting, divides the study area. To the west of the Wasatch fault zone is the Basin and Range physiographic province, a region of mountain ranges bounded by normal faults and surrounded by sediment-filled valleys. To the east of the Wasatch fault zone is the Middle Rocky Mountains physiographic province, including the Wasatch Range and its rugged hinterlands (Stokes, 1977).

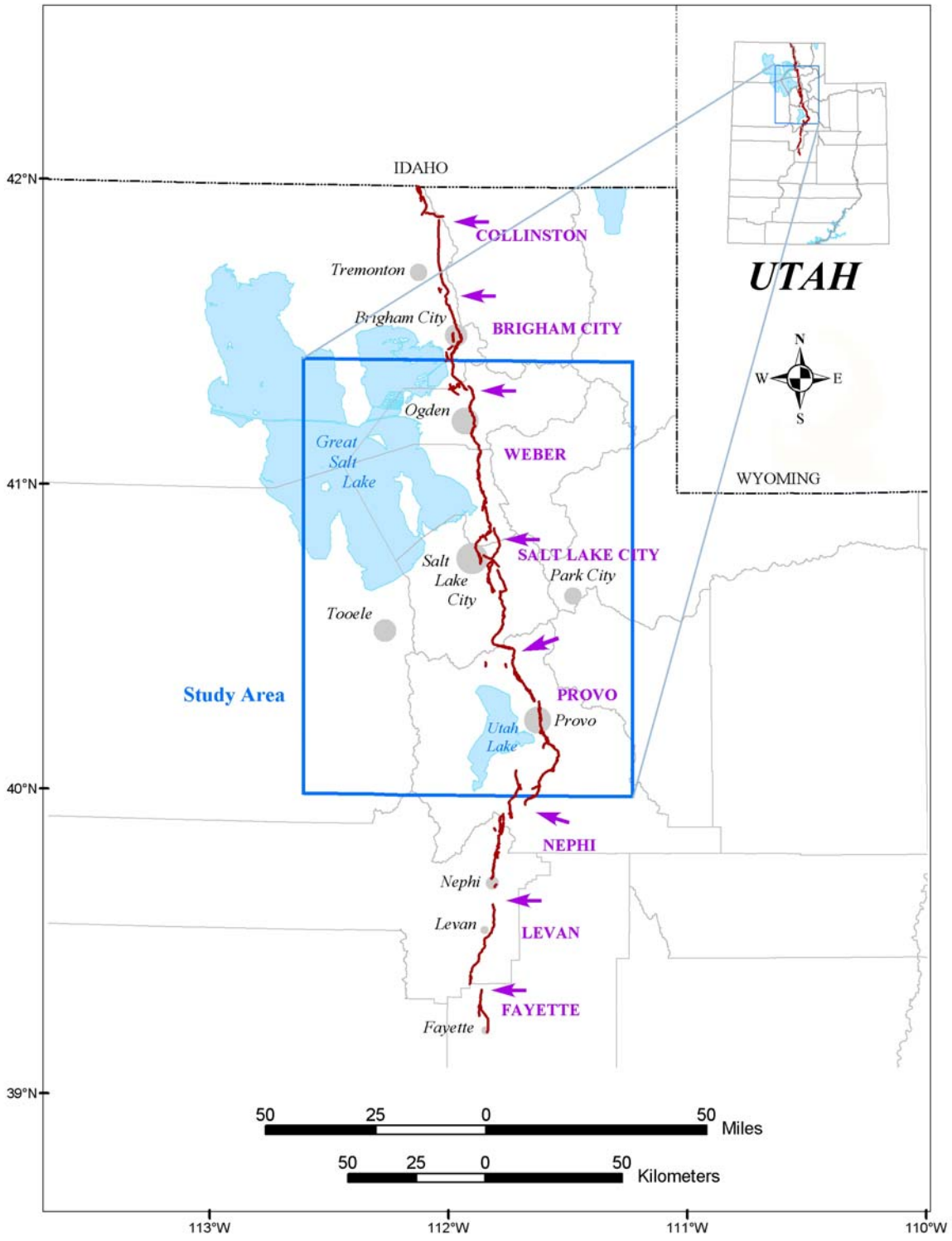

Figure 1. *Location of the study area and segments of the Wasatch fault zone, with arrows showing segment boundaries.*

Mountains in our study area within the Basin and Range Province include rocks of Precambrian through Cenozoic age, but are dominated by the Pennsylvanian-Permian Oquirrh Group. Tertiary and Quaternary sedimentary deposits fill the intervening valleys. Quaternary deposits extend to depths greater than 2,300 feet (700 m) in wedges along the Wasatch Range front (Arnow and others, 1970), but are commonly less than 800 feet (240 m) thick elsewhere and only about 200 feet (60 m) thick in Rush Valley in the southwest corner of the study area (figure 2). Surficial deposits in these valleys are mostly from latest Pleistocene Lake Bonneville, which occupied the area from about 32,000 to 10,000 years ago (Currey and Oviatt, 1985), and are underlain by Pleistocene alluvial and lacustrine sediments. Great Salt Lake and Utah Lake are two remnants of Lake Bonneville. Great Salt Lake, a saline lake with no outlet, occupies the northwest corner of the study area near Salt Lake City and Ogden. Utah Lake, a freshwater lake that drains into Great Salt Lake through the Jordan River in Salt Lake Valley, lies adjacent to Provo in the south-central part of the study area.

Predominant rocks in our study area within the Middle Rocky Mountains province include metamorphic rocks of the Precambrian Farmington Canyon Complex in the northern Wasatch Range; Precambrian quartzite, Mesozoic sedimentary, and Tertiary intrusive rocks in the central Wasatch Range; sandstone and limestone of the Oquirrh Group in the southern Wasatch Range; and Tertiary sedimentary and volcanic rocks surrounding most back valleys east of the Wasatch Range (Hintze and others, 2000). Unconsolidated sediment in the back valleys is less than 200 feet (60 m) thick.

Characteristics of the Scenario Earthquake

The Wasatch Front is located in the southern part of the Intermountain Seismic Belt, one of the most seismically active regions in the interior of the western U.S. (Smith and Arabasz, 1991). The region includes many faults that have been repeatedly active in the late Quaternary (past 130,000 years). The most significant of these faults is the 230-mile-long (370 km) range-bounding Wasatch fault zone, one of the longest and most active normal-slip faults in the world (figure 1). The Wasatch fault zone strikes north-south through north-central Utah and is divided into 10 segments, each capable of generating strong earthquakes (Machette and others, 1992). The five central segments (Brigham City, Weber, Salt Lake City, Provo, and Nephi segments) are the most active, exhibiting geologic evidence for repeated Holocene surface-faulting events. These five segments have estimated slip rates of 0.03 to 0.07 inches/year (0.8-1.9 mm/yr) (Black and others, 2003) and recurrence intervals typically between 1,000 and 3,000 years (McCalpin and Nishenko, 1996). Expected maximum earthquake magnitudes for these segments range from **M** 7 to 7¼ (Machette and others, 1992).

Recent observations from paleoseismic trenches indicate that the Salt Lake City segment, which extends along the eastern border of Salt Lake Valley, generated four surface-faulting earthquakes in the past 6,000 years. These earthquakes recur on average about every 1,350 ± 200 years, with the most recent surface-faulting earthquake occurring about 1,300 years ago (Black and others, 1996). The four earthquakes were preceded by surface-faulting earthquakes with longer recurrence intervals between about 6,000 and 9,000 years ago and by an extended period of fault quiescence from about 9,000 to 15,500 years ago (McCalpin, 2002). This irregular pattern of seismicity may be typical of the long-term behavior of the Wasatch fault zone

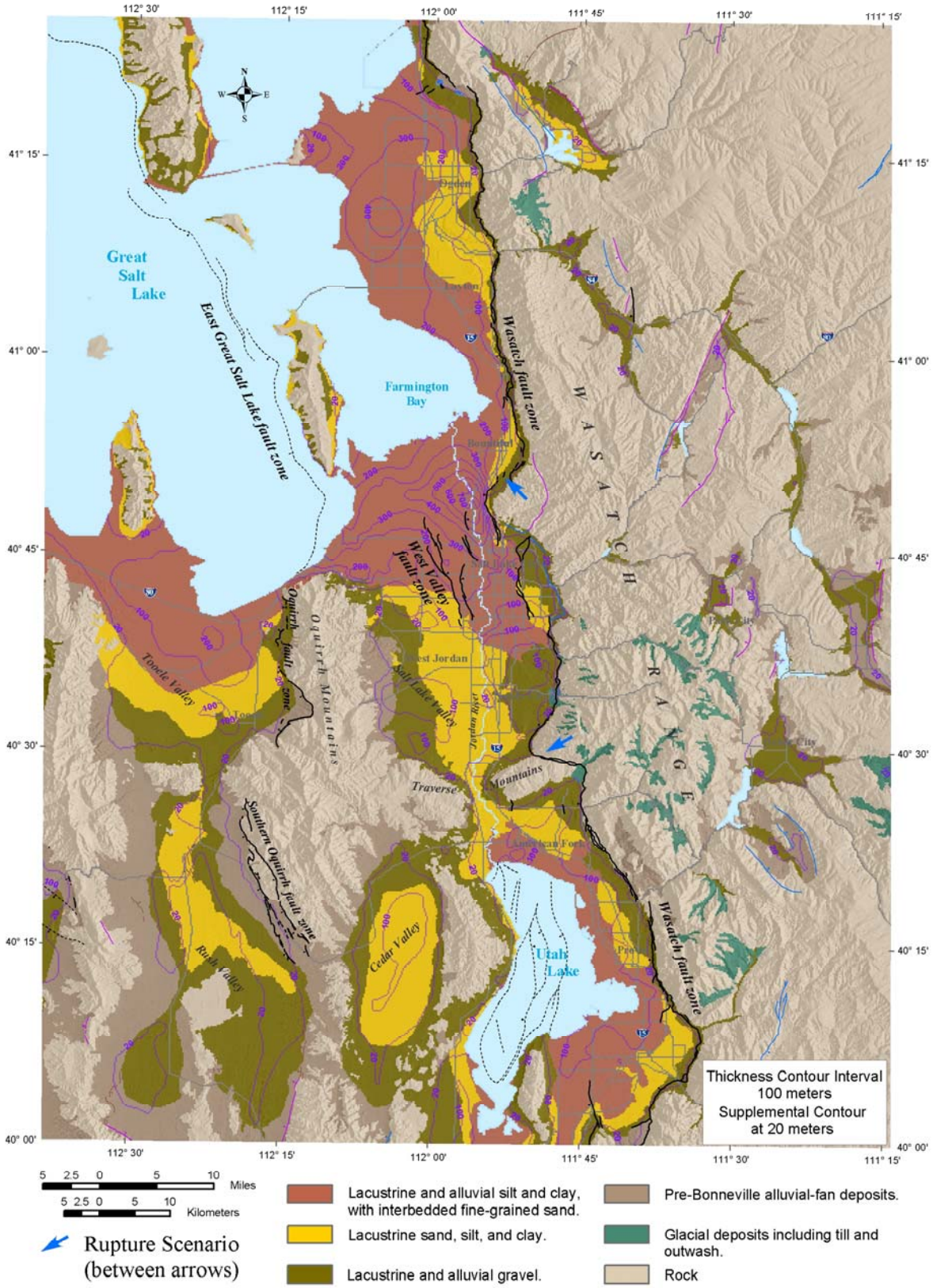

Figure 2. *Site-response units and contours showing thickness of unconsolidated deposits (from Ashland, 2001). See figure 3 for explanation of fault symbols, modified from Black and others (2003).*

or may be the consequence of unloading of the hanging wall after the regression of Lake Bonneville, returning local extension rates to the long-term regional rate (McCalpin, 2002).

Because a large earthquake on the Salt Lake City segment will affect the greatest number of people and probably generate the greatest losses along the central Wasatch Front, we selected an event on this segment as the scenario earthquake. The segment, as defined by Machette and others (1992), extends from the Salt Lake salient at the north end of the Warm Springs fault to the Traverse Mountains salient at the south end of the Cottonwood section of the fault (figure 3). We modeled the scenario earthquake as a **M** 7 event with a rupture plane 29 miles (46 km) long, 12 miles (19 km) wide, and dipping 55 degrees to the west, and assume that the fault spans the full thickness of the seismogenic (brittle) crust to a depth of 9 to 10 miles (15-16 km). The Salt Lake City segment exhibits a pronounced curvilinear nature at the surface and this geometry was incorporated into the ground motion calculations.

Geographic Information Systems Approach

We produced our maps using the vector- and raster-based ArcInfo®, ArcGIS®, and ArcView® software from Environmental Systems Research Institute, Inc. Data were analyzed through a series of query, overlay, and coincident raster calculation techniques. Ground-motion values were calculated using a 1.2-mile (2 km) grid spacing, resampled using a 650-foot (200 m) grid spacing, and then spatially smoothed using a circular window of 1,600-foot (500 m) radius to eliminate smaller features. The ground-motion grid was then resampled using a 100-foot (30 m) grid spacing and combined with additional raster grids to map liquefaction and landsliding hazards. Slope maps derived from U.S. Geological Survey (USGS) Digital Elevation Models (DEMs) required resampling at a different scale. Although 100-foot (30 m) DEMs were available in most of our study area, and 30-foot (10 m) DEMs were available for areas of high relief in the Wasatch Range, we resampled all DEMs at 300 feet (90 m) because of the poor quality of several level 1 100-foot (30 m) DEMs in areas of low relief on valley floors.

Limitations of Earthquake-Hazard Scenario Maps

Our scenario earthquake happens on average every thousand years or so, and our hazard maps pertain only to the effects of this scenario earthquake. Other active faults in the region, and other segments of the Wasatch fault zone, may also subject the study area to earthquakes. The effects of actual earthquakes will undoubtedly differ from this scenario. Some effects may be worse than the scenario suggests and some may not be as severe. The general kinds of effects described herein will likely occur in the scenario earthquake, and areas of high risk from the scenario earthquake will commonly correlate with areas of high risk from other earthquakes. However, hazards from other earthquakes occur throughout the study area, including in areas with low hazard potential for the scenario earthquake. For example, earthquake hazards from our scenario are typically lower near Ogden than Salt Lake City because of the distance from the earthquake source, but earthquake hazards near Ogden will likely be greater than those near Salt Lake City from an earthquake on the Weber segment of the Wasatch fault zone near Ogden. Thus, a low-hazard rating should not be interpreted as indicating the absence of earthquake hazards, but only a lower likelihood of hazards for this particular scenario.

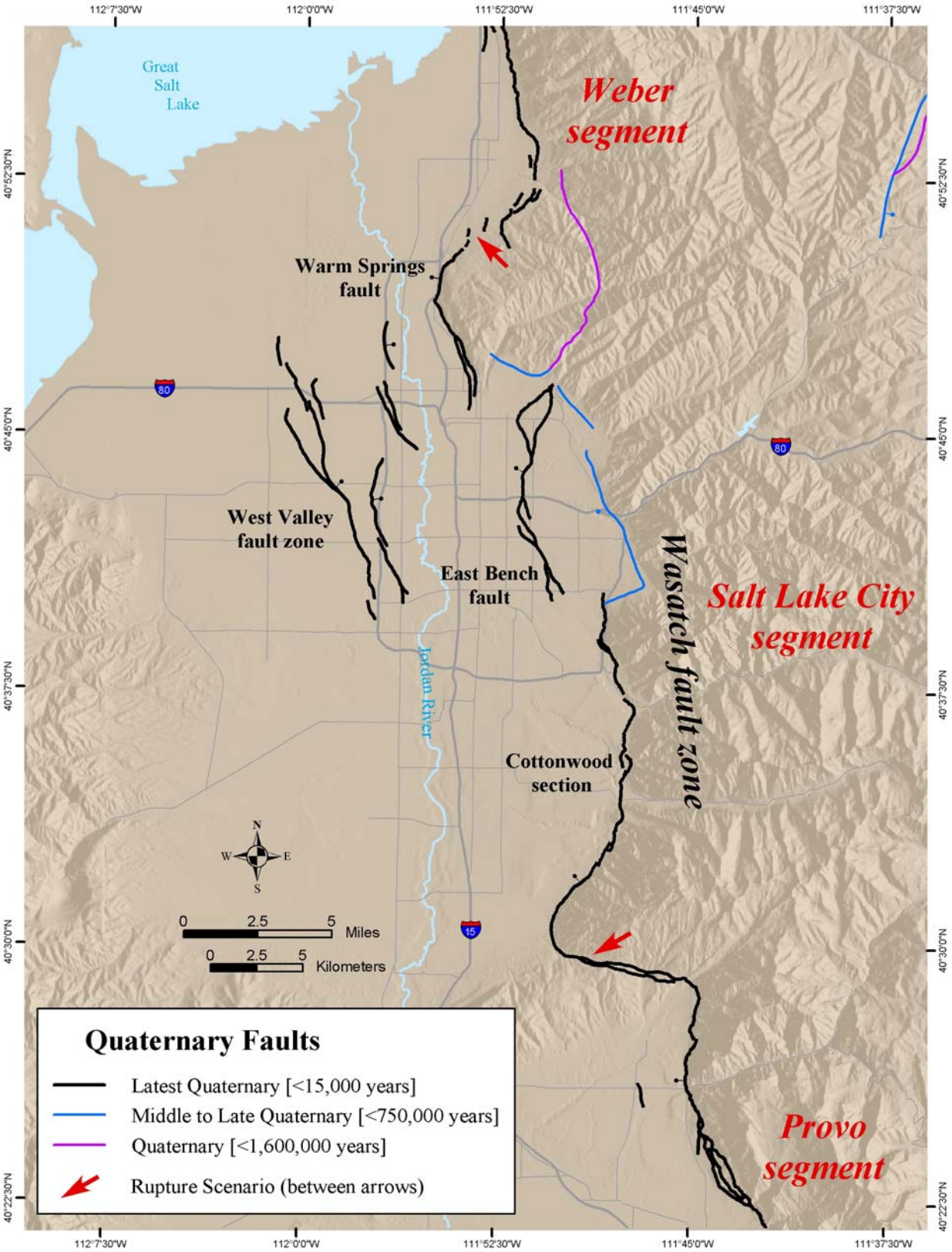

Figure 3. *Segments of the Wasatch fault zone along the central Wasatch Front, and sections of the Salt Lake City segment. Fault data modified from Black and others (2003).*

The predicted hazards are based on specific analytical techniques. Different techniques may yield different patterns of relative hazards. The hazard maps also depend on the quality of geologic information, which varies throughout the study area. We used only generalized geologic information in our hazard analysis, and more detailed information is needed for site-specific hazard studies. Because hazard boundaries are based on limited geologic data, the boundaries are approximate and subject to change with additional data. The hazards at any particular site may be different than shown because of geological variations within a hazard category, gradational and approximate map-unit boundaries, and the regional scale of the maps. The hazard maps are not intended for use at scales other than the published scale. The maps are designed for use in general planning, estimating losses, and raising awareness in the study area. They are not intended for use by local governments to define special-study areas, and do not preclude the need for site-specific studies to address hazards.

EARTHQUAKE HAZARDS

The earthquake hazards we map in this study include earthquake ground shaking, surface fault rupture, liquefaction, earthquake-induced landsliding, and tectonic subsidence. We map earthquake ground shaking using numerical modeling and empirical attenuation relationships for soft-rock site conditions and adjust these values for varying soil conditions over the map area using site-response analysis. We map surface fault rupture, liquefaction, and earthquake-induced landsliding hazards using published data, our predicted earthquake ground motions, and empirical relationships between characteristics of geologic materials and their observed association with historical earthquakes. Our report includes a map of the potential consequences of tectonic subsidence modified from the published maps of Keaton (1986) and Chang and Smith (1998a).

We also considered earthquake-induced flooding due to dam failure, seiches, and landslide-induced water waves. Current programs to modify existing large, high-hazard dams are designed to provide satisfactory performance with no uncontrolled releases during our scenario earthquake (Dan Grundvig, U.S. Bureau of Reclamation, written communication, 2001; Rick Hall, Utah Division of Water Rights, Office of Dam Safety, verbal communication, 2001), and we believe the potential for inundation by seiches in Great Salt Lake and Utah Lake is negligible. Although the potential for inundation by seiches in smaller intermontane lakes and reservoirs may be significant, seiche-inundation studies for most of these water bodies do not exist and are beyond the scope of this study. For landslide-induced seiches, the volume of water displaced by a landslide largely governs the height of waves and extent of inundation. For our scenario, landslide-source areas mapped near lake shores indicate a potential for nearby inundation from landslide-induced water waves, but we do not map the extent of inundation because the volume of displaced water is difficult to predict.

Ground Shaking

Our study of ground shaking expands upon another study supported by the USGS National Earthquake Hazards Reduction Program (NEHRP), which developed scenario and probabilistic ground-shaking hazard maps for the Salt Lake City metropolitan area (Wong and others, 2002).

Because the majority of cities and towns in this current study are located within sediment-filled valleys adjacent to the Wasatch fault and Wasatch Range, site-response effects on future ground shaking will be significant within the study area. Near-surface site amplification (Wong and Silva, 1993) and possibly basin amplification (Olsen and others, 1995, 1996) could increase ground-motion levels by a factor of two or more relative to rock depending on frequency. Empirical observations (for example, Abrahamson and Silva, 1997) and numerical modeling results (Wong and Silva, 1993) also suggest that near-source effects such as hanging-wall effects and possibly rupture directivity may also be significant along the Wasatch Front. Therefore, the maps we developed for this study depict surficial ground motions incorporating the site-response effects of unconsolidated sediments and near-source effects. The maps display peak horizontal acceleration (plate 1, simplified on figure 4) and horizontal spectral accelerations at periods of 0.2 and 1.0 second (figures 5 and 6).

To map ground shaking, we first defined and characterized geologic site-response units. We then computed amplification factors and characterized ground-motion attenuation, and used these results to calculate ground motions and develop the scenario ground-shaking maps.

Characteristics of Geologic Site-Response Units

We defined and characterized five site-response units within the study area to incorporate site-response effects into the computed ground motions (figure 2). Our site-response units are generally based on surficial geologic mapping and the Salt Lake Valley site-response units of Ashland (2001), which were characterized using the shear-wave velocities compiled by Ashland and Rollins (1999). Our site-response units include: (1) lacustrine and alluvial silt and clay, with interbedded fine-grained sand; (2) lacustrine sand, silt, and clay; (3) lacustrine and alluvial gravel; (4) pre-Bonneville alluvial-fan deposits (locally including post-Bonneville alluvial-fan deposits) and glacial deposits (shown on figure 2 as two separate units mapped by Ashland [2001]); and (5) rock. Each unit is characterized by an average shear-wave-velocity profile with its uncertainties, developed from the data of Tinsley and others (1991) and Schuster and Sun (1993), and shear-modulus reduction and damping curves to account for strain-dependent non-linear soil response (Electric Power Research Institute, 1993; Silva and others, 1997; Vucetic and Dobry, 1998).

For computational purposes, we divided the total thickness of unconsolidated sediments into six ranges: 10 to 50 feet (3-15 m), 50 to 100 feet (15-30 m), 100 to 200 feet (30-60 m), 200 to 400 feet (60-120 m), 400 to 800 feet (120-240 m), and 800 to 2,600 feet (240-800 m). This results in 24 categories defined by the six thickness ranges in each of the four unconsolidated site-response units. The categories span the full range of thickness for deposits overlying semi-consolidated sediments estimated in Salt Lake Valley by Arnow and others (1970) and beyond Salt Lake Valley by our study using drillers' logs of water wells. Possible overlaps in thickness between ranges were incorporated into the computation of amplification factors to accommodate uncertainties in amplification factors and estimated thickness. Areas with unconsolidated sediments less than 10 feet (3 m) thick were considered equivalent to areas underlain by rock.

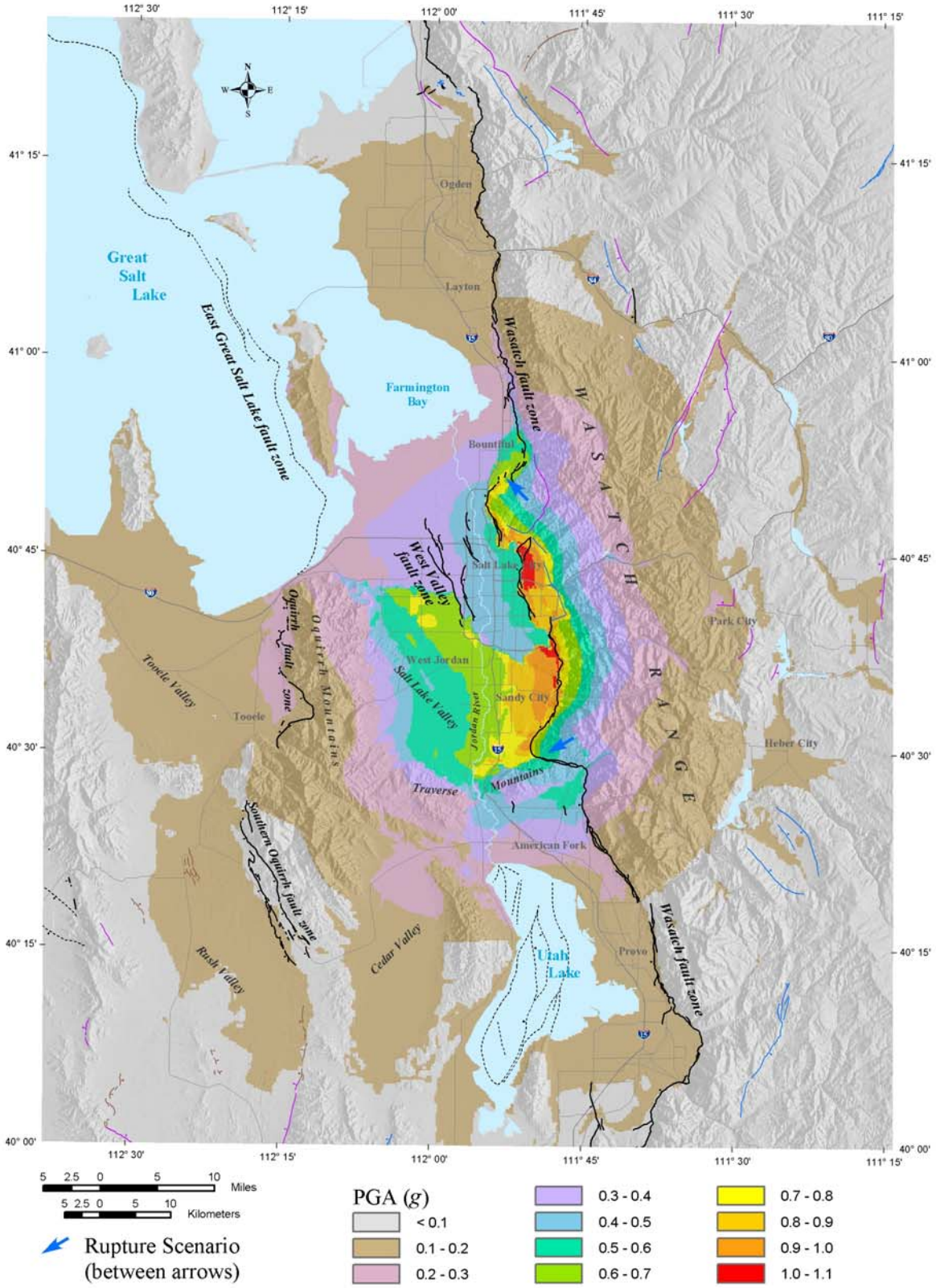

Figure 4. *Peak horizontal acceleration at the ground surface (PGA). Simplified from plate 1. See figure 3 for explanation of fault symbols (dotted where under water), modified from Black and others (2003).*

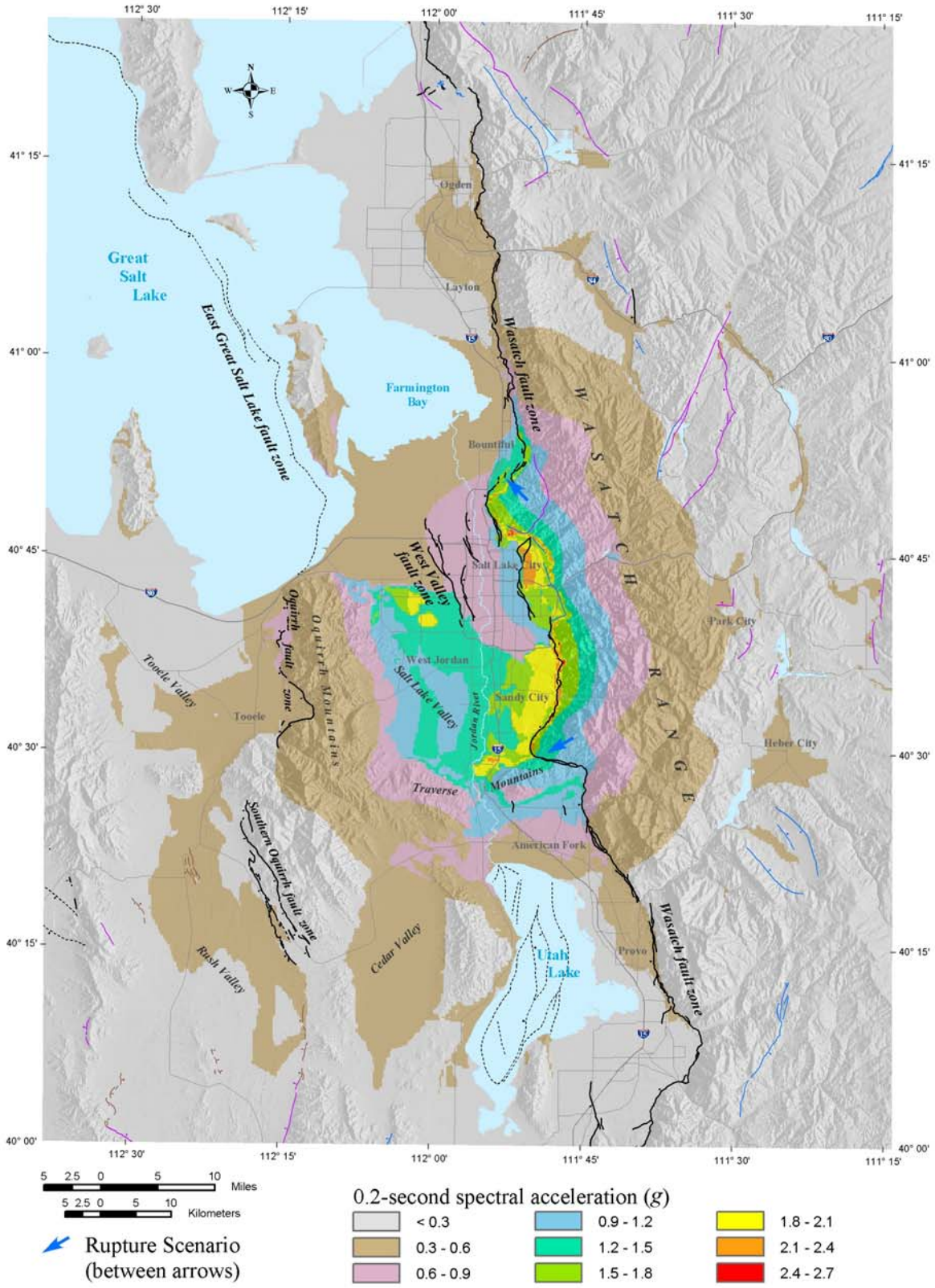

Figure 5. *0.2-second spectral acceleration at the ground surface. See figure 3 for explanation of fault symbols (dotted where under water), modified from Black and others (2003).*

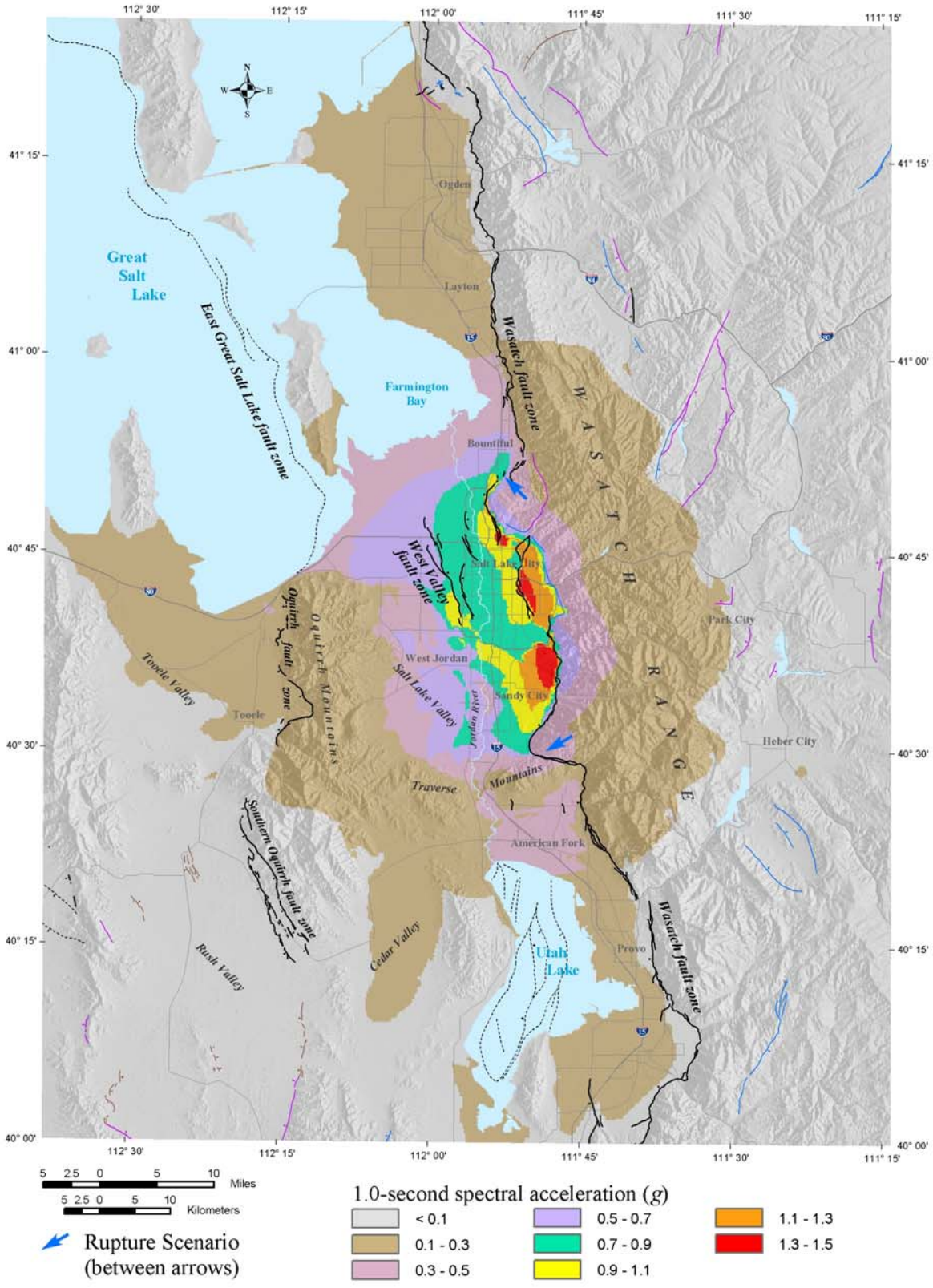

Figure 6. *1.0-second spectral acceleration at the ground surface. See figure 3 for explanation of fault symbols (dotted where under water), modified from Black and others (2003).*

Computation of Amplification Factors

We adapted frequency- and strain-dependent amplification factors as a function of site-response unit, ranges in thickness of unconsolidated sediment, and input rock motions, from Wong and others (2002). The stochastic numerical ground-motion modeling approach coupled with an equivalent-linear methodology (Silva and others, 1998) was used to calculate amplification factors for 5 percent-damped response spectra for each site-response unit. The point-source stochastic methodology was used to generate rock-acceleration response spectra for a **M** 6.5 earthquake, which were then propagated up through the site-response-unit profiles. We selected a **M** 6.5 event because it approximated the mean magnitude of the earthquakes contributing to the probabilistic hazard at return periods of 500 and 2,500 years in the Wong and others (2002) study. The **M** 6.5 event was placed at several distances to produce input peak accelerations of 0.05, 0.10, 0.20, 0.40, 0.50, and 0.75 *g*. Thus, the amplification factors (the ratios of the response spectra at the top of the profiles to the input spectra) are a strong function of the reference rock peak acceleration, spectral frequency, soil thickness, and nonlinear soil response. We used interpolation to obtain amplification factors at other reference rock peak accelerations. At peak horizontal acceleration, median amplification factors range from 0.62 to 2.09 (values less than 1.0 signify deamplification). At 0.2- and 1.0-second spectral accelerations, median amplification factors range from 0.50 to 2.19 and 0.94 to 3.13, respectively.

Attenuation Relationships and Calculation of Ground Motions

To compute ground motions for the scenario earthquake, we used empirical attenuation relationships appropriate for soft rock sites in the western U.S., and numerical modeling. An important consideration in the selection of attenuation relationships is that the study area is located in the extensional Basin and Range Province where normal faulting predominates. We therefore used the empirical relationships of Abrahamson and Silva (1997) with normal faulting factors (N. Abrahamson, consultant, written communication, 1997), and Spudich and others (1999), which was developed from an extensional earthquake strong-motion database. These relationships were subjectively assigned weights of 0.40 and 0.30, respectively. We also used the relationships of Sadigh and others (1997) and Campbell (1997), which are based primarily on California strong-motion data and were included to more fully address uncertainty. These relationships were weighted 0.15 each. Although none of the four relationships are specific to central Utah or the Basin and Range Province due to the lack of strong motion records from these areas, the greatest weight (0.70) was given to the two relationships most appropriate for extensional regimes.

To compensate for the lack of region-specific attenuation relationships, we also used the numerical stochastic finite-fault approach to calculate ground motions (Wong and others, 1996). This modeling explicitly incorporates the effects of the seismic source (fault geometry and dip, location of rupture, and sense of slip) and rupture propagation (directivity), which are particularly important in the near-field. Region-specific parameters for crustal attenuation (Q) were incorporated. We conducted 30 simulations, varying the slip models and depth of rupture initiation. Scenario ground-motion values were calculated by assigning a 0.40 weight to the values computed from the empirical attenuation relationships and a 0.60 weight to the numerically modeled values.

Ground-Shaking Maps

We produced ground-shaking maps by first assigning a site-response category to each map cell and then calculating surface ground motions at each cell by multiplying the rock ground motions by the appropriate amplification factor. For each map, the peak or spectral acceleration values were contoured and then color coded into intervals varying from 0.10 to 0.30 *g*.

The map for peak horizontal acceleration (plate 1, simplified on figure 4) indicates that high-frequency ground motions could approach and possibly exceed 1 *g* from the scenario earthquake. The rate of decay of ground motions on rock in the footwall is faster and more uniform than the rate of decay of ground motions on soil in the hanging wall. The pattern of high-frequency ground shaking mimics the distribution of site-response units. The highest peak accelerations (> 0.7 *g*) occur in stiff gravels and sands, particularly on the east side of Salt Lake Valley underlying foothills adjacent to the Wasatch fault. Lower peak accelerations occur in thick deposits of lacustrine and alluvial silts and clays that damp out stronger high-frequency ground motions. Site effects appear to be more dominant than the hanging-wall effect as illustrated by high peak accelerations in the footwall of the East Bench fault, east of the fault.

Although high-frequency ground motions are greatest in Salt Lake Valley, potentially damaging ground motions of 0.10 *g* and greater extend along the Wasatch Front to Ogden and Provo at distances of about 30 to 40 miles (50-60 km) from Salt Lake City (plate 1, simplified on figure 4). Lacustrine and alluvial silts and clays will amplify the weaker ground motions in these areas, as well as in Tooele, Rush, and Cedar Valleys west of the Wasatch Front. Potentially damaging ground motions may also occur in the back valleys of the Wasatch Range east (in the footwall) of the Wasatch fault, where peak acceleration will be amplified to levels greater than in surrounding rock by a thin cover of unconsolidated sediment (plate 1, simplified on figure 4).

The pattern of ground shaking for short-period (0.2 s) spectral acceleration (figure 5) resembles that for peak acceleration (plate 1, simplified on figure 4). The highest levels of peak acceleration and short-period spectral acceleration are found on the east side of Salt Lake Valley adjacent to the Wasatch fault zone because of their proximity to the fault and because the relatively thin (less than 300 feet [100 m] thick), dense gravelly and sandy soil amplifies ground shaking at short to moderate spectral periods. Levels of peak acceleration and short-period spectral acceleration decrease toward the thick sediments of north-central Salt Lake Valley. In contrast, this pattern is less distinct for long-period (1.0 s) spectral acceleration (figure 6), with higher ground motions (> 1.1 *g*) extending farther into deeper parts of the basin. Directivity effects, which are long period in nature (> 0.5 s), are not readily apparent in areas of thick, unconsolidated sediments because the effects have been diluted somewhat by the use of empirical attenuation relationships and/or masked by site effects.

Surface Fault Rupture

The Salt Lake City segment of the Wasatch fault zone lies between the Weber segment to the north and the Provo segment to the south (figure 1). The Salt Lake City segment consists of a main, active latest Quaternary trace; a northern bedrock fault with no conclusive evidence of Quaternary movement; and an eastern range-front fault with minimal post-Bonneville movement

(figure 3). The main trace is divided into three en echelon sections. These sections are, from north to south, the Warm Springs fault, the East Bench fault, and the Cottonwood section of the Wasatch fault zone (Personius and Scott, 1992). The northern bedrock fault, east of the Warm Springs fault, appears to connect the East Bench fault with the Weber segment of the Wasatch fault zone (Hecker, 1993). Faulting in the northeastern part of Salt Lake Valley shifted westward from the range-front fault to the East Bench fault during the late Quaternary.

Extent of Surface Fault Rupture

The active trace of the Salt Lake City segment ruptures to the surface during our scenario earthquake. Based on the structural geology of the Salt Lake City segment, distribution and size of fault scarps, and comparisons with large historical earthquakes elsewhere, surface rupture on the segment may initiate at the southern end of the Cottonwood section and propagate unilaterally northward (Bruhn and others, 1987; Personius and Scott, 1992), although we treated the rupture randomly when computing ground motions. Simultaneous rupture may also occur on the antithetic West Valley fault zone, west of the Salt Lake City segment, in north-central Salt Lake Valley (Keaton and others, 1987; Personius and Scott, 1992). However, the extent to which movement on the West Valley fault zone is independent of movement on the Salt Lake City segment of the Wasatch fault zone is unclear (Wong and others, 2002). For our study we assumed that such movement is independent and the West Valley fault zone did not rupture during the scenario earthquake. We also assumed that the scenario earthquake involved only the Salt Lake City segment of the Wasatch fault zone, although recent stress-interaction modeling suggests that some prehistoric earthquakes may have ruptured through segment boundaries, indicating multisegment ruptures (Chang and Smith, 1998b, 2002).

Amount of Permanent Ground Displacement

The median amount of permanent vertical ground displacement caused by surface fault rupture from our scenario earthquake is 6.1 feet (1.9 m). We estimated the displacement using the default HAZUS technique, which employs the correlation between maximum surface fault displacement and earthquake moment magnitude developed by Wells and Coppersmith (1994). This relationship, which the authors indicate may provide the most reliable results for normal faults, was determined using data from historical earthquakes worldwide associated with all fault-slip types.

The calculated displacement occurs along a main fault that may be accompanied by one or more minor faults. The zone between the faults may be faulted and tilted in a complex manner. McCalpin (1987) estimates that typical surface fault rupture on the Wasatch fault zone is accompanied by a single minor fault on the upthrown block within 3 feet (1 m) of the main fault, in contrast to an average of four faults on the downthrown block over a width of 40 to 45 feet (12-14 m).

For loss estimation, HAZUS assumes that the maximum displacement can potentially occur at any location along the fault, although displacement must drop to zero at the ends of the fault. However, considerable uncertainty exists in the maximum displacement estimate for this relationship. For this reason, HAZUS conservatively estimates the probability distribution for

values of displacement along the fault rupture segment. Wells and Coppersmith (1994) found that the average displacement along the fault rupture segment was approximately equal to one-half the maximum displacement. This is equivalent to a uniform probability distribution for values of displacement ranging from zero to the maximum displacement. As a conservative estimate, HAZUS incorporates a uniform probability distribution equivalent to average displacement with a minimum of one-half of the maximum fault displacement (rather than zero) for any location along the fault rupture.

Liquefaction

We evaluate liquefaction hazards using three steps. First, we characterize the relative liquefaction susceptibility of soil. Susceptibility depends in part upon soil properties, which we assume are consistent within each map unit. In reality each unit encompasses a range of liquefaction susceptibilities due to variations of soil properties, such as grain-size distribution and relative density, which cannot be recognized at the map scale. Portions of a susceptible map unit may be more or less susceptible to liquefaction or may not be susceptible. We therefore assess the probability of liquefaction at any given location due to variations in soil properties. Finally, we use probability as a factor in determining the amount of expected permanent ground displacement due to hazards associated with liquefaction, including lateral spreading and ground settlement. HAZUS suggests a method for evaluating liquefaction susceptibility, but we use a technique that is more appropriate for local geologic conditions. We then use our susceptibility maps and modified default HAZUS relationships to determine the probability of liquefaction occurring and the resulting ground displacement.

Susceptibility

HAZUS suggests characterizing susceptibility using geologic map information and the classification system presented by Youd and Perkins (1978). This system assigns a relative liquefaction susceptibility rating based on age, depositional environment, and material type of each map unit. However, Anderson and others (1982, 1986a, 1986b, 1990a, 1990b) believe that the criteria of Youd and Perkins (1978), defined for Quaternary deposits in California, are not applicable to Utah's closed basins and Pleistocene lacustrine deposits, and we concur. Instead, Anderson and others (1982, 1986a, 1986b, 1990a, 1990b) mapped liquefaction potential along the Wasatch Front in the central part of our study area by modifying the techniques of Seed and others (1983, 1985), using standard- and cone-penetration-test data to predict the critical acceleration required to initiate liquefaction. Because they did not map liquefaction potential over our entire study area, and because we wanted our mapping to be uniform and based on readily available geologic information, we mapped liquefaction susceptibility using the site-response units of this study (figure 2) and a statewide compilation of shallow ground water (Hecker and others, 1988). The site-response units are based on material type, and the map of shallow ground water shows depths to the shallow unconfined water table.

We assigned soil to one of four liquefaction-susceptibility categories, ranging from very low for most soils with deep ground water to high for granular soils with shallow ground water, and assume that bedrock is not susceptible (table 1). These categories are similar to those used in the liquefaction-potential maps of Anderson and others (1982, 1986a, 1986b, 1990a, 1990b).

Although we mapped liquefaction susceptibility (figure 7) and they mapped liquefaction potential, which includes components of both susceptibility (a function of the soil and site characteristics) and opportunity (a function of regional seismicity), the map patterns are very similar. In limited areas where significant differences arose between our map and those of Anderson and others (1982, 1986a, 1986b, 1990a, 1990b), we modified our map based on their more detailed area-specific geotechnical data or because local surficial geology was complex and beyond the resolution of geologic data that we used to map site-response units. These areas include (1) the Weber River flood plain, where we map a low susceptibility because of dense gravels identified by Anderson and others (1982, 1990a), (2) the Jordan River flood plain and small drainages in southern Salt Lake Valley and south of Ogden, where we map a high susceptibility because of the sandy alluvium which is included in site-response units with large amounts of fine-grained soil (Anderson and others, 1982, 1986b), (3) lower Spanish Fork Canyon, where we map a moderate susceptibility because of shallow ground water that extends beyond the limit mapped by Hecker and others (1988), and (4) the western shore of Utah Lake, where we map a moderate to high susceptibility because of shallow ground water that extends beyond the limit mapped by Hecker and others (1988).

Table 1. *Relative liquefaction susceptibility as a function of ground-water depth and site-response unit.*

		Ground-Water Depth (ft)		
		>30	<30	<10
Site-Response Unit	Lacustrine and alluvial silt and clay, with interbedded fine-grained sand	Low	Moderate	High
	Lacustrine sand, silt, and clay	Very Low	Moderate	Moderate
	Lacustrine and alluvial gravel	Very Low	Low	Moderate
	Pre-Bonneville alluvial-fan deposits	Very Low	Very Low	Low
	Glacial deposits	Very Low	Very Low	Very Low
	Rock	None	None	None

Liquefaction susceptibility is greatest around the margins of Great Salt Lake and Utah Lake, where saturated fine-grained sand layers are commonly interbedded in finer grained silty and clayey Lake Bonneville lake-bottom deposits. We map high liquefaction susceptibility in significant parts of the Provo, Salt Lake City, and Ogden metropolitan areas, including most of the central and northern Salt Lake Valley. Liquefaction susceptibility decreases in valleys not adjacent to Great Salt Lake and Utah Lake and on the margins of valleys near these lakes where, although the proportion of shallow granular soils increases, ground-water depth also increases. We map extensive areas of very low liquefaction susceptibility in Cedar Valley, Rush Valley, southern Tooele Valley, and southwestern Salt Lake Valley.

Probability

HAZUS determines the probability of liquefaction as a function of soil susceptibility, amplitude and duration of ground shaking (represented by PGA and **M**), and ground-water depth. We assume uniform soil properties within site-response units used for susceptibility mapping when, in reality, variations of soil properties exist within each susceptibility unit.

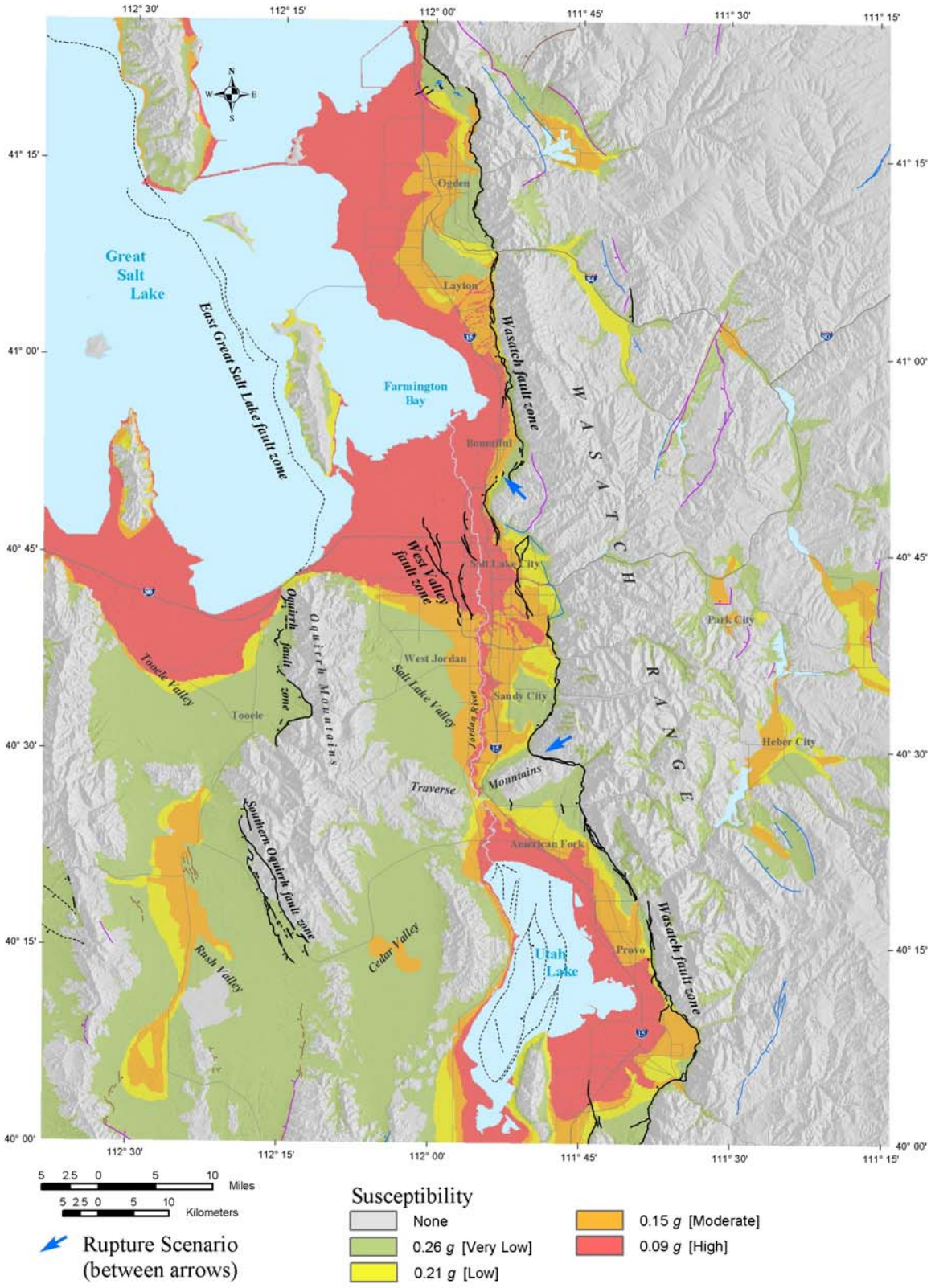

Figure 7. *Liquefaction susceptibility, as measured by threshold acceleration. See figure 3 for explanation of fault symbols (dotted where under water), modified from Black and others (2003).*

HAZUS accounts for this by estimating the proportion of the area of each susceptibility category that may be susceptible to liquefaction, based on preliminary examination of soil-property data compiled for geologic map units characterized for various regional liquefaction studies (for example, Power and others, 1991). Because we map four susceptibility categories (figure 7) but HAZUS maps five (our four categories plus Very High), we estimate the proportion of our High susceptibility category that may be susceptible to liquefaction by using the average of HAZUS proportions for the High and Very High categories (table 2).

HAZUS also relates liquefaction probability and PGA for each susceptibility category (the conditional liquefaction probability) based on empirical procedures and the statistical modeling of the empirical liquefaction catalog presented by Liao and others (1988) for representative penetration resistance characteristics of soils within each susceptibility category. The conditional liquefaction probability relationships were developed for a **M** 7.5 earthquake and an assumed ground-water depth of 5 feet (1.5 m), but HAZUS calculates correction factors (Seed and Idriss, 1982; Seed and others, 1985; National Research Council, 1985) for other values of **M** and ground-water depth. Because Hecker and others (1988) mapped ground-water depth by ranges rather than specific values, we estimated ground-water depth within ground-water map units (table 3). Where ground-water depth is not mapped, we estimate that ground-water depth is greater than 30 feet (9 m) and averages 50 feet (15 m), the depth below which soil is commonly too deep to liquefy (Seed, 1979). HAZUS determines the conditional probability relationships for five susceptibility categories, and we adapt these relationships to our four categories by conservatively assuming that the HAZUS relationships for their Very High category apply to our High category (table 4).

Because the probability of liquefaction is a function of soil susceptibility and PGA, liquefaction is more likely where highly susceptible soils (figure 7) are subject to the greatest levels of ground shaking (plate 1, simplified on figure 4). This includes most of the central and northern Salt Lake Valley, the Jordan River flood plain in southern Salt Lake Valley, and the northern end of Utah Valley, where the probability of liquefaction during the scenario earthquake commonly ranges from 20 to 25 percent (figure 8). Where levels of PGA are significantly lower, generally less than 0.2 *g*, the probability of liquefaction is also lower even in areas of high liquefaction susceptibility such as the Ogden and Provo metropolitan areas and Tooele Valley. In these areas, the probability of liquefaction commonly ranges from 1 to 10 percent, decreasing with increasing distance from the Salt Lake City segment. However, even in areas closer to the segment, strong ground shaking is unlikely to induce liquefaction in well-drained soils with very low liquefaction susceptibility. These areas include the east benches of Salt Lake and Utah Valleys, the bench east of Bountiful, and southwestern Salt Lake Valley, where the probability of liquefaction is commonly less than 1 percent.

Permanent Ground Displacement

Permanent ground displacement due to lateral spreads, flow slides, and differential settlement is a significant potential hazard associated with liquefaction. Lateral spreads are liquefaction-induced landslides occurring either on relatively uniform and gentle slopes or near abrupt topographic features (free faces such as incised streams or steep banks). Flow slides generally occur in liquefied material on steeper slopes. Settlement results from the

Table 2. *Proportion of map units susceptible to liquefaction (modified from National Institute of Building Sciences, 1999, table 4.12).*

Relative Liquefaction Susceptibility	Proportion of Map Unit	Source of Proportion
High	0.23	Average of HAZUS "High" and "Very High"
Moderate	0.10	HAZUS "Moderate"
Low	0.05	HAZUS "Low"
Very Low	0.02	HAZUS "Very Low"
None	0.00	HAZUS "None"

Table 3. *Estimated average ground-water depth within ground-water map units of Hecker and others (1988).*

Map-Unit Ground-Water Depth (ft)	Estimated Range of Ground-Water Depth (ft)	Estimated Average Ground-Water Depth (ft)
<10	0-10	5
<30	10-30	20
Not mapped	>30	50

Table 4. *Conditional liquefaction probability of relative liquefaction-susceptibility categories at a specified PGA (modified from National Institute of Building Sciences, 1999, table 4.13).*

Relative Liquefaction Susceptibility	Conditional Liquefaction Probability at a Specified Level of PGA[1]	Source of Conditional Probability
High	$0 \le 9.09\ PGA - 0.82 \le 1.0$ $0 \le 7.67\ PGA - 0.92 \le 1.0$	HAZUS "Very High" HAZUS "High"
Moderate	$0 \le 6.67\ PGA - 1.00 \le 1.0$	HAZUS "Moderate"
Low	$0 \le 5.57\ PGA - 1.18 \le 1.0$	HAZUS "Low"
Very Low	$0 \le 4.16\ PGA - 1.08 \le 1.0$	HAZUS "Very Low"
None	0	HAZUS "None"

[1] Values of conditional liquefaction probability range from 0 (liquefaction cannot occur) to 1 (liquefaction must occur). If values less than 0 or greater than 1 are calculated using the relationships in this table, then values of 0 and 1 are respectively used.

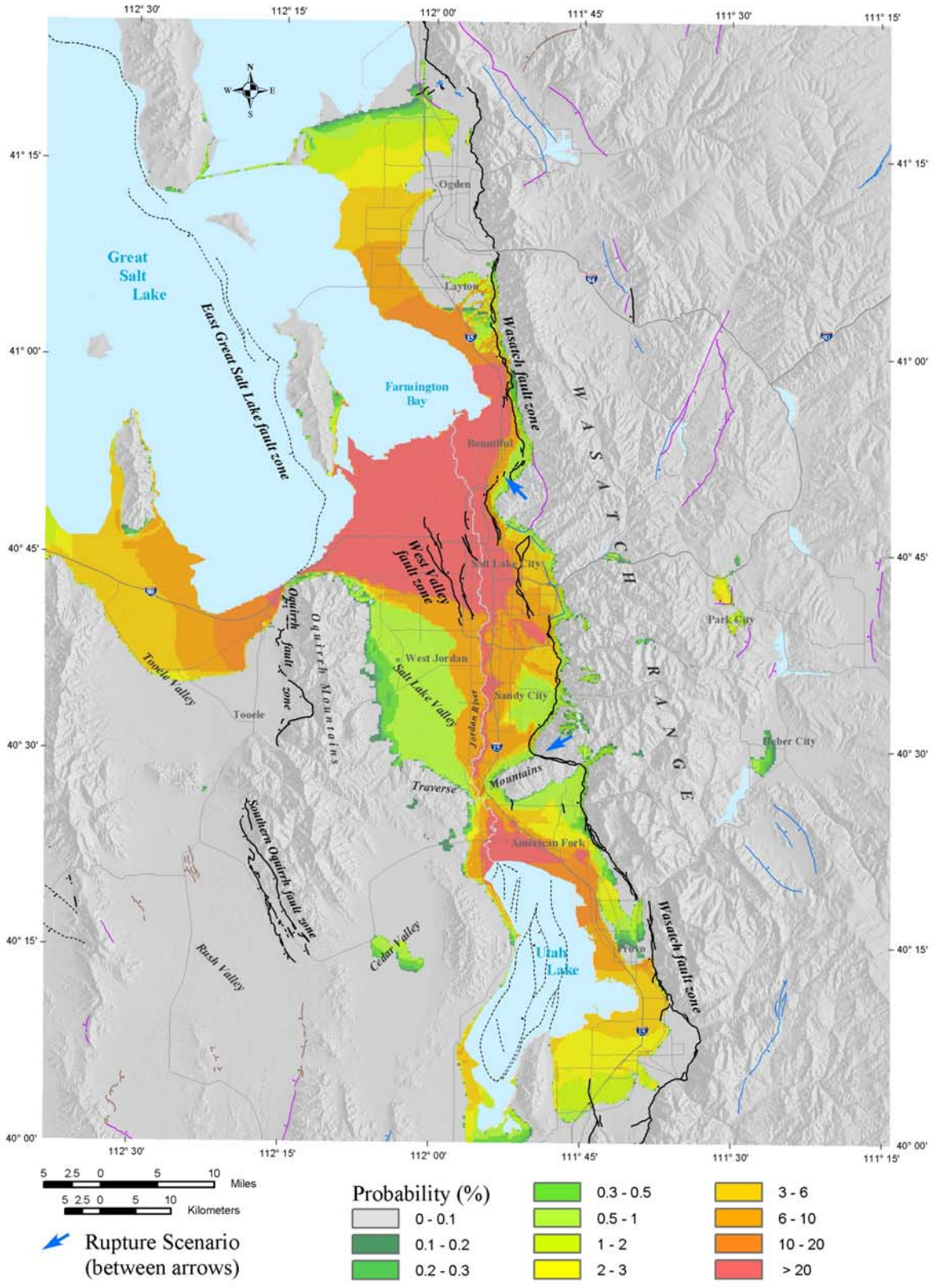

Figure 8. *Liquefaction probability. See figure 3 for explanation of fault symbols (dotted where under water), modified from Black and others (2003).*

rearrangement of loose soils into a denser configuration during earthquake ground shaking. Variations in soil properties may cause settlement to occur differentially. We estimate the potential for permanent ground displacement from the most common liquefaction-induced processes for which regional factors can be identified. These include lateral spreading on gentle slopes (plate 2, simplified on figure 9) and settlement (plate 3, simplified on figure 10). We do not estimate the potential for permanent ground displacement from lateral spreading near abrupt topographic features because these features are beyond the resolution of our topographic base map. We also do not estimate the potential for flow slides because most ground slopes in our study area underlain by susceptible material are too gentle for flow failure, although this may occur locally.

Lateral spreading: Although various techniques have been proposed to estimate lateral-spread displacement, only one has been used for a regional liquefaction study in Utah. McCalpin and Solomon (2001) used the relationship developed by Bartlett and Youd (1992) and revised by Youd and others (1999) to estimate lateral-spread displacement in the central Cache Valley, about 60 miles (100 km) north of Salt Lake City. This relationship relies upon observations of earthquake characteristics, geology, slope, and soil properties at sites of historical lateral spreading. Soil properties needed by this relationship to calculate lateral-spread displacement include the cumulative thickness of saturated granular layers, the average fines content of these layers, and the average grain size within the layers.

Bardet and others (2002), in their evaluation of techniques for regional modeling of lateral-spread displacement, recommend the method of Bartlett and Youd (1992) when information is available on the grain-size distribution of soils. However, when this information is not available and is estimated, the accuracy of the Bartlett and Youd (1992) method decreases. To overcome the need for extensive subsurface data, Bardet and others (2002) propose an alternate relationship that does not require knowledge of the average fines content of saturated granular layers and the average grain size within the layers. This relationship still requires knowledge of the cumulative thickness of the layers. Accurate values for thickness and grain-size distribution require collection of considerable field data that is impractical because of the regional scope of our study, and estimates for these properties would introduce a significant margin of error, negating the advantages of using either relationship.

HAZUS relies upon a relationship for lateral spreading, which we use for our study, developed by combining the Liquefaction Severity Index (LSI) of Youd and Perkins (1987) with the ground-motion attenuation relationship of Sadigh and others (1986) as presented in Joyner and Boore (1988). The LSI has the advantage of relying primarily on earthquake factors (distance from the causative earthquake and its magnitude), does not explicitly rely on soil properties, and is intended to provide a conservative upper bound for estimating horizontal ground displacement at sites having a moderate to high liquefaction susceptibility. The ground-motion attenuation relationship implicitly incorporates soil properties through the use of PGA, which is based in part on the properties of site-response units. Although Bardet and others (2002) demonstrate a poor agreement between measured and calculated displacements using the LSI alone, combining the LSI with a ground-motion attenuation relationship increases the accuracy of the HAZUS technique. We cannot quantify the accuracy of the HAZUS relationship

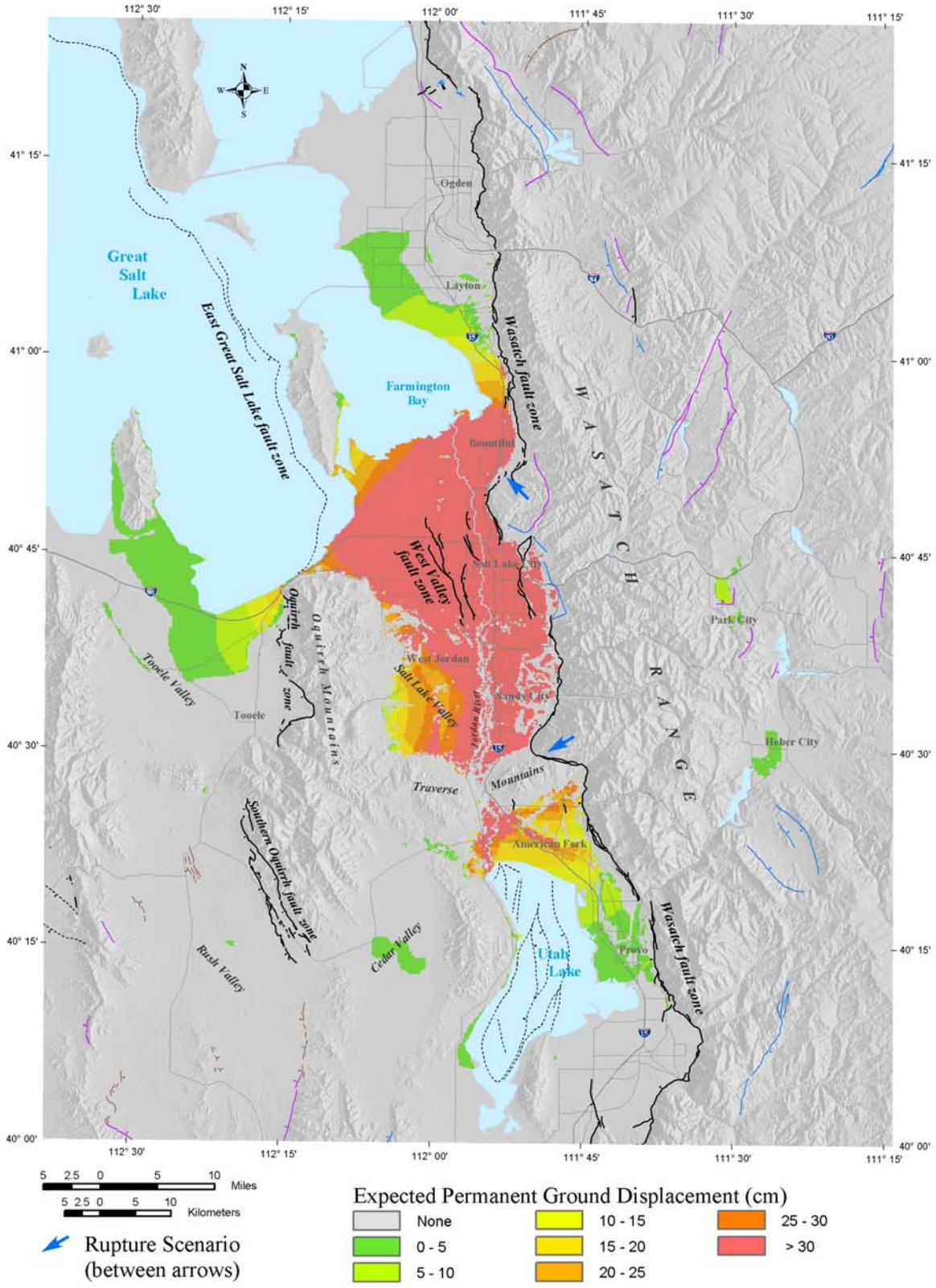

Figure 9. *Permanent ground displacement caused by liquefaction-induced lateral spreading. Simplified from plate 2. See figure 3 for explanation of fault symbols (dotted where under water), modified from Black and others (2003).*

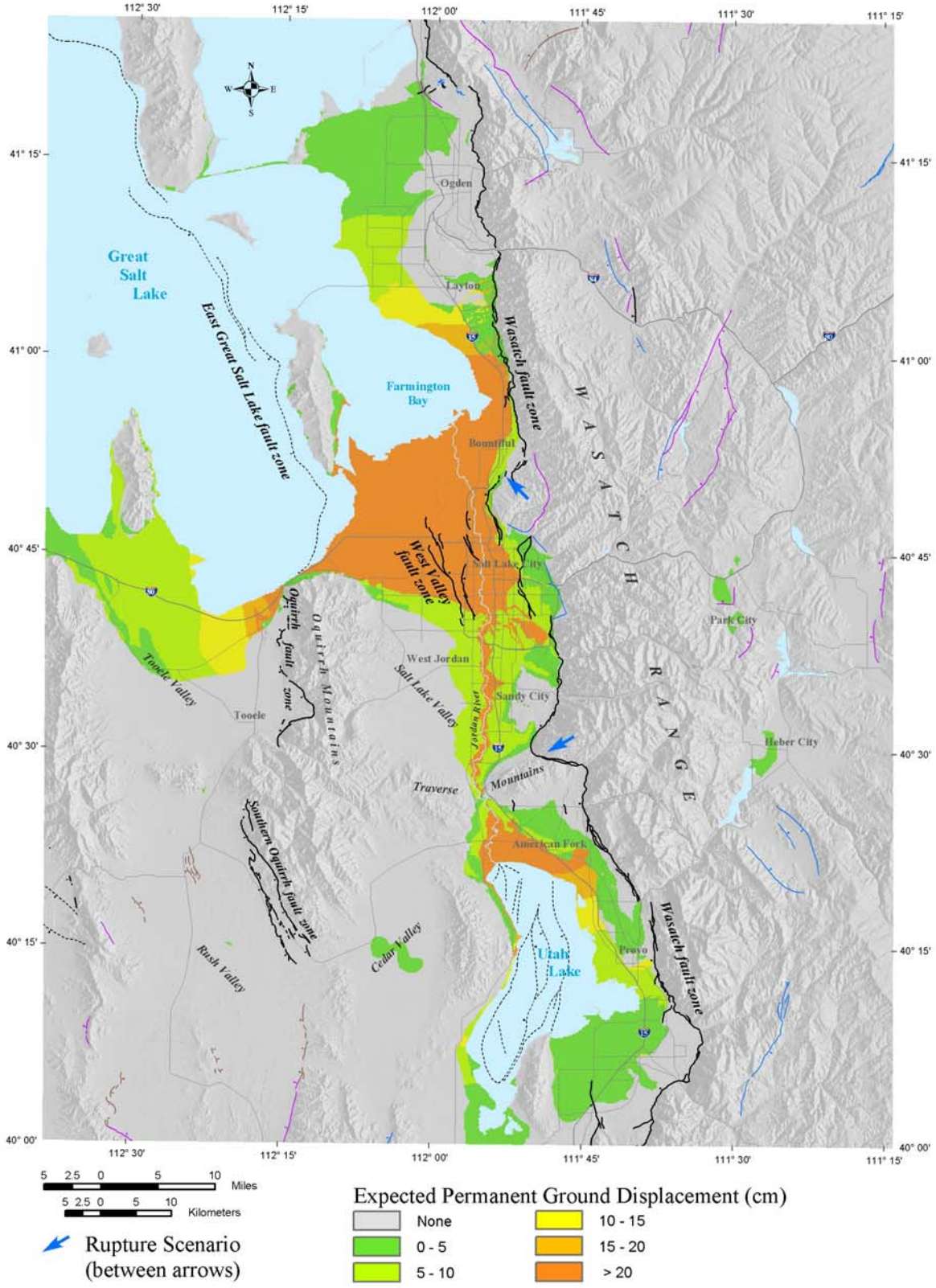

Figure 10. *Permanent ground displacement caused by liquefaction-induced ground settlement. Simplified from plate 3. See figure 3 for explanation of fault symbols (dotted where under water), modified from Black and others (2003).*

and do not recommend its use when a detailed geotechnical database is available, but the relationship appears appropriate for use in our regional study.

The HAZUS relationship calculates the expected permanent ground displacement for a given susceptibility category under a specified level of normalized ground shaking. Because this relationship was developed for a **M** 7.5 earthquake, displacements for other magnitudes are determined using a displacement correction factor calculated by HAZUS based on the work of Seed and Idriss (1982). We calculated displacements only on slopes less than 5 percent, which is the approximate maximum gradient of lateral spreads observed by Bartlett and Youd (1992).

The ground-shaking level used by the HAZUS relationship is normalized by the threshold PGA corresponding to zero probability of liquefaction for each susceptibility category (table 4). Because we use four susceptibility categories rather than the five used by HAZUS, the threshold PGA for our "High" category (0.09 *g*) is the same as that for the HAZUS "Very High" category (table 5). The larger threshold PGA for the HAZUS "High" category (0.12 *g*) lies conservatively within the range of PGAs required to initiate lateral spreading in susceptible soils within our "High" category. The factor termed the threshold PGA by HAZUS represents the minimum critical acceleration as defined by Anderson and others (1982, 1986a, 1986b, 1990a, 1990b) for each susceptibility category in their Wasatch Front liquefaction studies. Our values for threshold PGA are near the values for minimum critical acceleration calculated by Anderson and others (1986a) for Salt Lake County and our susceptibility categories are therefore approximately equivalent to theirs. If PGAs determined for this study (plate 1, simplified on figure 4) exceed the threshold PGAs for each susceptibility category (table 5), we can calculate expected permanent ground displacements.

Table 5. *Comparison of critical accelerations required to induce liquefaction (Anderson and others, 1986a) and threshold ground accelerations corresponding to zero probability of liquefaction (this study; modified from National Institute of Building Sciences, 1999, table 4.14).*

Relative Liquefaction Susceptibility	Critical Acceleration (Anderson and others, 1986a)	Threshold Ground Acceleration (this study)	Source of Threshold Ground Acceleration
High	< 0.13 g	0.09 g	HAZUS "Very High"
Moderate	0.13 g to 0.23 g	0.15 g	HAZUS "Moderate"
Low	0.23 g to 0.33 g	0.21 g	HAZUS "Low"
Very Low	> 0.33 g	0.26 g	HAZUS "Very Low"
None	N/A	N/A	N/A

Youd (1980) estimates that lateral-spread displacements greater than 1 foot (30 cm) tend to result in severe, irreparable building damage or building collapse. Our analysis for the scenario earthquake indicates that displacements of this level are possible in much of Salt Lake Valley and extending to Bountiful and northern Utah Valley (plate 2, simplified on figure 9). These areas lie within about 13 miles (21 km) of the Salt Lake City segment on the hanging wall where large displacements are most likely in soils with high liquefaction susceptibility, and are possible but improbable in soils with lower susceptibilities underlying areas of very strong

ground shaking. Smaller displacements may occur in back valleys and near the Great Salt Lake and Utah Lake shores north, west, and south of Salt Lake Valley, resulting in slight to severe, but repairable, damage.

Ground settlement: The HAZUS technique for estimating the amount of ground settlement associated with liquefaction, which we apply in our study, assumes that the amount of settlement is related to liquefaction susceptibility. This relationship is based on the research of Tokimatsu and Seed (1987) and Ishihara (1993), which demonstrates very little dependence of settlement on ground-motion level once liquefaction occurs. HAZUS also indicates a direct correlation between susceptibility and the thickness of potentially liquefiable soils. Therefore, the expected settlement at a given location is the product of the characteristic settlement amplitude appropriate to the susceptibility category (reflecting the relationship between susceptibility, amount of settlement, and thickness of potentially liquefiable soils; table 6) and the probability of liquefaction for a given ground-motion level (which is independent of the amount of settlement; figure 8). Characteristic settlement amplitudes for each susceptibility category are presented by HAZUS. We modify these values to reflect our use of four susceptibility categories rather than the five used by HAZUS by applying the average of values for the HAZUS "High" and "Very High" to our "High" category. Our values range from no settlement for soils with Very Low susceptibility to 9 inches (23 cm) for soils with High susceptibility.

Table 6. *Ground-settlement amplitudes for relative liquefaction-susceptibility categories (modified from National Institute of Building Sciences, 1999, table 4.15).*

Relative Liquefaction Susceptibility	Settlement (inches)	Source of Settlement Amplitude
High	9	Average of HAZUS "High" and "Very High"
Moderate	2	HAZUS "Moderate"
Low	1	HAZUS "Low"
Very Low	0	HAZUS "Very Low"
None	0	HAZUS "None"

Settlement displacements are commonly less than lateral-spread displacements. Settlement displacement is greatest in highly susceptible soils within about 13 miles (21 km) of the Salt Lake City segment on the hanging wall, where displacements of 9 inches (23 cm) may occur (plate 3, simplified on figure 10). According to Youd (1980), displacement of this size is insufficient to cause irreparable building damage but may cause severe but repairable damage. Displacements as small as 4 inches (10 cm) may cause similar damage, but areas subject to settlement displacements greater than 4 inches (10 cm) but less than 9 inches (23 cm) extend only a small distance beyond areas subject to displacement of 9 inches (23 cm). Settlement displacements smaller than 4 inches (10 cm), resulting in little damage, may occur in a larger area than lateral spreading along the Great Salt Lake and Utah Lake shores.

Summary

The extent of soils having the potential for the largest lateral-spread displacements (greater than 1 foot [30 cm]) is deceiving. Their widespread distribution is due to large ground accelerations, which exceed threshold accelerations for all soils regardless of susceptibility. However, such displacements are most likely in areas underlain by highly susceptible soils, with a 20 to 25 percent probability of occurrence. These areas include the densely populated northern part of Salt Lake Valley, the Bountiful area to the north, and the northern end of Utah Valley, which are underlain by saturated Lake Bonneville deposits, and alluvium in the Jordan River flood plain along the axis of Salt Lake Valley. The probability of liquefaction decreases with decreasing susceptibility to less than 1 percent in areas underlain by soils of very low susceptibility. Therefore, although large lateral-spread displacements may be possible during our scenario earthquake in much of Salt Lake Valley and nearby areas to the north and south, they are not probable in a significant portion of these areas, particularly where susceptibility is very low (southwest Salt Lake Valley and the Sandy area in southeast Salt Lake Valley). Moreover, the technique we employed to estimate lateral-spread displacements yields conservative results, thereby likely overestimating the probability and size of displacements.

The extent of soils having the potential for the largest settlement displacements (9 inches [23 cm]) mirrors the distribution of highly susceptible soils in areas where ground shaking exceeds 0.2 *g*. These are essentially the same areas subject to large, high-probability lateral-spread displacements. Settlement is unlikely in soils having very low liquefaction susceptibility. This is particularly significant in southern Salt Lake Valley, where negligible settlement displacement contrasts with large but low-probability lateral-spread displacements.

Landsliding

Our evaluation of landslide hazards involves steps similar to those for evaluation of liquefaction hazards. These steps include assessing the susceptibility of geologic materials to landsliding, determining the probability of landsliding in susceptible materials, and estimating permanent ground displacements due to landsliding. This results in an estimate of the hazard in the landslide source area. Because landslide debris moves downslope, an additional hazard exists in the landslide runout zone, but we did not assess its potential.

Earthquake-induced landsliding occurs when forces within the slide mass cause the factor of safety to temporarily drop below 1.0. The value of PGA required to cause the factor of safety to drop to 1.0 is called the critical acceleration. Determining the factor of safety requires knowledge of the shear strength and dry density of slope materials. HAZUS assigns landslide-susceptibility categories to geologic-map units based on assumed shear strengths and dry densities of the predominant soil or rock type within each unit, associating each category with a critical acceleration. We use this procedure for assessing the susceptibility of geologic materials to landsliding.

Once susceptibility categories are assigned to geologic-map units, HAZUS determines the probability of a landslide-susceptible deposit occurring within each category. Thus, at any given location the probability of landslide occurrence is specified, and landsliding occurs within

susceptible deposits if the PGA exceeds the critical acceleration. If landsliding is anticipated, HAZUS then calculates the amount of likely ground displacement.

The probability of landslide-susceptible deposits assigned by HAZUS is based on the research of Wieczorek and others (1985), who examined the percentage of area involved in slope failures in areas of strong ground shaking during historical earthquakes. However, more recent research by Jibson and others (1998), revised by Jibson and others (2000) with additional data, estimates the probability of landslide-susceptible deposits by statistically comparing predicted Newmark displacements with an inventory of landslides triggered by the **M** 6.7 1994 Northridge, California earthquake. We use the relationship of Jibson and others (2000) to estimate probability of slope failure as a function of Newmark displacement rather than as a function of susceptibility. We calculate Newmark displacement using another relationship of Jibson and others (2000) that is based on the analysis of strong-motion records from 280 recording stations in 13 earthquakes, rather than on the relationship used by HAZUS that is derived from the results of Makdisi and Seed (1978).

Our use of the relationships of Jibson and others (2000) is appropriate based on published comparisons with other techniques. Newmark displacements refer to the method developed by Newmark (1965) to calculate the cumulative permanent displacement of a sliding block as it is subjected to the effects of an earthquake acceleration-time history. Miles and Keefer (2000) note that the original Newmark method, although yielding an accurate index of relative slope performance during earthquakes, is numerically cumbersome. To overcome this problem, several investigators developed alternative methods to calculate Newmark displacement through double integration of those parts of an earthquake accelerogram that exceed the critical acceleration of a slope. Jibson (1993) considers the method developed by Wilson and Keefer (1983) to be one of the most useful rigorous double-integration techniques. However, some researchers developed simplified approaches to calculating Newmark displacements because of the numerical complexity of double-integration techniques and the difficulty of selecting the required acceleration time histories. Miles and Keefer (2000) evaluated several simplified techniques and recommend the approach of Jibson and others (1998), later modified by Jibson and others (2000), because its results are most similar to those of the double-integration approach regarding the areal distribution of Newmark displacements and probability of exceeding values greater than 1 inch (2 cm).

Susceptibility

HAZUS uses relationships between critical acceleration (the acceleration required to initiate slope movement), slope inclination, lithology, and ground-water depth developed by Wilson and Keefer (1985) as the basis for mapping landslide susceptibility. These relationships are based both on studies of 40 historical earthquakes and on a numerical analysis of dynamic slope stability. Keefer (1993) refined the method of Wilson and Keefer (1985) by revising assessment criteria for rock slopes. However, the additional information required to implement the Keefer (1993) method, including the degree of weathering, the presence of fissures, and fissure spacing, is not readily available to map susceptibility at the regional scale of our scenario study. We therefore use the Wilson and Keefer (1985) relationship to map susceptibility to earthquake-induced landsliding.

Wilson and Keefer (1985) define three geologic groups (A, B, and C) containing rock and soil having similar shear strengths. HAZUS divides the groups into 10 susceptibility categories (I through X) based on slope angle, considering both dry and wet conditions (ground water below the level of sliding and at the ground surface, respectively; table 7), and relates each category to a critical acceleration (table 8). HAZUS defines minimum slope angles and critical accelerations for each geologic group, below which geologic materials are not susceptible to landsliding (table 9). Within the study area, we assigned each bedrock geologic unit from the statewide geologic map (Hintze and others, 2000), existing landslides from the statewide landslide compilation (Harty, 1991), and soil site-response units (figure 2) to a geologic group (table 10). We then subdivided the groups into categories based on slope and mapped susceptibility under both wet and dry conditions (figures 11 and 12, respectively).

Table 7. *Characteristics and landslide-susceptibility categories of geologic groups (modified from National Institute of Building Sciences, 1999, table 4.16).*

Geologic Group	Material Type	Characteristic Lithologies	Estimated Shear Strength		Landslide-Susceptibility Categories (Dry/Wet)							
			Cohesion (psf)	Friction Angle (°)	Slope Angle (°)							
					0-3	3-5	5-10	10-15	15-20	20-30	30-40	>40
A	Strongly cemented rocks	Crystalline rocks and well-cemented sandstone	300	35	None/ None	None/ None	None/ None	None/ III	I/ VI	II/ VII	IV/ VIII	VI/ VIII
B	Weakly cemented rocks and soils	Sandy soils and poorly cemented sandstone	0	35	None/ None	None/ None	None/ V	III/ VIII	IV/ IX	V/ IX	VI/ IX	VII/ X
C	Argillaceous rocks and soils	Shale, clayey soil, existing landslides, and poorly compacted fills	0	20	None/ None	None/ VII	V/ VII	VI/ IX	VII/ X	IX/ X	IX/ X	IX/ X

Table 8. *Critical accelerations and relative landslide susceptibility for landslide-susceptibility categories (modified from National Institute of Building Sciences, 1999, table 4.18).*

Susceptibility Category	None	I	II	III	IV	V	VI	VII	VIII	IX	X
Critical Acceleration (g)	None	0.60	0.50	0.40	0.35	0.30	0.25	0.20	0.15	0.10	0.05
Relative Landslide Susceptibility	None	Very Low				Low		Moderate			High

Table 9. *Lower bounds for slope angles and critical accelerations for landslide susceptibility (modified from National Institute of Building Sciences, 1999, table 4.17).*

Geologic Group	Slope Angle (°)		Critical Acceleration (g)	
	Dry Conditions	Wet Conditions	Dry Conditions	Wet Conditions
A	15	10	0.20	0.15
B	10	5	0.15	0.10
C	5	3	0.10	0.05

Table 10. *Bedrock geologic units (Hintze and others, 2000), existing landslides (Harty, 1991), and site-response units of unconsolidated deposits (Ashland, 2001) within landslide-susceptibility geologic groups.*

Geologic Group	Map Symbol	Age	Description	Predominant Lithologies
A	Tpb	Pliocene	Volcanic rocks	Basalt
	Tmv	Miocene	Volcanic rocks	Quartz latite
	Tmr		Volcanic rocks	Rhyolite
	Ti	Tertiary	Intrusive rocks	Granodiorite, quartz monzonite
	Jg	Jurassic	Navajo and Nugget Sandstone	Sandstone
	PIP	Pennsylvanian-Permian	Oquirrh Group; Wells, Weber, and other formations	Sandstone, limestone
	IP	Pennsylvanian	Morgan, Round Valley, and other formations	Limestone
	M2	Mississippian	Great Blue, Humbug, Deseret, and other formations	Limestone, sandstone
	M1		Gardison, Lodgepole, and other formations	Limestone
	D	Devonian	Devonian Formations	Dolomite, sandstone
	S	Silurian	Laketown and Bluebell Dolomite	Dolomite
	O	Ordovician	Fish Haven, Swan Peak, Garden City, Eureka, and other formations	Limestone, quartzite
	-C3	Cambrian	St. Charles, Nounan, and other Upper Cambrian formations	Limestone, dolomite
	-C1		Prospect Mountain, Tintic, Geertsen Canyon, and other formations	Quartzite
	P-Cs	Proterozoic	Sedimentary and metasedimentary formations	Quartzite, argillite
	P-Cm	Precambrian	Metamorphic rocks	Gneiss, schist
B	Q03	Quaternary	Lacustrine and alluvial gravel	Sand, gravel
	Q04		Pre-Bonneville alluvial-fan deposits	Sand, gravel
	Q05		Glacial deposits (except Snow Basin and Wasatch County)	Gravel, sand
	QT	Miocene-Pleistocene	High-level alluvial deposits	Gravel, sand, conglomerate
	T3	Eocene-Oligocene	Duchesne River, Uinta, and other formations	Sandstone, conglomerate
	J1	Jurassic	Summerville, Entrada, Carmel, Arapien, Twin Creek, and other formations	Limestone, shale, sandstone
	TR2	Triassic	Ankareh Formation	Siltstone, shale, sandstone
	TR1		Dinwoody, Woodside, Thaynes, and other formations	Limestone, shale, sandstone
	P2	Permian	Gerster, Park City, and other formations	Limestone, shale
	P1		Diamond Creek, Arcturus, and other formations	Sandstone, shale
	-C2	Cambrian	Middle Cambrian formations	Limestone, shale

Table 10. *(continued).*

Geologic Group	Map Symbol	Age	Description	Predominant Lithologies
C	Q01	Quaternary	Lacustrine and alluvial silt and clay, with interbedded fine-grained sand	Silt, clay, sand
	Q02		Lacustrine sand, silt, and clay	Sand, silt, clay
	Q05		Glacial deposits (Snow Basin and Wasatch County)	Gravel, sand, clay
	Land-slides		Existing landslides	Gravel, sand, silt, clay
	Tov	Oligocene	Norwood and Keetley Volcanics	Tuff, tuffaceous sedimentary rocks
	T4	Oligocene-Pliocene	Salt Lake Formation and other valley-filling alluvial, lacustrine, and volcanic units	Tuffaceous sedimentary rocks
	T2	Eocene	Green River, Fowkes, and other formations	Shale, limestone, tuffaceous sedimentary rocks
	T1	Cretaceous-Eocene	Wasatch, Colton, Flagstaff, White Sage, and other formations	Conglomerate, siltstone
	TK	Cretaceous-Paleocene	Evanston, North Horn, Currant Creek, and other formations	Conglomerate, siltstone
	K3	Cretaceous	Mesaverde Group, Price River, Echo Canyon, and other formations	Sandstone, shale, conglomerate
	K2		Indianola, Mancos, Frontier, and other formations	Shale, sandstone
	K1		Dakota, Cedar Mountain, Kelvin, and other formations	Sandstone, siltstone, shale
	J2	Jurassic	Morrison Formation	Shale, sandstone
	M3	Mississippian	Chainman, Manning Canyon, Doughnut, and other formations	Shale, siltstone, limestone

Depending on foundation type, buildings generally cannot withstand more than 4 to 12 inches (10-30 cm) of ground displacement without severe damage (Youd, 1980). To be conservative, Wieczorek and others (1985) assumed that 2 inches (5 cm) or more of ground displacement was potentially hazardous to structures and human life and designated 2 inches (5 cm) of ground displacement as the "design threshold." They then used strong-motion records from earthquakes in California to calculate ground displacements for a variety of critical accelerations, and characterized landslide susceptibility by comparing calculated displacements with the design threshold. Ground displacements resulting from critical accelerations greater than 0.3 *g* were less than the design threshold, and geologic materials with such critical accelerations were considered to have a very low susceptibility. Ground displacements resulting from critical accelerations less than 0.1 *g* were greater than the design threshold, and geologic materials with such critical accelerations were considered to have a high susceptibility. Ground displacements resulting from critical accelerations from 0.1 to 0.3 *g* were less than the design threshold for some earthquakes and greater for others, depending upon earthquake intensity and ground motions, and geologic materials with such critical accelerations were considered to have either low or moderate susceptibilities.

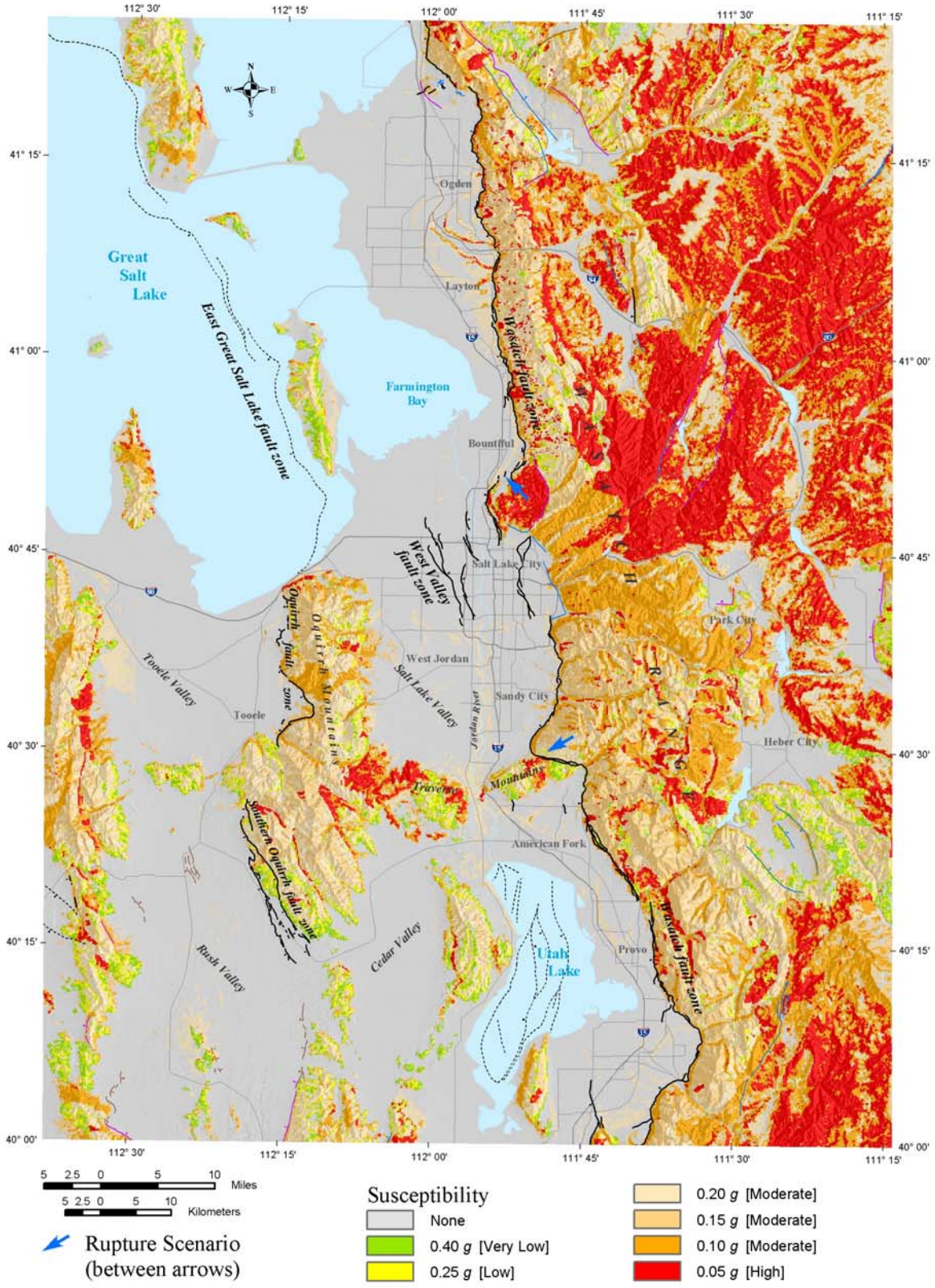

Figure 11. *Landslide susceptibility under wet conditions, as measured by critical accelerations. Saturation of all soil and rock is very unlikely and represents a worst-case condition. Saturation is most likely during spring snowmelt. See figure 3 for explanation of fault symbols (dotted where under water), modified from Black and others (2003).*

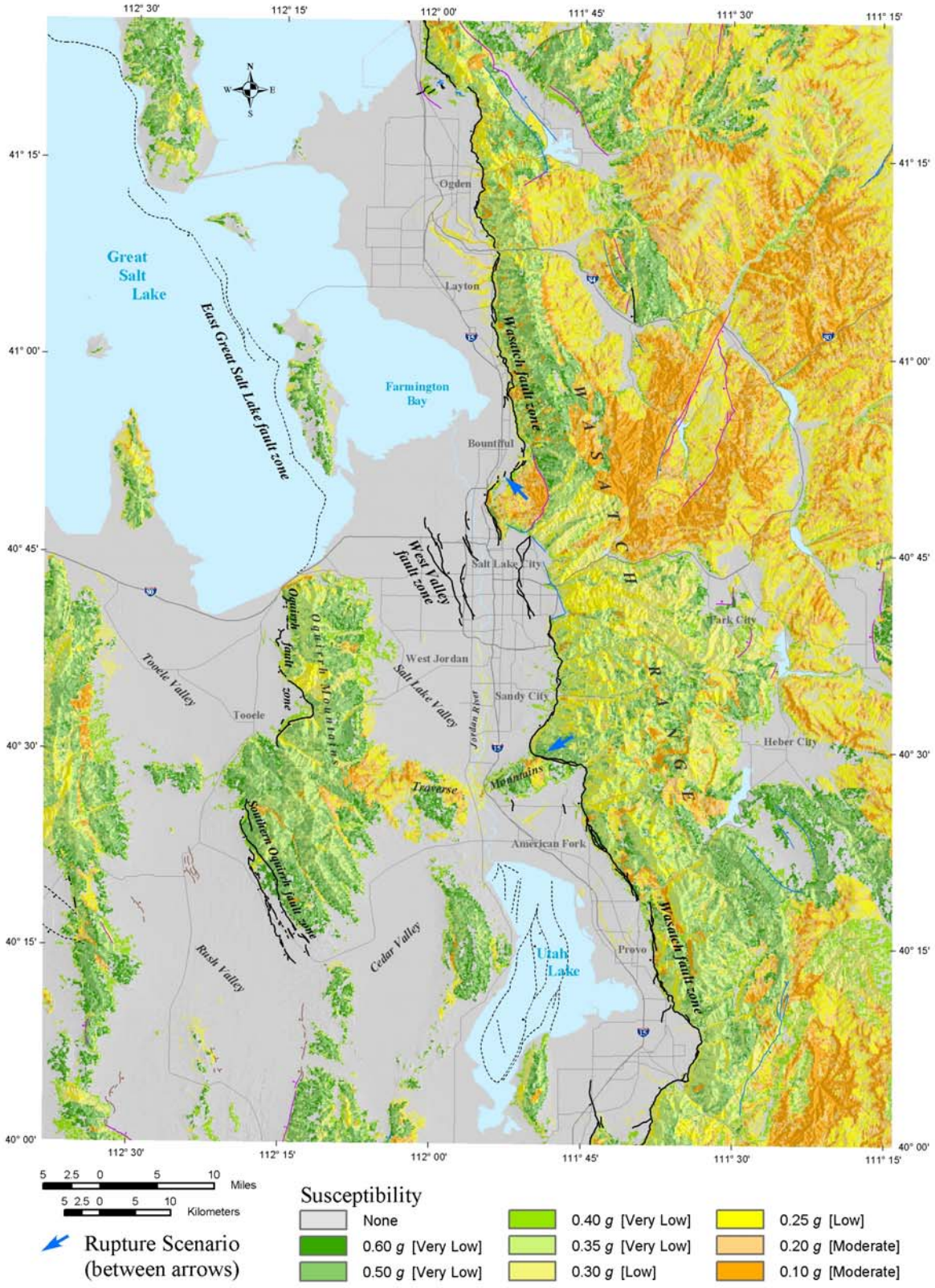

Figure 12. *Landslide susceptibility under dry conditions, as measured by critical accelerations. When soil and rock are dry, susceptibility decreases and represents a best-case condition. Actual susceptibility will likely be intermediate between that shown in figures 11 and 12. See figure 3 for explanation of fault symbols (dotted where under water), modified from Black and others (2003).*

We use the relationship of Wieczorek and others (1985) between ground displacement and critical acceleration to characterize relative landslide susceptibility within our study area (table 8). Geologic materials in landslide susceptibility categories I through IV, with critical accelerations greater than 0.3 *g*, have a very low susceptibility. Geologic materials in landslide susceptibility category X, with a critical acceleration less than 0.1 *g*, have a high susceptibility. Geologic materials in landslide susceptibility categories V through IX, with critical accelerations from 0.1 to 0.3 *g*, have either a low (categories V and VI) or moderate susceptibility (categories VII through IX).

The most extensive areas of high landslide susceptibility when geologic materials are wet (figure 11) lie in the Wasatch Range east of Ogden, underlain predominantly by low-strength conglomerate in the Wasatch Formation of Cretaceous to Eocene age, and east of Utah Valley, underlain predominantly by the conglomeratic North Horn Formation of Cretaceous to Paleocene age and the shale-rich Green River Formation of Eocene age. These areas are predominantly rural, but smaller areas of highly susceptible deposits are present near urban areas, notably the salient north of Salt Lake City, underlain by Tertiary conglomerate and tuffaceous rocks. When dry, susceptibility decreases to moderate in these areas, and highly susceptible rocks are absent (figure 12). Most rocks along the Wasatch Range front near urban areas, as well as soil along the steep banks of the Jordan River in Salt Lake Valley, are moderately susceptible when wet and have only a very low to low susceptibility when dry.

Permanent Ground Displacement

HAZUS calculates the amount of permanent ground displacement due to landsliding using the approach originally developed by Newmark (1965), who calculated the cumulative permanent displacement of a sliding block as it is subjected to the effects of an earthquake acceleration time history. Downslope deformations occur during the time periods when the induced PGA within the slide mass exceeds the critical acceleration. The amount of downslope movement also depends on the duration or number of cycles of ground shaking. The HAZUS relationship calculates permanent ground displacements from an expected displacement factor, the PGA, and the number of cycles of ground shaking. The expected displacement factor, calculated as a function of the ratio of critical acceleration to induced acceleration, is derived from the results of Makdisi and Seed (1978). The number of cycles of ground shaking is related to earthquake magnitude by Seed and Idriss (1982).

We did not use the HAZUS technique, but rather used a more recent approach to predict permanent ground displacement from earthquake-induced landsliding using modified Newmark methods suggested by Jibson (1993), who established an empirical relationship between Arias intensity (a comprehensive and quantitative measure of total shaking intensity developed by Arias [1970]) and Newmark displacement. We calculate Newmark displacements using the empirical equation of Jibson and others (2000), a modification of the equation presented by Jibson (1993). The equation of Jibson and others (2000) is:

Eq.1 $\quad \log D_n = 1.521 \log I_a - 1.993 \log a_c - 1.546$

where:

D_n = Newmark displacement in centimeters.

I_a = Arias intensity, in meters per second.

a_c = critical acceleration, in *g*.

Equation 1 requires values for Arias intensity and critical acceleration. HAZUS provides values for critical acceleration for each susceptibility category (table 8). Jibson (1993) presents two additional equations that we combine to calculate Arias intensity. The first equation, developed by R.C. Wilson (U.S. Geological Survey) using strong-motion records, is a function of the duration of strong ground shaking and PGA:

Eq. 2 $I_a = 0.9Ta^2$

where:

T = Dobry duration (the time required to build up 90 percent of the Arias intensity), in seconds.

a = PGA, in *g*.

The second equation, developed by Dobry and others (1978), allows us to calculate the duration of strong ground shaking from its relationship to earthquake magnitude:

Eq. 3 $\text{Log } T = 0.432M - 1.83$

where:

M = earthquake magnitude (type unspecified, but we use moment magnitude).

Combining the two equations creates a third relationship that permits us to calculate Arias intensity from PGA (plate 1, simplified on figure 4) and **M**:

Eq. 4 $I_a = 0.9(10^{0.432\mathbf{M}-1.83})a^2$

For our **M** 7 scenario earthquake, equation 4 simplifies to:

Eq. 5 $I_a = 14.1a^2$

We solved equation 5 for I_a using PGA values from plate 1 (simplified on figure 4) and then solved Equation 1 using these values of I_a and values for a_c from table 8. The amount of permanent ground displacement caused by landsliding from the scenario earthquake is mapped for both wet (plate 4, simplified on figure 13) and dry (plate 5, simplified on figure 14) conditions. Because Jibson and others (2000) calibrated equation 1 by analyzing predominantly shallow and disrupted landslides (such as rock falls and debris slides), mapped displacements are most appropriate for estimating the hazard posed by these landslide types. However, they are the

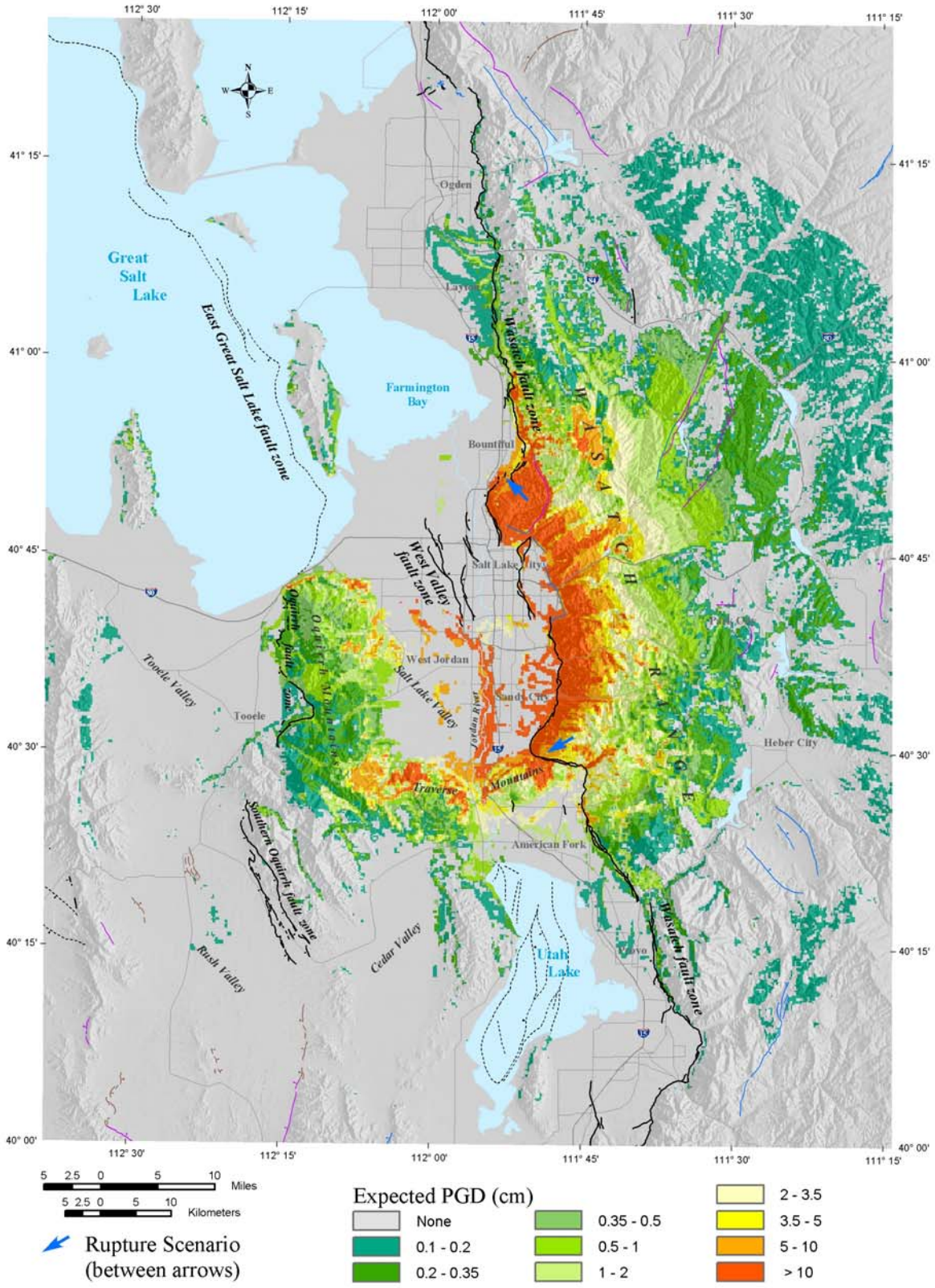

Figure 13. *Permanent ground displacement (PGD) caused by landsliding under wet conditions. Simplified from plate 4. See figure 3 for explanation of fault symbols (dotted where under water), modified from Black and others (2003).*

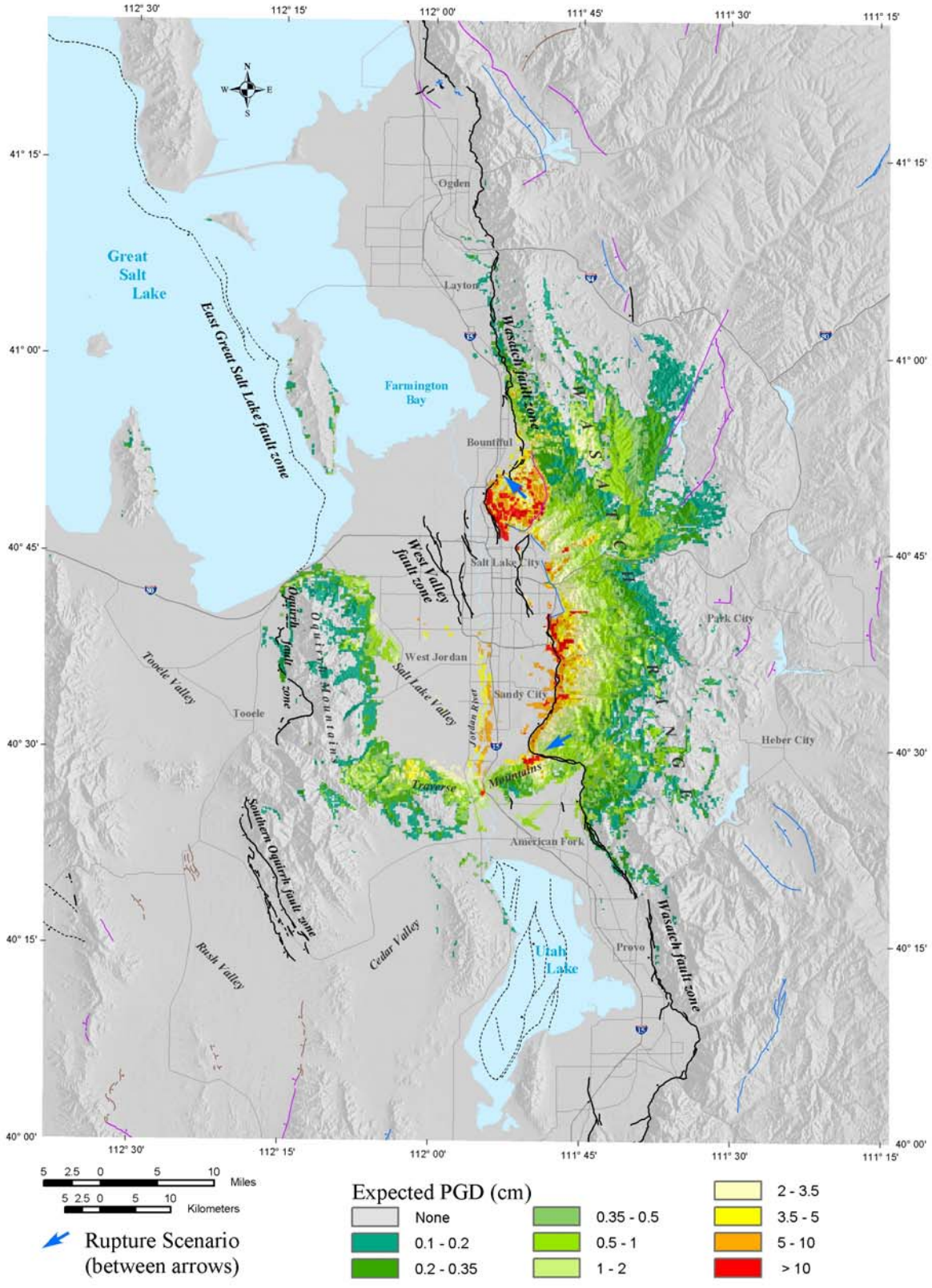

Figure 14. *Permanent ground displacement (PGD) caused by landsliding under dry conditions. Simplified from plate 5. See figure 3 for explanation of fault symbols (dotted where under water), modified from Black and others (2003).*

most abundant landslides in the historical earthquakes studied by Keefer (1984), and will likely be most common in our scenario.

Wilson and Keefer (1985) estimate that damage to structures is likely when permanent ground displacement from landsliding exceeds 4 inches (10 cm). Slope movement of this size may occur along Wasatch Range front bedrock spurs on the east side of Salt Lake Valley and the north slope of the Traverse Mountains on the south side of Salt Lake Valley in our scenario earthquake if slopes are wet (plate 4, simplified on figure 13). Similar movement in soil could be expected on steep banks of the Jordan River in southern Salt Lake Valley and in small areas of steeper slopes on the east bench near Sandy underlain by Lake Bonneville shoreline deposits. However, under dry conditions, bedrock displacements greater than 2 inches (5 cm) are unlikely, as are slope movements greater than 4 inches (10 cm) near the Jordan River (plate 5, simplified on figure 14). Although slope movement of at least 0.1 inch (0.2 cm), the threshold of significant slope movement estimated by Wilson and Keefer (1985), may occur as much as 30 miles (50 km) from the Salt Lake City segment under wet conditions, this distance decreases to 15 miles (25 km) under dry conditions. Small but significant displacements may also occur in the Oquirrh and Traverse Mountains when wet, but are limited to the foothills of the Oquirrh Mountains, underlain by unconsolidated to semiconsolidated Pleistocene alluvial-fan deposits, when dry.

Probability

Wieczorek and others (1985) point out that the relationships developed by Wilson and Keefer (1985) (table 7) are conservative, representing the most landslide-susceptible geologic types likely to be found in the geologic group. Thus, in using these relationships, further consideration must be given to evaluating the probability of slope failure. Jibson and others (2000) estimate the probability of slope failure by comparing predicted Newmark displacements with an inventory of landslides triggered by the Northridge earthquake. They found that the proportion of landslide-source areas increases with increasing displacement, with the proportion increasing rapidly in the first few centimeters of displacement and leveling off abruptly when displacement reaches from 4 to 6 inches (10-15 cm). This relationship is a direct estimate of the probability that any location will be occupied by a landslide source.

Jibson and others (2000) expressed the relationship mathematically by fitting their data to a curve originally developed by Weibull (1939) to model the failure of rock samples. After calibrating the curve and its corresponding equation to Northridge earthquake data by determining area-specific regression constants, Jibson and others (2000) used the equation to predict the probability of slope failure as a function of Newmark displacement. The calibrated equation is:

Eq. 6 $P(f) = 0.335[1-\exp(-0.048\ D_n^{1.565})]$

where:

$P(f)$ = the proportion of grid cells occupied by landslide-source areas.

D_n = Newmark displacement in centimeters.

We use equation 6 to map the probability of slope failure resulting from our scenario earthquake as a function of Newmark displacement under both wet and dry conditions (figures 15 and 16, respectively). However, because the formula was calibrated using data from southern California, applying it to northern Utah increases the uncertainty due to differences in climate, rock type, vegetation, and topography. Recalibration for local use is desirable, but detailed data required for recalibration are lacking.

Because probability is a function of displacement, the mapped patterns of landslide probability and displacement are similar. Where expected displacements are greater than 4 inches (10 cm), the probability of landsliding is commonly greater than 20 percent, under both wet and dry conditions. Probability rapidly decreases with increasing distance from the trace of the Salt Lake City segment and is generally less than 1 percent farther than 10 to 15 miles (15-25 km) under wet conditions (figure 15) and 5 miles (8 km) under dry conditions (figure 16). Although the probability of landsliding is significant on the north slope of the Traverse Mountains on the southern edge of Salt Lake Valley under wet conditions, the probability of landsliding is small in that area under dry conditions and in the Oquirrh Mountains on the west side of Salt Lake Valley whether wet or dry.

Summary

During our scenario earthquake, the landslide hazard will be greatest on saturated bedrock spurs of the Wasatch Range adjacent to densely populated areas on the east side of Salt Lake Valley. These slopes are underlain by varied lithologies of differing shear strengths, but ground shaking is so strong (PGA >0.4 *g*) that failure of even moderately susceptible rock slopes may result in large ground displacements. In these areas, buildings and other structures may suffer significant damage, and the potential for catastrophic slope failure increases as displacements increase. However, bedrock displacement greater than 8 inches (20 cm) is only likely when the ground is wet, a condition that is widespread during spring snowmelt and long-duration area-wide rainstorms. Under dry conditions, the landslide hazard is greatest in scattered areas of the east bench underlain by soil rather than rock. Actual slope failures will be affected by unmapped factors, including the orientation and frequency of rock discontinuities such as fractures, joints, and bedding planes. Unlike the probability of liquefaction, which spans a wide range of values in areas subject to relatively large displacements, the probability of landsliding is greatest in areas subject to the largest displacements and decreases as the amount of displacement decreases.

Our scenario earthquake may also trigger landslides into lakes and reservoirs that produce large waves. The height of waves generated by this mechanism, and therefore the extent of inundation, is governed largely by the volume of water displaced by the landslide. Landslide-source areas mapped near lake and reservoir shores indicate a potential for nearby inundation from landslide-induced water waves, but we have not mapped the extent of inundation because the volume of displaced water is difficult to predict. For our scenario, most intermontane lakes and reservoirs are in areas where expected permanent ground displacements are small and slope failures have a low probability of occurrence, although some lake and reservoir shores may be subject to inundation from landslide-induced water waves. Large, high-probability slope failures are not expected near Great Salt Lake and Utah Lake from our scenario earthquake, so we do not

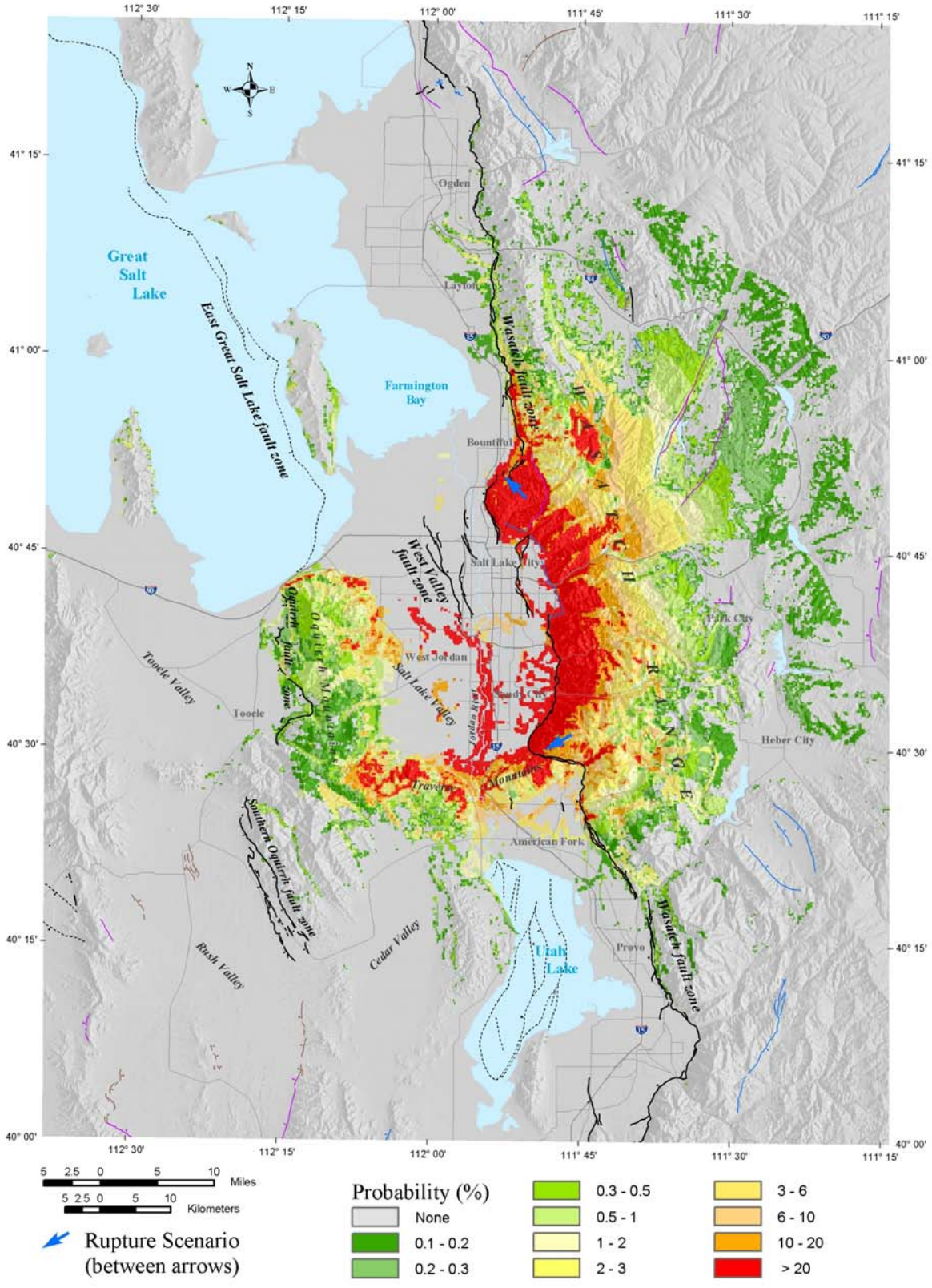

Figure 15. *Landslide probability under wet conditions. See figure 3 for explanation of fault symbols (dotted where under water), modified from Black and others (2003).*

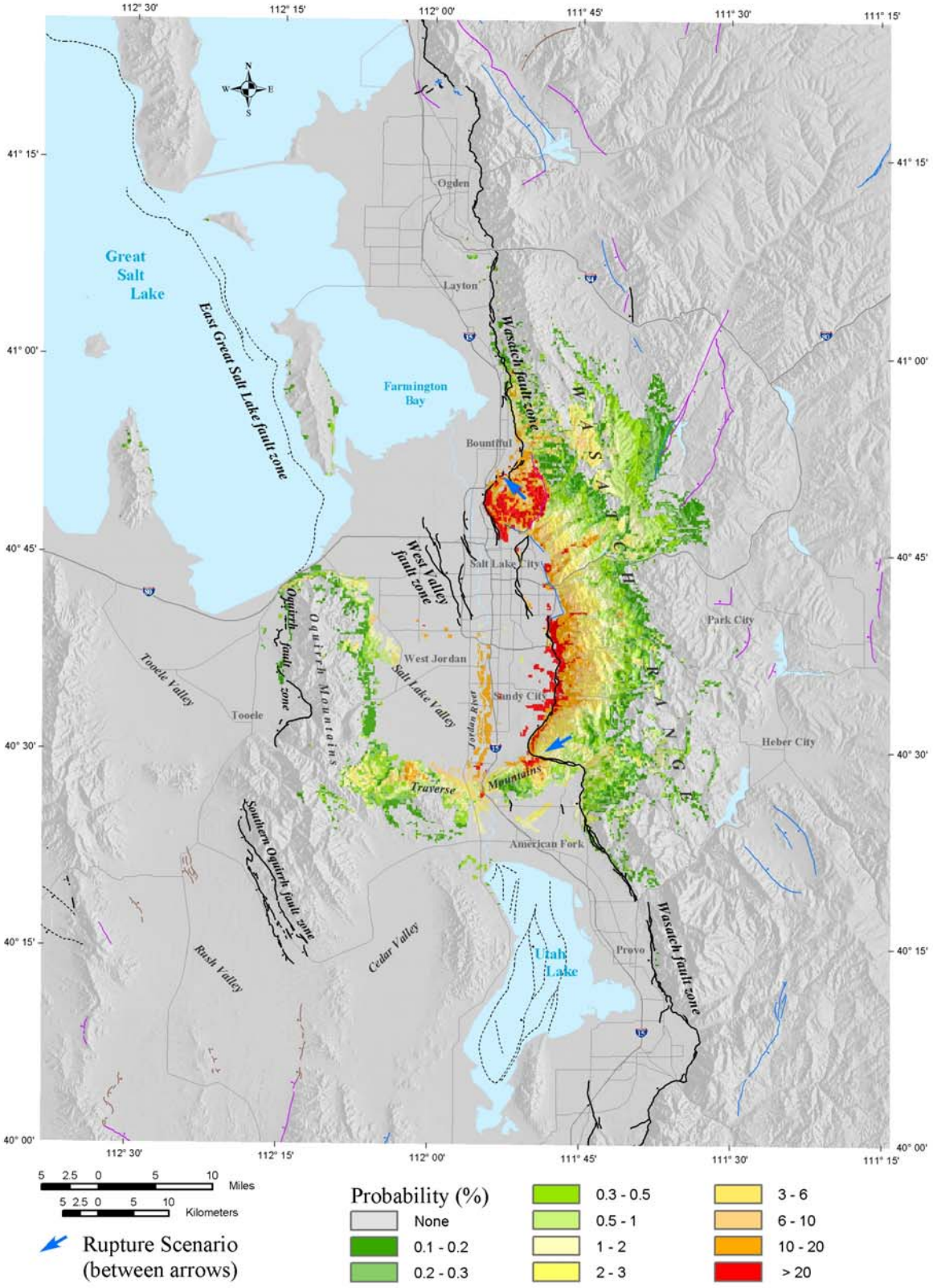

Figure 16. *Landslide probability under dry conditions. When soil and rock are dry they are less susceptible to landsliding than when wet and therefore less likely to fail. See figure 3 for explanation of fault symbols (dotted where under water), modified from Black and others (2003).*

consider their shores to be at significant risk from landslide-induced water waves generated by our scenario earthquake.

Tectonic Subsidence

The floor of Salt Lake Valley will drop and tilt toward the Wasatch fault zone on the downdropped side of the surface fault rupture during our scenario earthquake. As a result, areas along the shore of Great Salt Lake will permanently subside, causing local flooding. Other potential consequences include ponding of shallow ground water that may flood basements and buried facilities, and tilting of the ground surface that may compromise the performance of gravity-flow structures such as wastewater-treatment plants and sewer lines.

Ground-Deformation Modeling

Smith and Richins (1984) first modeled potential ground deformation along the Wasatch Front associated with tectonic subsidence by subtracting observed crustal deformation of the 1959 **M** 7.3 Hebgen Lake, Montana earthquake (Myers and Hamilton, 1964) from ground elevations in the Great Salt Lake and Utah Lake areas. Keaton (1986) applied the profile of maximum subsidence observed from that earthquake to each segment of the Wasatch fault zone. The profile shows subsidence extending 10 miles (16 km) from the fault, with maximum subsidence of 20 feet (6.1 m) occurring 1 mile (1.6 km) from the fault. However, Keaton (1986) concluded that the Hebgen Lake model represented a worst-case scenario for the Wasatch fault zone because displacement caused by surface faulting associated with the Hebgen Lake earthquake (about 20 feet [6.1 m]) was much larger than typical displacements (about 7 feet [2 m]) along the Wasatch fault zone. Keaton (1986) subsequently modeled potential ground deformation along the Salt Lake City segment of the Wasatch fault zone with an elastic dislocation model developed by Okada (1985). This model is a function of fault-plane dimensions and amount and direction of slip, which Keaton (1986) estimated using source parameters appropriate for a characteristic Wasatch fault earthquake of **M** 7.1. This model shows that about 6.9 feet (2.1 m) of maximum fault displacement results in maximum subsidence of about 4.9 feet (1.5 m). Keaton (1986) assumes a fault-rupture length for the Salt Lake City segment of 20 miles (32 km) and a dip of 60 degrees.

Chang and Smith (1998a) conducted a detailed assessment of potential ground deformation along the Wasatch Front associated with tectonic subsidence by developing high-resolution digital topographic data from orthophoto maps to improve the resolution and accuracy of earlier studies. They used boundary-element methods, which they describe as more flexible and refined than earlier analytical techniques, as well as Hebgen Lake data to model ground deformation under various scenarios. One of their scenarios is similar to ours, with a surface-wave magnitude of 7 (essentially equivalent to **M** 7; Kanamori, 1983), a rupture plane 28 miles (45 km) long dipping 45 degrees to the west, and about 6.5 feet (2 m) of maximum fault displacement. We assume a rupture plane with a length of 28.6 miles (46 km), dipping 55 degrees, and a maximum displacement of 6.1 feet (1.9 m).

We use the results of Chang and Smith (1998a) to map the amount of tectonic subsidence and resulting inundation along the Great Salt Lake shore (plate 6, simplified on figure 17), which

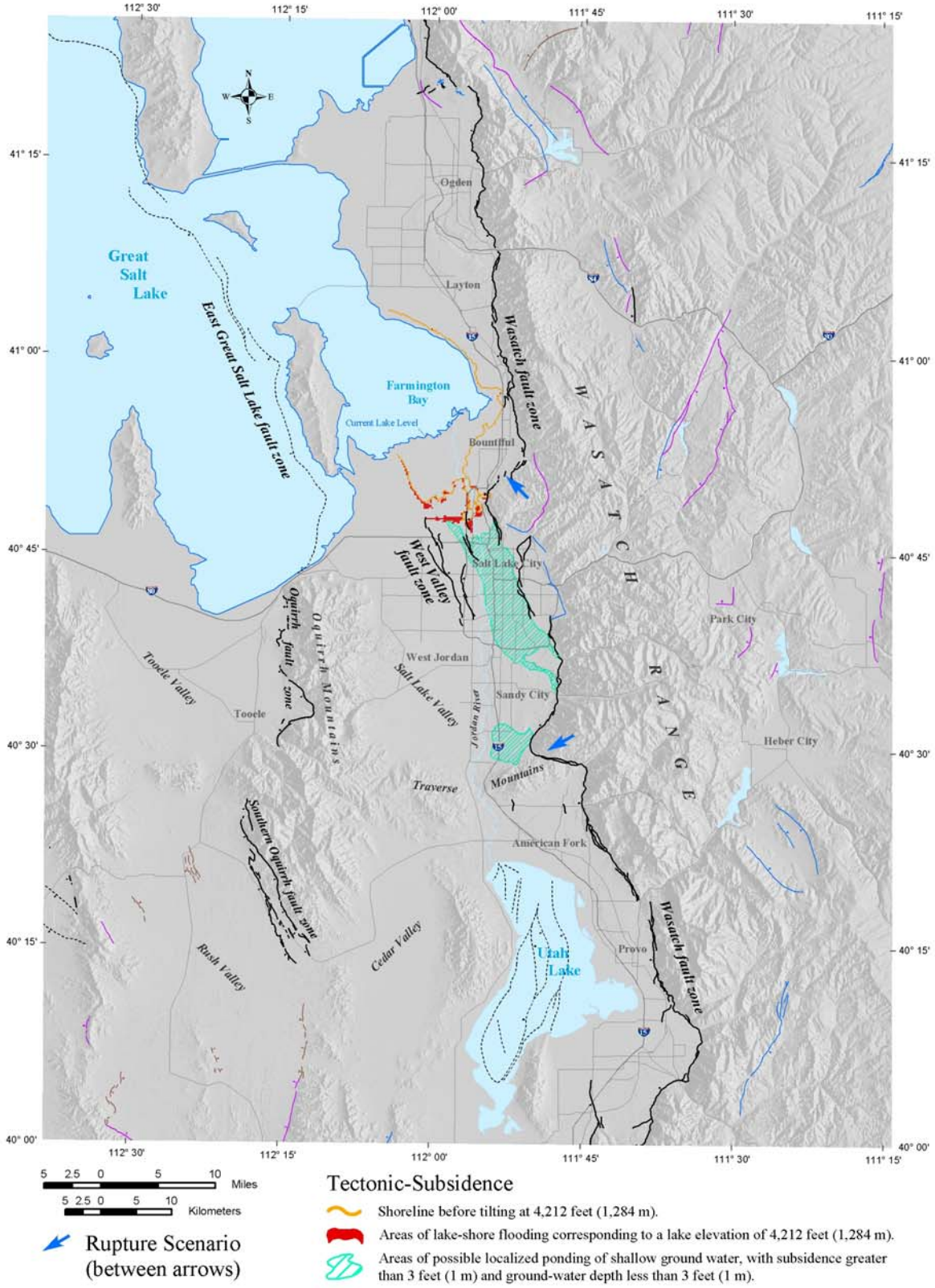

Figure 17. *Tectonic subsidence hazards (modified from Keaton, 1986, and Chang and Smith, 1998a). Simplified from plate 6. See figure 3 for explanation of fault symbols (dotted where under water), modified from Black and others (2003).*

depend in part on the fault dip. Because our study assumes a steeper dip than the modeled scenario of Chang and Smith (1998a), a model based on our dip would result in a larger amount of tectonic subsidence. This difference would be on the order of only a few centimeters, greatest nearer the fault and likely negligible near Great Salt Lake. Because slopes along the Great Salt Lake shore are gentle, small changes in lake levels result in significant changes in areas of inundation. Chang and Smith (1998a) consider changing lake levels by mapping the extent of inundation due to tectonic subsidence assuming Great Salt Lake shoreline elevations of 4,212 feet (1,284 m) (the maximum historical lake elevation reached in 1986), 4,200 feet (1,280 m) (the long-term average lake elevation), and 4,191 feet (1,278 m) (the minimum historical lake elevation reached in 1965) (Arnow and Stephens, 1990).

We use the results of Keaton (1986) to map the extent of possible inundation from ponding of shallow ground water. The extent of inundation from ponding reflects areas where ground-water depth may be less than 3 feet (1 m) and tectonic subsidence may be greater than 3 feet (1 m). Although the earthquake parameters used by Keaton (1986) are slightly different from ours, at the map scale we do not expect his mapped inundation extent to significantly differ from the extent of inundation resulting from our scenario earthquake.

Summary

Ground deformation associated with tectonic subsidence, modeled by Chang and Smith (1998a), causes no significant flooding along the shore of Great Salt Lake when lake levels are at or below the long-term average lake elevation of 4,200 feet (1,280 m). However, as the lake rises above this level, lake waters will increasingly inundate the Jordan River flood plain upstream from where the river enters Farmington Bay (plate 6, simplified on figure 17). At the maximum historical lake elevation of 4,212 feet (1,284 m), water could flood approximately 3 miles (4.8 km) southward along the flood plain, 2 miles (3.2 km) westward through a shallow depression south of the lake shore, and one mile (1.6 km) eastward to the subsidence trough along the Wasatch Range front (Chang and Smith, 1998a). Although flood-control dikes protect much of the area, the permanent change in the position of the lake shore may result in unequal water levels on opposite sides of the dikes. Long-term equilibration of water levels across the dikes would result in ground-water underflow beneath them or infiltration through them. Should this occur, or should the dikes fail, flood-plain inundation may affect oil refineries, a sewage disposal facility, and a significant amount of residential and commercial development in rapidly growing areas northwest of Salt Lake City, and may disrupt major transportation routes through the valley. To the west, floodwaters would reach the northern part of Salt Lake City International Airport, and to the east floodwaters would approach Interstate Highway 15, the principal north-south transportation route through Utah. Although such an event could have devastating effects, it would be less likely to occur than other hazards modeled in this study. The probability of a large earthquake occurring simultaneously with a historic lake highstand would be much smaller than the chances of each event occurring independently.

Areas of potential ponding of shallow ground water, mapped by Keaton (1986), may occur in the subsidence trough west of the Wasatch fault during periods of shallow ground water. The trough lies on the east side of the valley along the Wasatch Range front in a zone about 4 miles (6.4 km) wide (plate 6, simplified on figure 17). This zone includes the most densely

populated areas of Salt Lake Valley, including much of downtown Salt Lake City. However, most areas along the range front will not be subject to this hazard because of relatively deep ground water. These areas include the east margin of the valley (locally referred to as the east bench), the footwall of the active East Bench fault (which would not subside), and eastern Sandy and vicinity (overlying well-drained Lake Bonneville deltaic deposits).

Earthquake-Induced Flooding from Dam Failure

HAZUS includes information on 247 dams within our study area from a database developed from the National Inventory of Dams (FEMA, 1993). The failure of any of the high-hazard dams could pose a threat to human life and property. However, the U.S. Bureau of Reclamation, U.S. Army Corps of Engineers, and Utah Division of Water Rights have dam-safety programs to evaluate the expected performance of large, high-hazard dams during earthquakes. If these dams were not initially designed and constructed to withstand large earthquakes, the programs require modification of the dams to provide better performance. Some of the modifications are complete, and the rest are expected to be complete in the next few years. Once the dams are modified, officials believe all large, high-hazard dams in our study area will provide satisfactory performance with no uncontrolled releases during an earthquake similar to our scenario earthquake (Dan Grundvig, U.S. Bureau of Reclamation, written communication, 2001; Rick Hall, Utah Division of Water Rights, Office of Dam Safety, verbal communication, 2001). Smaller high-hazard dams, including debris basins and flood-control structures, are not subject to seismic criteria but are generally dry and unlikely to contain significant amounts of water during large earthquakes. Thus, our scenario does not include an evaluation of earthquake-induced dam-failure flooding.

Seiches

Seiches are oscillations of enclosed bodies of water. The term was first used in Switzerland by Forel (1895) to apply to standing waves set up on the surface of Lake Geneva by wind and by changes in barometric pressure. However, seiches often occur following an earthquake. Reid (1914) reported that earthquake seiches were first noticed at the time of the 1755 Lisbon, Portugal earthquake when seiching motions were noted in small bodies of water throughout Europe as far away as Finland. To restrict the term "seiches" to those events caused by earthquakes, Kvale (1955) qualified the phenomenon as "seismic seiches." Although strong ground shaking most commonly causes seismic seiches, more dramatic seiching motion may be produced by a permanent vertical ground displacement, such as may be caused by surface faulting or tectonic subsidence, beneath a water body. Myers and Hamilton (1964) documented large-amplitude waves generated during the 1959 **M** 7.3 Hebgen Lake, Montana earthquake resulting from subsidence of the lake floor and called these waves "surges" to differentiate them from much milder but otherwise similar oscillations of closed water bodies caused by ground shaking.

Recent Estimates of the Potential for Seiches in Great Salt Lake

Recent interest in possible seiches in Great Salt Lake results from the potential for lakeshore flooding associated with historically high lake levels in the 1980s. Pechmann (1987)

first discussed possible seiches in this context in an analysis of earthquake-design considerations for the inter-island diking project, which was incorporated into the final design report for the project prepared for the Utah Division of Water Resources (Rollins, Brown, and Gunnell, Inc., and Creamer & Noble Engineers, 1987). Pechmann (1987) specifically discussed the potential for surges. He noted surges described by Myers and Hamilton (1964) over 10 feet (3 m) high resulting from non-uniform subsidence of the Hebgen Lake floor following the 1959 Hebgen Lake earthquake and described accounts of waves generated in Great Salt Lake by the 1909 M 6+ Hansel Valley, Utah earthquake. Although felt reports placed the location of the 1909 earthquake about 9 miles (15 km) northeast of the north lake shore, the accounts of waves generated by this event suggested to Pechmann that the earthquake might actually have occurred beneath the lake and caused displacement of the lake bottom, generating a surge. The 1934 **M** 6.6 Hansel Valley earthquake apparently did not generate similar lake waves, consistent with instrumental location of the earthquake epicenter and with surface faulting located just northeast of the north lake shore.

Lowe (1993) refined the analysis of Pechmann (1987) by estimating the size of the wave generated by the 1909 Hansel Valley earthquake, using elevations of Great Salt Lake and the Lucin Cutoff railroad trestle, which was overtopped by the wave. Assuming accurate reports of the lake and trestle elevations, Lowe (1993) estimated a wave height of more than 12 feet (3.7 m). However, Lowe did not differentiate the mechanism of wave generation, stating that all earthquake-generated water waves (whether from ground shaking, surface fault rupture, or earthquake-induced landslides) are classified as seiches. Thereafter, earthquake-induced lakeshore flooding by waves is generally attributed to seiches in Utah Geological Survey (UGS) publications (see, for example, Black and others, 1999) without specifying the mechanism of wave generation, and the hazard along the Great Salt Lake shore was estimated using the wave height calculated by Lowe (1993). In most assessments of hazard potential around the shore of Great Salt Lake, the mechanism of wave-induced flooding is irrelevant; Lowe's estimate is a reasonable approximation of the hazard potential that may be generated by differential subsidence of the lake floor associated with one of several active faults underlying the lake. However, when describing the consequences of an earthquake with a specified magnitude and location (a scenario earthquake), the mechanism is important and depends upon the relative locations of the lake, earthquake epicenter, and surface fault rupture.

The Potential for Seiches Resulting from the Scenario Earthquake

Great Salt Lake: Seiches with significant amplitude may be generated in a lake when the period of earthquake ground motion is close to the natural period of the lake (Houston, 1979). The natural period of a lake depends on water depth, shape, size, and bottom topography. The system of waves related to this period includes an infinite number of wave species, called the normal modes, and a fundamental mode referring to the wave having the longest wavelength. Theoretically, the fundamental mode is easier to excite and more difficult to damp, and normal modes having successively shorter wavelengths are increasingly difficult to excite. Lin and Wang (1978) determined that the three major modes of the south basin of Great Salt Lake (the part of the lake nearest the Salt Lake City segment of the Wasatch fault zone) have periods of 6.33 (the fundamental mode), 3.13, and 1.79 hours. Thus, earthquake ground motions should have periods close to these values in order to generate significant seiches.

Seismic energy to stimulate seiches is carried in surface waves rather than body waves because periods of body waves are too short to generate sufficient energy to stimulate seiche modes (McGarr, 1965). Earthquake motions from fundamental-mode surface waves will be strongest at periods in the range of about 15 to 25 seconds. Because the period of strong earthquake ground motions (15 to 25 s) is not close to the natural period of the south basin of Great Salt Lake (6.33 hr), seiches generated by ground shaking during a strong earthquake will not be significant. A quantitative estimate of peak wave height is less than one centimeter, calculated using equation 7 (National Institute of Building Sciences, 1999, equation 9-1):

Eq. 7 $H = \sqrt{A/(L(\pi f)^2)}$

where:

H = peak wave height (cm).

A = PGA (*g*).

f = frequency of the lake.

L = wavelength = $5.12/f^2$.

Resonance due to local nearshore topographic configuration (shallow areas or where the water is constricted) may amplify the seiche motion. The degree of amplification depends on the detailed time history of the ground motions and the response characteristics of the lake, but even with amplification factors of up to 20 times, similar to those observed during the 1964 Alaska earthquake in Kenai Lake (Donn, 1964; McCulloch, 1966), seiches due to ground shaking appear to be a negligible hazard in Great Salt Lake. However, our hazard assessment is preliminary, and more detailed studies are needed to fully understand the scope and role of seiches due to ground shaking in alternative scenarios.

The magnitude of a surge is governed by the amount of lake-floor subsidence rather than lake and earthquake-ground-motion frequency. Although the relationship between surge height and lake-floor subsidence is unclear, an estimate of surge height generated by a scenario earthquake can be obtained by applying data from a study of the 1959 Hebgen Lake earthquake. Myers and Hamilton (1964) report that the first (and highest) surge of water from that earthquake rose 10 feet (3 m) above the post-earthquake static water level at Hebgen Dam (the deepest part of Hebgen Lake), and the height of the highest surge decreased away from the dam (as water depth decreased). Subsequent surges, decreasing in height, continued for about 12 hours at about 15-minute intervals. The timing of the surges was governed by the period of the lake, with the interval between surges about equal to the first harmonic of the fundamental period (Wiegel and Camotim, 1962). Maximum subsidence in the West Yellowstone basin was about 22 feet (7.7 m), but the lake floor near the dam subsided only half as much (about 10 feet [3 m]) as the deepest part of the subsidence trough. Therefore, the ratio of surge height to subsidence at the location of maximum surge height (Hebgen Dam) is about 1.0, and the ratio of surge height to maximum subsidence is about 0.5.

To estimate the surge height resulting from our scenario earthquake, we assume that maximum surge height will occur where the floor of Great Salt Lake subsides the most and surge height will be approximately equal to the amount of subsidence (a ratio of 1.0). Chang and Smith (1998a) estimate 6.5 feet (2 m) of displacement for an **M** 7 earthquake along the Salt Lake City segment of the Wasatch fault zone (plate 6, simplified on figure 17). Because most movement on normal faults results in subsidence of the hanging wall, maximum subsidence from this scenario would be 6.5 feet (2 m) near the fault, decreasing to 0 within 6 miles (10 km). Should maximum subsidence occur beneath Great Salt Lake, we would estimate a potential surge height of 6.5 feet (2 m). However, because our scenario only postulates rupture along the Salt Lake City segment and the lakeshore is no closer than about 8 miles (13 km) to the fault at its northern end, subsidence beneath the lake and concurrent surge will be negligible. The potential for surge is greater from a strong earthquake along the Weber segment of the Wasatch fault zone, where Farmington Bay is close to the fault, and from displacement of faults beneath the lake, such as the East Great Salt Lake fault zone. In the case of a strong earthquake along the Weber segment, the problem of shoreline flooding will be compounded because shoreline elevations will subside at the same time a surge is generated.

Other Lakes: Our previous discussion applies only to the potential for seismically generated seiches and surges in Great Salt Lake. However, because the potential for seiches is related to the lake period, any lake with a fundamental mode (or low-order normal modes) substantially larger than the fundamental mode of surface waves (with periods in the range of about 15 to 25 seconds) will not have a significant potential for a large seiche. For example, we estimate that the periods of major modes for Utah Lake are about 3.6 hours (the fundamental mode), 1.8 hours, and 1.2 hours, calculated using Merian's equation (Ruttner, 1953), which is a function of basin length, number of modes, gravitational acceleration, and water depth:

Eq. 8 $T_n = 2l_b/\sqrt{gd}$

where:

T_n = period in seconds.

l_b = length of the basin.

n = number of modes.

g = gravitational acceleration.

d = depth of water.

These periods are not conducive to generating a seiche, but as length decreases and depth increases Merian's equation yields shorter periods. Merian's equation, though, is based on the assumption of uniform and constant basin cross section. Jeffreys (as quoted by Hutchinson [1957, p. 307-308]) emphasizes that long, narrow lakes, especially those with cuspate ends, have periods markedly shorter than indicated by the simple Merian formula. Therefore, the seismic-seiche hazard may be greater in lakes and reservoirs within Utah mountains, and the hazard may

be amplified by shoreline topography. These water bodies are typically smaller and deeper than Utah Lake and Great Salt Lake, and are commonly long and narrow with complex shorelines.

SUMMARY AND CONCLUSIONS

We mapped geologic hazards for a scenario earthquake of **M** 7 in the central Wasatch Front, Utah. In our scenario, this populous urban corridor is subjected to earthquake ground shaking stronger than experienced in historical times but characteristic of large prehistoric earthquakes that have repeatedly occurred in the region. The earthquake occurs on the Salt Lake City segment of the Wasatch fault zone, one of the longest and most active normal faults in the world.

Severe ground shaking occurs in our scenario, with maximum PGA possibly exceeding 1 *g*. Potentially damaging ground motions (> 0.1 *g*) occur over a wide area including major valleys west of the fault and back valleys in the Wasatch Range. The hazard maps dramatically show the frequency-dependent amplification of unconsolidated sediments along the Wasatch Front. The pattern of both amplification and deamplification in the map area is clearly a function of the distribution and thickness of the surficial geologic units. High-frequency site amplification is particularly significant along the foothills at the base of the Wasatch Range. Strong low-frequency ground motions extend farther into the middle of Salt Lake Valley where thick alluvial deposits amplify long-period ground motions. Hanging-wall effects are also evident on the ground-shaking maps.

The strong ground shaking initiates liquefaction and landsliding in our scenario that may impact urban areas and result in significant loss of life and property. Much of Salt Lake Valley has a potential for large liquefaction-induced lateral-spread displacements that may exceed 1 foot (30 cm), but such displacements are most likely in the northern part of the valley. Liquefaction-induced settlement will probably be greatest in the same area, possibly exceeding 8 inches (20 cm). Landsliding will likely be most severe on Wasatch Range front mountain spurs adjacent to Salt Lake Valley, threatening downslope development in areas such as the east bench. The greater extent of landsliding under wet conditions, as opposed to dry conditions, indicates a springtime earthquake during the snowmelt would be much more damaging than one during a drier time of the year. Although seiches are not a significant threat to shoreline areas near Great Salt Lake, they may be important in intermontane lakes and reservoirs, though we did not evaluate this hazard.

Our scenario earthquake is also accompanied by surface fault rupture with a median maximum displacement of about 6.1 feet (1.9 m), resulting in tilting of the Salt Lake Valley floor and subsidence near the fault. Subsidence may cause ponding of shallow ground water in the subsidence trough and, if the level of Great Salt Lake is near its historical maximum, inundation of developed areas near the lake shore and northern Jordan River flood plain as the shoreline migrates towards the fault and up the Jordan River. Tilting may also compromise the performance of gravity-flow structures such as wastewater-treatment plants and sewer lines.

Our geologic-hazard maps demonstrate that the central Wasatch Front is one of the most seismically hazardous major urban areas in the interior of the western U.S. We hope that government agencies and the engineering, urban planning, and emergency preparedness and response communities will use these maps as part of an overall program to reduce earthquake risks and losses near the Salt Lake City segment of the Wasatch fault zone. Because our mapping relied on existing geologic data at a regional scale, our hazard maps are only for general planning, estimating losses, and raising awareness, and should not be used as special-study-area maps or as a substitute for site-specific geologic investigations.

ACKNOWLEDGEMENTS

This study was completed through a cooperative project funded by the USGS NEHRP, the UGS, URS Corporation, Pacific Engineering & Analysis, and the Utah Division of Emergency Services and Homeland Security (DES). We thank Doug Bausch, FEMA, for helpful discussions related to HAZUS software. We also thank Robert Carey, DES, for encouraging the use of our geologic-hazard scenario in future HAZUS loss-estimation studies and for help in funding this project. Discussions with Francis Ashland, Gary Christenson, and Jon King, UGS, and Susan Olig, URS Corporation, were helpful throughout this project. Thoughtful reviews by Gary Christenson, Randall Jibson (USGS), and Matthew Mabey (Brigham Young University) improved our report.

REFERENCES

Abrahamson, N.A., and Silva, W.J., 1997, Empirical response spectral attenuation relations for shallow crustal earthquakes: Seismological Research Letters, v. 68, p. 94-127.

Anderson, L.R., Keaton, J.R., Aubrey, Kevin, and Ellis, S.J., 1982, Liquefaction potential map for Davis County, Utah: Logan, Utah State University Department of Civil and Environmental Engineering and Dames and Moore unpublished Final Technical Report prepared for the U.S. Geological Survey, National Earthquake Hazards Reduction Program Award No. 14-08-0001-19127, 50 p.; published as Utah Geological Survey Contract Report 94-7, 1994.

Anderson, L.R., Keaton, J.R., and Bay, J.A., 1990a, Liquefaction potential map for the northern Wasatch Front, Utah: Logan, Utah State University Department of Civil and Environmental Engineering unpublished Final Technical Report prepared for the U.S. Geological Survey, National Earthquake Hazards Reduction Program Award No. 14-08-0001-22015, 150 p.; published as Utah Geological Survey Contract Report 94-6, 1994.

Anderson, L.R., Keaton, J.R., and Bischoff, J.E., 1986a, Liquefaction potential map for Utah County, Utah: Logan, Utah State University Department of Civil and Environmental Engineering and Dames and Moore unpublished Final Technical Report prepared for the U.S. Geological Survey, National Earthquake Hazards Reduction Program Award No.

14-08-0001-21359, 46 p.; published as Utah Geological Survey Contract Report 94-8, 1994.

Anderson, L.R., Keaton, J.R., and Rice, J.D., 1990b, Liquefaction potential map for central Utah: Logan, Utah State University Department of Civil and Environmental Engineering unpublished Final Technical Report prepared for the U.S. Geological Survey, National Earthquake Hazards Reduction Program Award No. 14-08-0001-G1384, 134 p.; published as Utah Geological Survey Contract Report 94-10, 1994.

Anderson, L.R., Keaton, J.R., Spitzley, J.E., and Allen, A.C., 1986b, Liquefaction potential map for Salt Lake County, Utah: Logan, Utah State University Department of Civil and Environmental Engineering and Dames and Moore unpublished Final Technical Report prepared for the U.S. Geological Survey, National Earthquake Hazards Reduction Program Award No. 14-08-0001-19910, 48 p.; published as Utah Geological Survey Contract Report 94-9, 1994.

Arias, A., 1970, A measure of earthquake intensity, *in* Hansen, R.J., editor, Seismic design for nuclear power plants: Cambridge, Massachusetts Institute of Technology Press, p. 438-483.

Arnow, Ted, and Stephens, Doyle, 1990, Hydrologic characteristics of the Great Salt Lake, Utah—1847-1986: U.S. Geological Survey Water-Supply Paper 2332, 32 p.

Arnow, T., Van Horn, R., and LaPray, R., 1970, The pre-Quaternary surface in the Jordan Valley, Utah: U.S. Geological Survey Professional Paper 700, p. D257-D261.

Ashland, F.X., 2001, Site-response characterization for implementing ShakeMap in northern Utah: Utah Geological Survey Report of Investigation 248, 10 p.

Ashland, F.X., and Rollins, K., 1999, Seismic zonation using geotechnical site-response mapping, Salt Lake Valley, Utah: Utah Geological Survey unpublished Final Technical Report prepared for the U.S. Geological Survey, National Earthquake Hazards Reduction Program Award No. 1434-HQ-97-GR-03126, 33 p.

Bardet, J.-P., Tobita, Tetsuo, Mace, Nicholas, and Hu, Jianping, 2002, Regional modeling of liquefaction-induced ground deformation: Earthquake Spectra, v. 18, no. 1, p. 19-46.

Bartlett, S.F., and Youd, T.L., 1992, Empirical analysis of horizontal ground displacement generated by liquefaction-induced lateral spreads: National Center for Earthquake Engineering Research Technical Report NCEER-92-0021, 114 p.

Black, B.D., Hecker, Suzanne, Hylland, M.D., Christenson, G.E., and McDonald, G.N., 2003, Quaternary fault and fold database and map of Utah: Utah Geological Survey Map 193DM, scale 1:500,000, compact disc.

Black, B.D., Lund, W.R., Schwartz, D.P., Gill, H.E., and Mayes, B.H., 1996, Paleoseismic investigation of the Salt Lake City segment of the Wasatch fault zone at the South Fork Dry Creek and Dry Gulch sites, Salt Lake County, Utah: Utah Geological Survey Special Study 92, 22 p.

Black, B.D., Solomon, B.J., and Harty, K.M., 1999, Geology and geologic hazards of Tooele Valley and the West Desert Hazardous Industry Area, Tooele County, Utah: Utah Geological Survey Special Study 96, 65 p.

Bruhn, R.L., Gibler, P.R., and Parry, W.T., 1987, Rupture characteristics of normal faults—an example from the Wasatch fault zone, Utah, *in* Coward, M.P., Dewey, J.F., and Hancock, P.L., editors, Continental extensional tectonics: Geological Society of America Special Publication No. 28, p. 337-353.

Campbell, K.W., 1997, Empirical near-source attenuation relationships for horizontal and vertical components of peak ground acceleration, peak ground velocity, and pseudo-absolute acceleration response spectra: Seismological Research Letters, v. 68, p. 154-179.

Chang, Wu-Lung, and Smith, R.B., 1998a, Potential for tectonically induced tilting and flooding by the Great Salt Lake, Utah, from large earthquakes on the Wasatch fault, *in* Lund, W.R., editor, Proceedings volume, Basin and Range Province Seismic-Hazards Summit: Utah Geological Survey Miscellaneous Publication 98-2, p. 128-138.

—1998b, Stress interaction and its application to the earthquake hazard analysis of the Wasatch fault, Utah: Seismological Research Letters, v. 69, p. 161.

—2002, Integrated seismic-hazard analysis of the Wasatch Front, Utah: Bulletin of the Seismological Society of America, v. 92, no. 5, p. 1904-1922.

Currey, D.R., and Oviatt, C.G., 1985, Durations, average rates, and probable causes of Lake Bonneville expansions, stillstands, and contractions during the last deep-lake cycle, 32,000 to 10,000 years ago, *in* Kay, P.A., and Diaz, H.F., editors, Problems of and prospects for predicting Great Salt Lake levels—Proceedings of a NOAA conference, March 26-28, 1985: Salt Lake City, University of Utah, Center for Public Affairs and Administration, p. 9-24.

Dobry, R., Idriss, I.M., and Ng, E., 1978, Duration characteristics of horizontal components of strong-motion earthquake records: Bulletin of the Seismological Society of America, v. 68, no. 5, p. 1487-1520.

Donn, W.L., 1964, Alaska earthquake of 27 March 1964—remote seiche stimulation: Science, v. 145, p. 261-262.

Electric Power Research Institute, 1993, Guidelines for determining design basis ground motions—vol. 1 – Method and guidelines for estimating earthquake ground motion in eastern North America: Palo Alto, California, EPRI TR-102293, v. 1, 426 p.

Federal Emergency Management Agency, 1993, Water control infrastructure, National Inventory of Dams 1992: Washington, D.C., Federal Emergency Management Agency and U.S. Army Corps of Engineers, FEMA 246.

Forel, F.A., 1895, Le Leman—monographie limnologique, v. 2, Mecanique, Chimie, Thermique, Optique, Acoustique: Lausanne, F. Rouge, 651 p.

Harty, K.M., 1991, Landslide map of Utah: Utah Geological Survey Map 133, scale 1:500,000.

Hecker, Suzanne, 1993, Quaternary tectonics of Utah with emphasis on earthquake-hazard characterization: Utah Geological Survey Bulletin 127, 157 p.

Hecker, Suzanne, Harty, K.M., and Christenson, G.E., 1988, Shallow ground water and related hazards in Utah: Utah Geological Survey Map 110, scale 1:750,000.

Hintze, L.F., Willis, G.C., Laes, D.Y.M., Sprinkel, D.A., and Brown, K.D., 2000, Digital geologic map of Utah: Utah Geological Survey Map 179DM, scale 1:500,000, compact disc.

Houston, J.R., 1979, State-of-the-art for assessing earthquake hazards in the United States—Tsunamis, seiches, and landslide-induced water waves: U.S. Army Waterways Experiment Station, Miscellaneous Paper S-73-1, Report 15, 88 p.

Hutchinson, G.E., 1957, A treatise on limnology: New York, Wiley, v. 1, 1015 p.

Ishihara, K., 1993, Liquefaction and flow failure during earthquakes: Géotechnique, v. 43, p. 351-415.

Jibson, R.W., 1993, Predicting earthquake-induced landslide displacements using Newmark's sliding block analysis: Transportation Research Record, no. 1411, p. 9-17.

Jibson, R.W., Harp, E.L., and Michael, J.A., 1998, A method for producing digital probabilistic seismic landslide hazard maps—an example from the Los Angeles, California, area: U.S. Geological Survey Open-File Report 98-113, 17 p.

—2000, A method for producing digital probabilistic seismic landslide hazard maps: Engineering Geology, v. 58, p. 271-289.

Joyner, W.B., and Boore, D.M., 1988, Measurement, characterization, and prediction of strong ground motion, *in* Von Thun, J.L., editor, Proceedings of Earthquake Engineering & Soil Dynamics II, Recent Advances in Ground-Motion Evaluation: New York, Geotechnical Engineering Division of the American Society of Civil Engineers, Geotechnical Special Publication No. 20, p. 43-102.

Kanamori, Hiroo, 1983, Magnitude scale and quantification of earthquakes: Tectonophysics, v. 93, p. 185-199.

Keaton, J.R., 1986, Potential consequences of tectonic deformation along the Wasatch fault: Logan, Utah State University, Department of Civil and Environmental Engineering unpublished Final Technical Report prepared for the U.S. Geological Survey, 23 p.; published as Utah Geological Survey Contract Report 93-8, 1993.

Keaton, J.R., Currey, D.R., and Olig, S.J., 1987, Paleoseismicity and earthquake hazards evaluation of the West Valley fault zone, Salt Lake City urban area, Utah: Salt Lake City, Dames and Moore, unpublished Final Technical Report prepared for the U.S. Geological Survey, Contract No. 14-08-0001-22048, 55 p.

Keefer, D.K., 1984, Landslides caused by earthquakes: Geological Society of America Bulletin, v. 95, no. 4, p. 406-421.

—1993, The susceptibility of rock slopes to earthquake-induced failure: Bulletin of the Association of Engineering Geologists, v. 30, p. 353-361.

Kvale, Anders, 1955, Seismic seiches in Norway and England during the Assam earthquake of August 15, 1950: Bulletin of the Seismological Society of America, v. 45, p. 93-112.

Liao, S.S., Veneziano, D., and Whitman, R.V., 1988, Regression models for evaluating liquefaction probability: Journal of the Geotechnical Engineering Division, American Society of Civil Engineers, v. 114, p. 389-409.

Lin, Anching, and Wang, Po, 1978, Wind tides of the Great Salt Lake: Utah Geology, v. 5, p. 17-25.

Lowe, Mike, 1993, Hazards from earthquake-induced ground failure in sensitive clays, vibratory settlement, and flooding due to seiches, surface-drainage disruptions, and increased ground-water discharge, Davis County, Utah, *in* Gori, Paula L., editor, Applications of research from the U.S. Geological Survey program, Assessment of Regional Earthquake Hazard and Risk along the Wasatch Front, Utah: U.S. Geological Survey Professional Paper 1519, p. 163-167.

Machette, M.N., Personius, S.F., and Nelson, A.R., 1992, Paleoseismology of the Wasatch fault zone – A summary of recent investigations, conclusions, and interpretations, *in* Gori, P.L., and Hays, W.W., editors, Assessment of regional earthquake hazard and risk along the Wasatch Front, Utah: U.S. Geological Survey Professional Paper 1500, p. A1-A71.

Makdisi, F.I., and Seed, H.B., 1978, Simplified procedure for estimating dam and embankment earthquake-induced deformations: Journal of the Geotechnical Engineering Division, American Society of Civil Engineers, v. 104, no. GT7, p. 849-867.

McCalpin, J.P., 1987, Recommended setbacks from active normal faults, *in* McCalpin, J.P., editor, Proceedings of the 23rd Symposium on Engineering Geology and Soils Engineering: Boise, Idaho Department of Transportation, p. 35-56.

—2002, Post-Bonneville paleoearthquake chronology of the Salt Lake City segment, Wasatch fault zone, from the 1999 "megatrench" site: Utah Geological Survey Miscellaneous Publication 02-7, 37 p.

McCalpin, J.P., and Nishenko, S.P., 1996, Holocene paleoseismicity, temporal clustering, and probabilities of future large (M>7) earthquakes on the Wasatch fault zone, Utah: Journal of Geophysical Research, v. 101, p. 6,233-6,253.

McCalpin, J.P., and Solomon, B.J., 2001, Seismic-hazards mapping of the central Cache Valley, Utah—a digital pilot project: Utah Geological Survey unpublished Final Technical Report prepared for the U.S. Geological Survey, National Earthquake Hazards Reduction Program Award No. 1434-HQ-98-GR-00024, 59 p.

McCulloch, D.S., 1966, Slide-induced waves, seiching, and ground fracturing caused by the earthquake of March 27, 1964, at Kenai Lake, Alaska: U.S. Geological Survey Professional Paper 543-A, p. A1-A41.

McGarr, Arthur, 1965, Excitation of seiches in channels by seismic waves: Journal of Geophysical Research, v. 70, p. 847-854.

Miles, S.B., and Keefer, D.K., 2000, Evaluation of seismic slope-performance models using a regional case study: Environmental & Engineering Geoscience, v. 6, p. 25-39.

Myers, W.B., and Hamilton, Warren, 1964, Deformation accompanying the Hebgen Lake earthquake of August 17, 1959: U.S. Geological Survey Professional Paper 435, p. 55-98.

National Institute of Building Sciences, 1999, Earthquake loss estimation methodology—HAZUS user's manual: Washington, D.C., Federal Emergency Management Agency, 11 chapters and 8 appendices, variously paginated.

National Research Council, 1985, Liquefaction of soils during earthquakes: Washington, D.C., Committee on Earthquake Engineering, Commission on Engineering and Technical Systems, National Academy Press, 240 p.

Newmark, N.M., 1965, Effects of earthquakes on dams and embankments: Géotechnique, v. 15, p. 139-160.

Okada, Yoshimitsu, 1985, Surface deformation due to shear and tensile faults in a half-space: Bulletin of the Seismological Society of America, v. 75, p. 1135-1154.

Olsen, K.B., Pechmann, J.C., and Schuster, G.T., 1995, Simulation of 3-D elastic wave propagation in the Salt Lake basin: Bulletin of the Seismological Society of America, v. 85, p. 1688-1710.

—1996, An analysis of simulated and observed blast records in the Salt Lake basin: Bulletin of the Seismological Society of America, v. 86, p. 1061-1076.

Pechmann, J.C., 1987, Earthquake design considerations for the inter-island diking project, Great Salt Lake, Utah: Unpublished technical report for Rollins, Brown, and Gunnell, Inc., 31 p.

Personius, S.F., and Scott, W.E., 1992, Surficial geologic map of the Salt Lake City segment and parts of adjacent segments of the Wasatch fault zone, Davis, Salt Lake, and Utah Counties, Utah: U.S. Geological Survey Miscellaneous Investigations Series Map I-2106, scale 1:50,000.

Power, M.S., Perman, R.G., Wesling, J.R., Youngs, R.R., and Shimamoto, M.K., 1991, Assessment of liquefaction potential in the San Jose, California urban area: Stanford, Proceedings of the 4th International Conference on Microzonation, v. II, p. 677-684.

Reid, H.F., 1914, The Lisbon earthquake of November 1, 1755: Bulletin of the Seismological Society of America, v. 4, p. 53-80.

Rollins, Brown, and Gunnell, Inc., and Creamer & Noble Engineers, 1987, Great Salt Lake inter-island diking project: Unpublished final design reports for Utah Division of Water Resources, 2 volumes, variously paginated.

Ruttner, Franz, 1953, Fundamentals of limnology: Toronto University Press, 242 p.

Sadigh, K., Chang, C.-Y., Egan, J.A., Makdisi, F., and Youngs, R.R., 1997, Attenuation relationships for shallow crustal earthquakes based on California strong motion data: Seismological Research Letters, v. 68, p. 180-189.

Sadigh, K., Egan, J.A., and Youngs, R.R., 1986, Specification of ground motions for seismic design on long-period structures [abs.]: Earthquake Notes, v. 57, p. 13.

Schuster, G.T., and Sun, Y., 1993, Surface wave inversion of near-surface shear-wave velocities in Salt Lake Valley: University of Utah unpublished Final Technical Report prepared for the U.S. Geological Survey, National Earthquake Hazards Reduction Program Award No. 1434-92-G-2175, 31 p.

Seed, H.B., 1979, Soil liquefaction and cyclic mobility evaluation for level ground during earthquakes: Journal of the Geotechnical Engineering Division, American Society of Civil Engineers, v. 102, p. 201-255

Seed, H.B., and Idriss, I.M., 1982, Ground motions and soil liquefaction during earthquakes: Oakland, California, Earthquake Engineering Research Institute, Monograph Series, p. 13.

Seed, H.B., Idriss, I.M., and Arango, I., 1983, Evaluation of liquefaction potential using field performance data: Journal of the Geotechnical Engineering Division, American Society of Civil Engineers, v. 109, p. 458-482.

Seed, H.B., Tokimatsu, K., Harder, L.F., and Chung, R., 1985, Influence of SPT procedures on soil liquefaction resistance evaluations: Journal of the Geotechnical Engineering Division, American Society of Civil Engineers, v. 111, p. 1425-1445.

Silva, W.J., Abrahamson, N.A., Toro, G., and Constantino, C., 1997, Description and validation of the stochastic ground motion model: Upton, New York, Associated Universities, Inc., unpublished report prepared for the Brookhaven National Laboratory.

Silva, W.J., Wong, I.G., and Darragh, R.B., 1998, Engineering characterization of earthquake strong ground motions in the Pacific Northwest, *in* Rogers, A.M., Walsh, T.J., Kockelman, W.J., and Priest, G.R., editors, Assessing earthquake hazards and reducing risk in the Pacific Northwest: U.S. Geological Survey Professional Paper 1560, v. 2, p. 313-324.

Smith, R.B., and Arabasz, W.J., 1991, Seismicity of the Intermountain seismic belt, *in* Slemmons, D.B., Engdahl, E.R., Zoback, M.D., Zoback, M.L., and Blackwell, D., editors, Neotectonics of North America: Geological Society of America, Decade Map v. 1, p. 185-228.

Smith, R.B., and Richins, W.D., 1984, Seismicity and earthquake hazards of Utah and the Wasatch Front—paradigm and paradox: U.S. Geological Survey Open-File Report 84-763, 27 p.

Spudich, P., Joyner, W.B., Lindh, A.G., Boore, D.M., Margaris, B.M., and Fletcher, J.B., 1999, SEA99 – A revised ground motion prediction relation for use in extensional tectonic regimes: Bulletin of the Seismological Society of America, v. 89, p. 1156-1170.

Stokes, W.L., 1977, Subdivisions of the major physiographic provinces in Utah: Utah Geology, v. 4, no. 1, p. 1-17.

Tinsley, J.C., King, K.W., Trumm, D.A., Carver, D.L., and Williams, R., 1991, Geologic aspects of shear-wave velocity and relative ground response in Salt Lake Valley, Utah, *in* McCalpin, J.P., editor, Proceedings of the 27th Symposium on Engineering Geology and Geotechnical Engineering: Pocatello, Idaho State University, p. 25-1 – 25-9.

Tokimatsu, A.M., and Seed, H.B., 1987, Evaluation of settlements in sands due to earthquake shaking: Journal of the Geotechnical Division, American Society of Civil Engineers, v. 113, p. 681-878.

Vucetic, M., and Dobry, R., 1998, Degradation of marine clays under cyclic loading: Journal of Geotechnical Engineering, American Society of Civil Engineers, v. 114, p. 133-149.

Wald, D.J., Quitoriano, V., Heaton, T.H., and Kanamori, H., 1999, Relationships between peak ground acceleration, peak ground velocity and Modified Mercalli intensity in California: Earthquake Spectra, v. 15, p. 557-564.

Weibull, W.A., 1939, A statistical theory of the strength of materials: Stockholm, Sweden, Ingenioers Vetenskaps Akademien Handlingar, No. 151, p. 1-45.

Wells, D.L., and Coppersmith, K.J., 1994, New empirical relationships among magnitude, rupture length, rupture width, and surface displacement: Bulletin of the Seismological Society of America, v. 84, p. 974-1002.

Wieczorek, G.F., Wilson, R.C., and Harp, E.L., 1985, Map of slope stability during earthquakes in San Mateo County, California: U.S. Geological Survey Miscellaneous Investigations Map I-1257-E, scale 1:62,500.

Wiegel, R.L., and Camotim, Data, 1962, Model study of oscillations of Hebgen Lake: Bulletin of the Seismological Society of America, v. 52, p. 273-277.

Wilson, R.C., and Keefer, D.K., 1983, Dynamic analysis of a slope failure from the 6 August, 1979 Coyote Lake, California, earthquake: Bulletin of the Seismological Society of America, v. 73, p. 863-877.

—1985, Predicting areal limits of earthquake induced landsliding, *in* Ziony, J.I., editor, Evaluating earthquake hazards in the Los Angeles region—an earth-science perspective: U.S. Geological Survey Professional Paper 1360, p. 317-345.

Wong, I.G., and Silva, W.J., 1993, Site-specific strong ground motion estimates for the Salt Lake Valley, Utah: Utah Geological Survey Miscellaneous Publication 93-9, 34 p.

Wong, Ivan, Silva, Walter, Olig, Susan, Thomas, Patricia, Wright, Douglas, Ashland, Francis, Gregor, Nick, Pechmann, James, Dober, Mark, Christenson, Gary, and Gerth, Robyn, 2002, Earthquake scenario and probabilistic ground shaking maps for the Salt Lake City metropolitan area, Utah: Utah Geological Survey Miscellaneous Publication MP 02-05, 50 p.

Wong, I.G., Silva, W.J., Youngs, R.R., and Stark, C.L., 1996, Numerical earthquake ground motion modeling and its use in microzonation: Pergamon Press, Proceedings, 11th World Conference on Earthquake Engineering, compact disc.

Youd, T.L., 1980, Ground failure displacement and earthquake damage to buildings: American Society of Civil Engineers Conference on Civil Engineering and Nuclear Power, 2d, Knoxville, Tennessee, 1980, v. 2, p. 7-6-2 - 7-6-26.

Youd, T.L, Hansen, C.M., and Bartlett, S.F., 1999, Revised MLR equations for predicting lateral spread displacement, *in* Proceedings, 7th U.S.-Japan Workshop on Earthquake Resistant Design of Lifeline Facilities and Countermeasures against Liquefaction, Seattle, Washington: Multidisciplinary Center for Earthquake Engineering Research Technical Report MCEER-99-0019, p. 99-114.

Youd, T.L., and Perkins, D.M., 1978, Mapping liquefaction-induced ground failure potential: Journal of the Geotechnical Engineering Division, American Society of Civil Engineers, v. 104, p. 433-446.

—1987, Mapping of liquefaction severity index: Journal of Geotechnical Engineering Division, American Society of Civil Engineers, v. 118, p. 1374-1392.

Peak Horizontal Acceleration (*g*) at the Ground Surface

by
Ivan Wong[1], Walter Silva[2],
Douglas Wright[2], and Nick Gregor[1]

Research supported by U.S. Geological Survey (USGS), Department of the Interior, under USGS award number 99HQGR0091. The views and conclusions contained in this document are those of the authors and should not be interpreted as necessarily representing the official policies, either expressed or implied, of the U.S. Government.

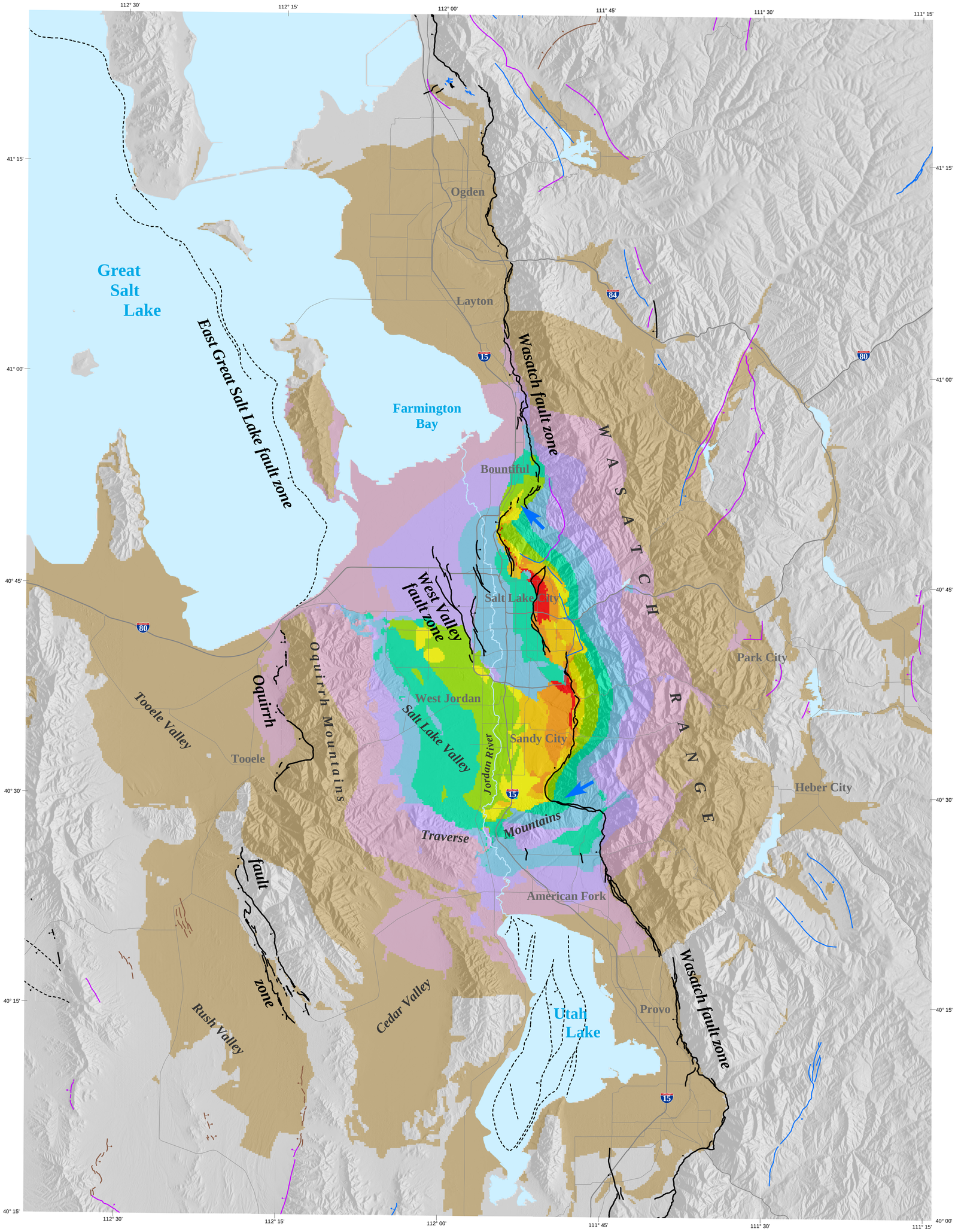

Peak Horizontal Acceleration (g)

	Modified Mercalli Intensity (from Wald and others, 1999)
< 0.1	**I-V** Weak to moderate shaking. Very light damage at MM V.
0.1 - 0.2	**VI** Strong Shaking. Felt by all, many frightened and run outdoors. Some heavy furniture moved; a few instances of fallen plaster and damaged chimneys. Damage light.
0.2 - 0.3	
0.3 - 0.4	**VII** Very strong shaking. Negligible damage in buildings of good design and construction; slight to moderate in well-built ordinary structures; considerable in poorly built or designed structures.
0.4 - 0.5	
0.5 - 0.6	**VIII** Severe shaking. Slight damage in specially designed structures; considerable in ordinary substantial buildings with partial collapse; great in poorly built structures.
0.6 - 0.7	
0.7 - 0.8	
0.8 - 0.9	**IX** Violent shaking. Considerable damage in specially designed structures; well-designed frame structures thrown out of plumb; great in substantial buildings, with partial collapse.
0.9 - 1.0	
1.0 - 1.1	

Quaternary Faults

Dashed where location is inferred

- Latest Quaternary [<15,000 years]
- Late Quaternary [<130,000 years]
- Middle to Late Quaternary [<750,000 years]
- Quaternary [<1,600,000 years]
- Bar and ball on down-thrown side

Fault data modified from Black and others (2003).

Rupture scenario (between arrows)

Explanation

This map illustrates the ground shaking that could occur if a moment magnitude (**M**) 7.0 earthquake were to rupture the Salt Lake City segment of the Wasatch fault. The intent of illustrating the strong ground shaking from such a scenario is to indicate that the severity of ground motions could be very strong and very damaging within the map area.

Limitations

There are large uncertainties associated with earthquake ground motion prediction in Utah due to a lack of region-specific information and data on the characteristics of ground motions. Additional uncertainty stems from the characterization of the subsurface geology beneath the mapped area and the estimation of the associated site response effects on ground motions. Thus the maps should not be used for site-specific design or in place of site-specific hazard evaluations.

[1] URS Corporation, 500 12th Street, Suite 200, Okland, California 94607
Phone: (510) 874-3014, Fax: (510) 874-3628, e-mail: Ivan_Wong@urscorp.com

[2] Pacific Engineering & Analysis, 311 Pomona Avenue, El Cerrito, California 94530
Phone (510) 528-2821, Fax: (510) 528-2135, e-mail: pacificengineering@juno.com

N W E S

Scale 1:250,000

10 5 0 10 Miles

10 5 0 10 Kilometers

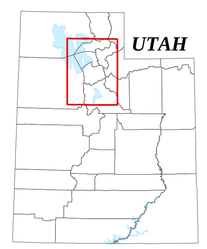

Study Area Index Map

ISBN 1-55791-704-3

Basemap source data modified from the Utah Automated Geographic Reference Center; Utah State Geographic Information Database. Relief shading derived from 1:24,000 scale USGS Digital Elevation Models.

Universal Transverse Mercator Projection, Zone 12. 1927 North American Datum.

UTAH GEOLOGICAL SURVEY
UTAH GEOLOGICAL SURVEY
a division of
Department of Natural Resources

Permanent Ground Displacement caused by Liquefaction (Lateral Spreading)

by
Barry J. Solomon and Neil D. Storey

Research supported by U.S. Geological Survey (USGS), Department of the Interior, under USGS award number 99HQGR0091. The views and conclusions contained in this document are those of the authors and should not be interpreted as necessarily representing the official policies, either expressed or implied, of the U.S. Government.

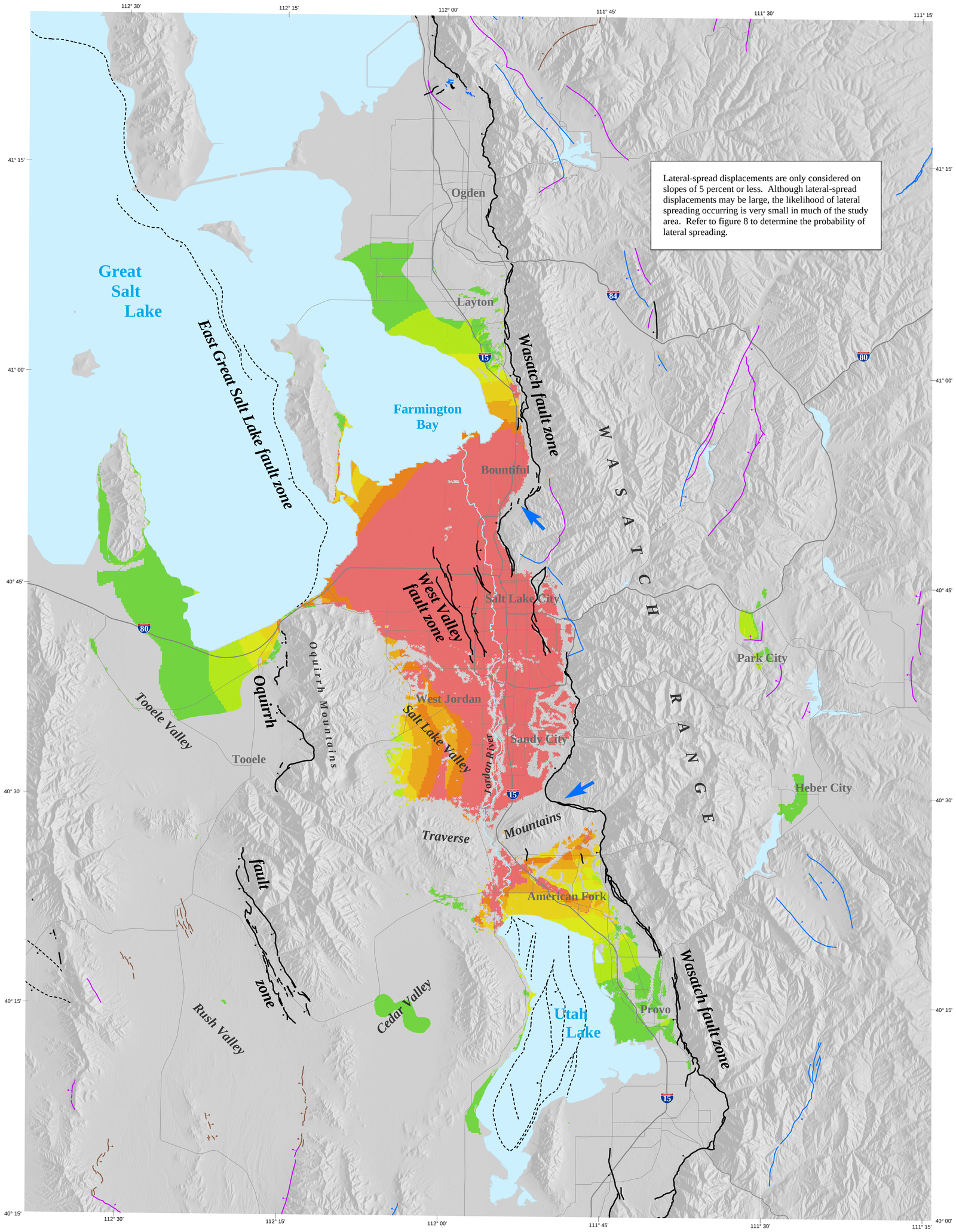

Expected Permanent Ground Displacement (cm) — Expected Damage to Buildings (Youd, 1980)

0 - 5	Little damage, repairable
5 - 10	
10 - 15	Severe damage, repairable
15 - 20	
20 - 25	
25 - 30	
>30	Severe damage or collapse, nonrepairable

Quaternary Faults

Dashed where location is inferred

- Latest Quaternary [<15,000 years]
- Late Quaternary [<130,000 years]
- Middle to Late Quaternary [<750,000 years]
- Quaternary [<1,600,000 years]
- Bar and ball on down-thrown side

Fault data modified from Black and others (2003).

Rupture scenario (between arrows)

Explanation

This map illustrates the liquefaction-induced lateral spreading that could occur if a moment magnitude (**M**) 7.0 earthquake were to rupture the Salt Lake City segment of the Wasatch fault zone. Liquefaction happens during earthquakes when shallow, water-saturated, cohesionless soils are subjected to strong ground shaking. Mapped potential hazards associated with liquefaction include lateral spreading (landslides on gentle slopes or near embankments) and settlement (lowering of the ground surface caused by rearrangement of loose soils into denser configurations). However, liquefaction-induced ground displacement may also be caused by flow failure or ground oscillation. We do not map displacement from these mechanisms because most ground slopes underlain by susceptible material are too gentle for flow failure and there is no widely accepted technique to estimate displacements generated by liquefaction-induced ground oscillation. Buildings and infrastructure may suffer severe damage if liquefaction-induced ground displacement is sufficiently large.

Limitations

The earthquake described here happens every thousand years or so. Other active faults in the region may subject the study area to earthquakes, and their effects will undoubtedly differ from this scenario. Some effects may be worse than the scenario suggests and some may not be as severe. Because the predicted earthquake hazards are based on specific analytical techniques, different techniques may alter the scale and extent of mapped hazards. In addition, this map does not address man-made alterations to ground conditions (fill) because they could not be distinguished on a regional basis with available data. The properties of fills vary from dense, engineered fills with a very low liquefaction susceptibility to loose fills with a very high liquefaction susceptibility. The use of fill may increase or decrease the hazard at a site. Because the hazards at any particular site may be different than shown, the maps should not be used for site-specific design or in place of site-specific hazard evaluations.

N W E S

Scale 1:250,000

10 5 0 10 Miles

10 5 0 10 Kilometers

Study Area Index Map

ISBN 1-55791-704-3

Basemap source data modified from the Utah Automated Geographic Reference Center; Utah State Geographic Information Database. Relief shading derived from 1:24,000 scale USGS Digital Elevation Models.

Universal Transverse Mercator Projection, Zone 12. 1927 North American Datum.

UTAH GEOLOGICAL SURVEY
UTAH GEOLOGICAL SURVEY
a division of
Department of Natural Resources

Permanent Ground Displacement caused by Liquefaction (Ground Settlement)

by
Barry J. Solomon and Neil D. Storey

Research supported by U.S. Geological Survey (USGS), Department of the Interior, under USGS award number 99HQGR0091. The views and conclusions contained in this document are those of the authors and should not be interpreted as necessarily representing the official policies, either expressed or implied, of the U.S. Government.

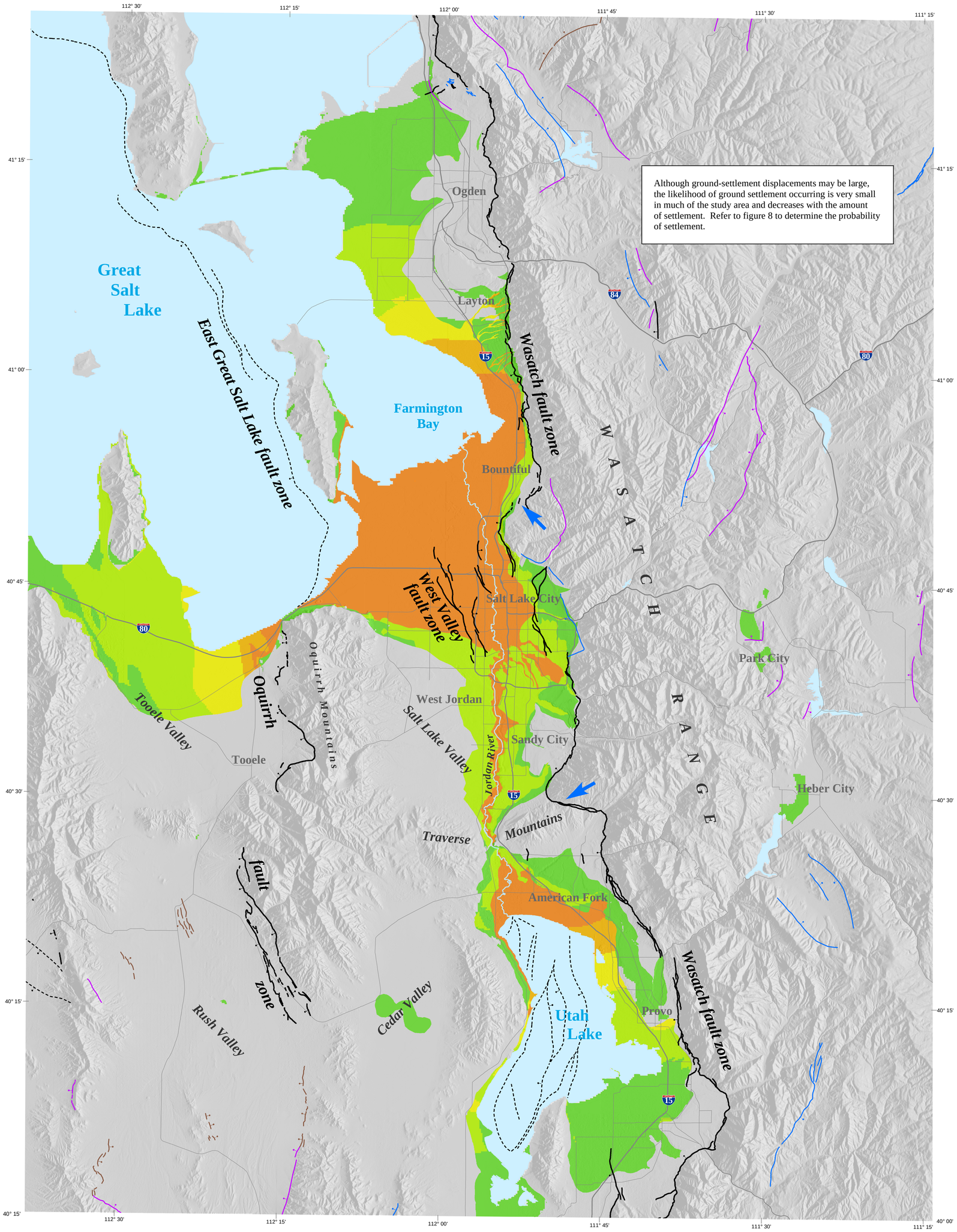

Although ground-settlement displacements may be large, the likelihood of ground settlement occurring is very small in much of the study area and decreases with the amount of settlement. Refer to figure 8 to determine the probability of settlement.

Expected Permanent Ground Displacement (cm)

Expected Damage to Buildings (Youd, 1980)

- 0 - 5
- 5 - 10 — Little damage, repairable
- 10 - 15
- 15 - 20 — Severe damage, repairable
- > 20

Quaternary Faults

Dashed where location is inferred

- Latest Quaternary [<15,000 years]
- Late Quaternary [<130,000 years]
- Middle to Late Quaternary [<750,000 years]
- Quaternary [<1,600,000 years]
- Bar and ball on down-thrown side

Fault data modified from Black and others (2003).

Rupture scenario (between arrows)

Explanation

This map illustrates the liquefaction-induced ground settlement that could occur if a moment magnitude (**M**) 7.0 earthquake were to rupture the Salt Lake City segment of the Wasatch fault zone. Liquefaction happens during earthquakes when shallow, water-saturated, cohesionless soils are subjected to strong ground shaking. Mapped potential hazards associated with liquefaction include lateral spreading (landslides on gentle slopes or near embankments) and ground settlement (lowering of the ground surface caused by rearrangement of loose soils into denser configurations). However, liquefaction-induced ground displacement may also be caused by flow failure or ground oscillation. We do not map displacement from these mechanisms because most ground slopes underlain by susceptible material are too gentle for flow failure and there is no widely accepted technique to estimate displacements generated by liquefaction-induced ground oscillation. Buildings and infrastructure may suffer severe damage if liquefaction-induced ground displacement is sufficiently large.

Limitations

The earthquake described here happens every thousand years or so. Other active faults in the region may subject the study area to earthquakes, and their effects will undoubtedly differ from this scenario. Some effects may be worse than the scenario suggests and some may not be as severe. Because the predicted earthquake hazards are based on specific analytical techniques, different techniques may alter the scale and extent of mapped hazards. In addition, this map does not address man-made alterations to ground conditions (fill) because they could not be distinguished on a regional basis with available data. The properties of fills vary from dense, engineered fills with a very low liquefaction susceptibility to loose fills with a very high liquefaction susceptibility. The use of fill may increase or decrease the hazard at a site. Because the hazards at any particular site may be different than shown, the maps should not be used for site-specific design or in place of site-specific hazard evaluations.

N
W E
S

Scale 1:250,000

10 5 0 10 Miles

10 5 0 10 Kilometers

Study Area Index Map

ISBN 1-55791-704-3

Basemap source data modified from the Utah Automated Geographic Reference Center; Utah State Geographic Information Database. Relief shading derived from 1:24,000 scale USGS Digital Elevation Models.

Universal Transverse Mercator Projection, Zone 12. 1927 North American Datum.

UTAH GEOLOGICAL SURVEY
UTAH GEOLOGICAL SURVEY
a division of
Department of Natural Resources

Permanent Ground Displacement caused by Landsliding under Wet Conditions

by
Barry J. Solomon and Neil D. Storey

Research supported by U.S. Geological Survey (USGS), Department of the Interior, under USGS award number 99HQGR0091. The views and conclusions contained in this document are those of the authors and should not be interpreted as necessarily representing the official policies, either expressed or implied, of the U.S. Government.

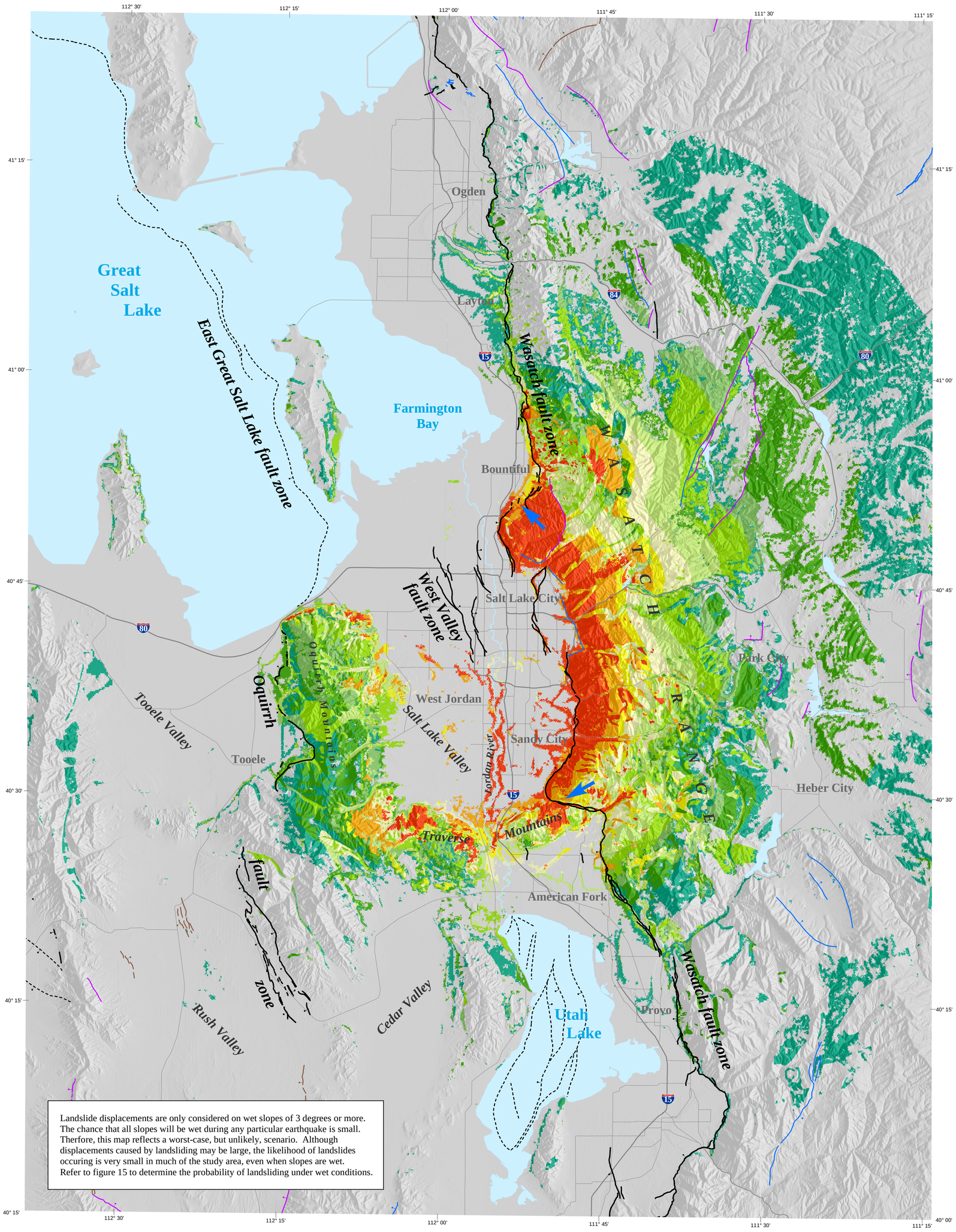

Landslide displacements are only considered on wet slopes of 3 degrees or more. The chance that all slopes will be wet during any particular earthquake is small. Therfore, this map reflects a worst-case, but unlikely, scenario. Although displacements caused by landsliding may be large, the likelihood of landslides occuring is very small in much of the study area, even when slopes are wet. Refer to figure 15 to determine the probability of landsliding under wet conditions.

Expected Permanent Ground Displacement (cm)

Expected Deformation (Wilson and Keefer, 1985)

0.0 - 0.1	Little slope movement or damage to overlying structures
0.1 - 0.2	
0.2 - 0.35	Significant slope movement and damage to overlying structures from landslides broken into chaotic masses of soil and rock
0.35 - 0.5	
0.5 - 1	
1 - 2	
2 - 3.5	
3.5 - 5	
5 - 10	
> 10	Significant slope movement and damage to overlying structures from all landslides; the possibility of catastrophic slope failure increases with larger displacement

Quaternary Faults

Dashed where location is inferred

- Latest Quaternary [<15,000 years]
- Late Quaternary [<130,000 years]
- Middle to Late Quaternary [<750,000 years]
- Quaternary [<1,600,000 years]
- Bar and ball on down-thrown side

Fault data modified from Black and others (2003).

Rupture scenario (between arrows)

Explanation

This map illustrates the landsliding that could occur if a moment magnitude (**M**) 7.0 earthquake were to rupture the Salt Lake City segment of the Wasatch fault zone when slopes are wet. Landsliding is the downslope movement of rock or soil, under the force of gravity, which may be triggered by earthquake ground shaking. Although wet slopes are more susceptible to landsliding than dry slopes, periods of moisture may be temporary. In this map, we assume that all slopes will be wet when affected by the scenario earthquake. We map the landslide hazard under dry conditions, a less conservative estimate of the hazard, on plate 5. Buildings and infrastructure may suffer severe damage if landslide-induced ground displacement is sufficiently large.

Limitations

The earthquake described here happens every thousand years or so. Other active faults in the region may subject the study area to earthquakes, and their effects will undoubtedly differ from this scenario. Some effects may be worse than the scenario suggests and some may not be as severe. Because the predicted earthquake hazards are based on specific analytical techniques, different techniques may alter the scale and extent of mapped hazards. In addition, mapped landslide hazards only indicate the source zone of landslides (the parts of slopes that may fail). This map does not show how far downslope the failed material may travel before stopping. Proposed development in areas downslope of landslide source zones should consider this in site-specific investigations. Because the hazards at any particular site may be different than shown, the maps should not be used for site-specific design or in place of site-specific hazard evaluations.

N
W E
S

Scale 1:250,000

10 5 0 10 Miles

10 5 0 10 Kilometers

Study Area Index Map

ISBN 1-55791-704-3

Basemap source data modified from the Utah Automated Geographic Reference Center; Utah State Geographic Information Database. Relief shading derived from 1:24,000 scale USGS Digital Elevation Models.

Universal Transverse Mercator Projection, Zone 12. 1927 North American Datum.

UTAH GEOLOGICAL SURVEY
UTAH GEOLOGICAL SURVEY
a division of
Department of Natural Resources

Permanent Ground Displacement caused by Landsliding under Dry Conditions

by
Barry J. Solomon and Neil D. Storey

Research supported by U.S. Geological Survey (USGS), Department of the Interior, under USGS award number 99HQGR0091. The views and conclusions contained in this document are those of the authors and should not be interpreted as necessarily representing the official policies, either expressed or implied, of the U.S. Government.

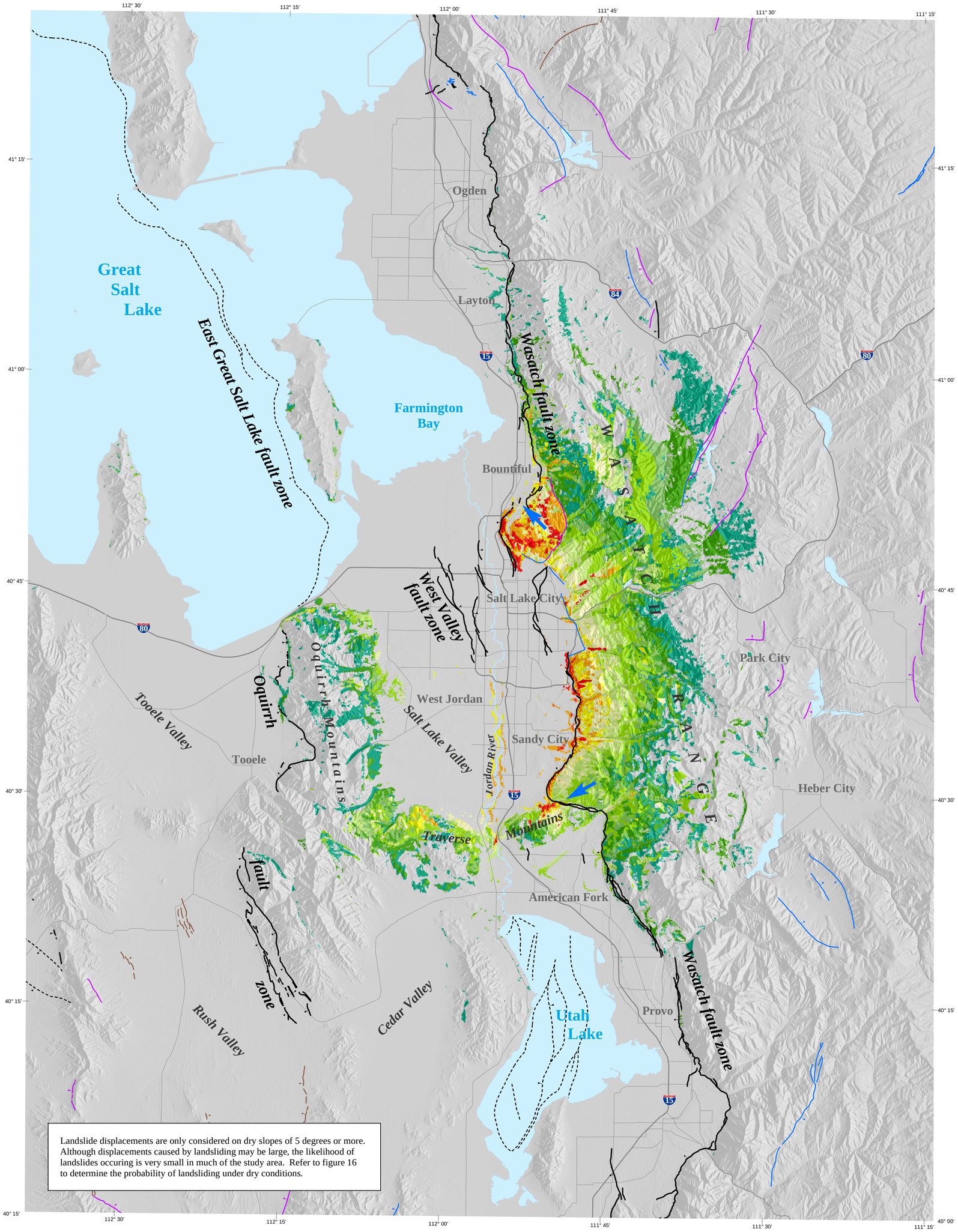

Landslide displacements are only considered on dry slopes of 5 degrees or more. Although displacements caused by landsliding may be large, the likelihood of landslides occuring is very small in much of the study area. Refer to figure 16 to determine the probability of landsliding under dry conditions.

Expected Permanent Ground Displacement (cm)

Expected Deformation (Wilson and Keefer, 1985)

0.0 - 0.1	Little slope movement or damage to overlying structures
0.1 - 0.2	
0.2 - 0.35	Significant slope movement and damage to overlying structures from landslides broken into chaotic masses of soil and rock
0.35 - 0.5	
0.5 - 1	
1 - 2	
2 - 3.5	
3.5 - 5	
5 - 10	
> 10	Significant slope movement and damage to overlying structures from all landslides; the possibility of catastrophic slope failure increases with larger displacement

Quaternary Faults

Dashed where location is inferred

- Latest Quaternary [<15,000 years]
- Late Quaternary [<130,000 years]
- Middle to Late Quaternary [<750,000 years]
- Quaternary [<1,600,000 years]
- Bar and ball on down-thrown side

Fault data modified from Black and others (2003).

Rupture scenario (between arrows)

Explanation

This map illustrates the landsliding that could occur if a moment magnitude (**M**) 7.0 earthquake were to rupture the Salt Lake City segment of the Wasatch fault zone when slopes are dry. Landsliding is the downslope movement of rock or soil, under the force of gravity, which may be triggered by earthquake ground shaking. Although wet slopes are more susceptible to landsliding than dry slopes, periods of moisture may be temporary. In this map, we assume that all slopes will be dry when affected by the scenario earthquake. We map the landslide hazard under wet conditions, a more conservative estimate of the hazard, on plate 4. Buildings and infrastructure may suffer severe damage if landslide-induced ground displacement is sufficiently large.

Limitaions

The earthquake described here happens every thousand years or so. Other active faults in the region may subject the study area to earthquakes, and their effects will undoubtedly differ from this scenario. Some effects may be worse than the scenario suggests and some may not be as severe. Because the predicted earthquake hazards are based on specific analytical techniques, different techniques may alter the scale and extent of mapped hazards. In addition, mapped landslide hazards only indicate the source zone of landslides (the parts of slopes that may fail). This map does not show how far downslope the failed material may travel before stopping. Proposed development in areas downslope of landslide source zones should consider this in site-specific investigations. Because the hazards at any particular site may be different than shown, the maps should not be used for site-specific design or in place of site-specific hazard evaluations.

N
W E
S

Scale 1:250,000

10 5 0 10 Miles

10 5 0 10 Kilometers

Study Area Index Map

ISBN 1-55791-704-3

Basemap source data modified from the Utah Automated Geographic Reference Center; Utah State Geographic Information Database. Relief shading derived from 1:24,000 scale USGS Digital Elevation Models.

Universal Transverse Mercator Projection, Zone 12. 1927 North American Datum.

UTAH GEOLOGICAL SURVEY
UTAH GEOLOGICAL SURVEY
a division of
Department of Natural Resources

Tectonic-Subsidence Hazards

by
Barry J. Solomon and Neil D. Storey

Research supported by U.S. Geological Survey (USGS), Department of the Interior, under USGS award number 99HQGR0091. The views and conclusions contained in this document are those of the authors and should not be interpreted as necessarily representing the official policies, either expressed or implied, of the U.S. Government.

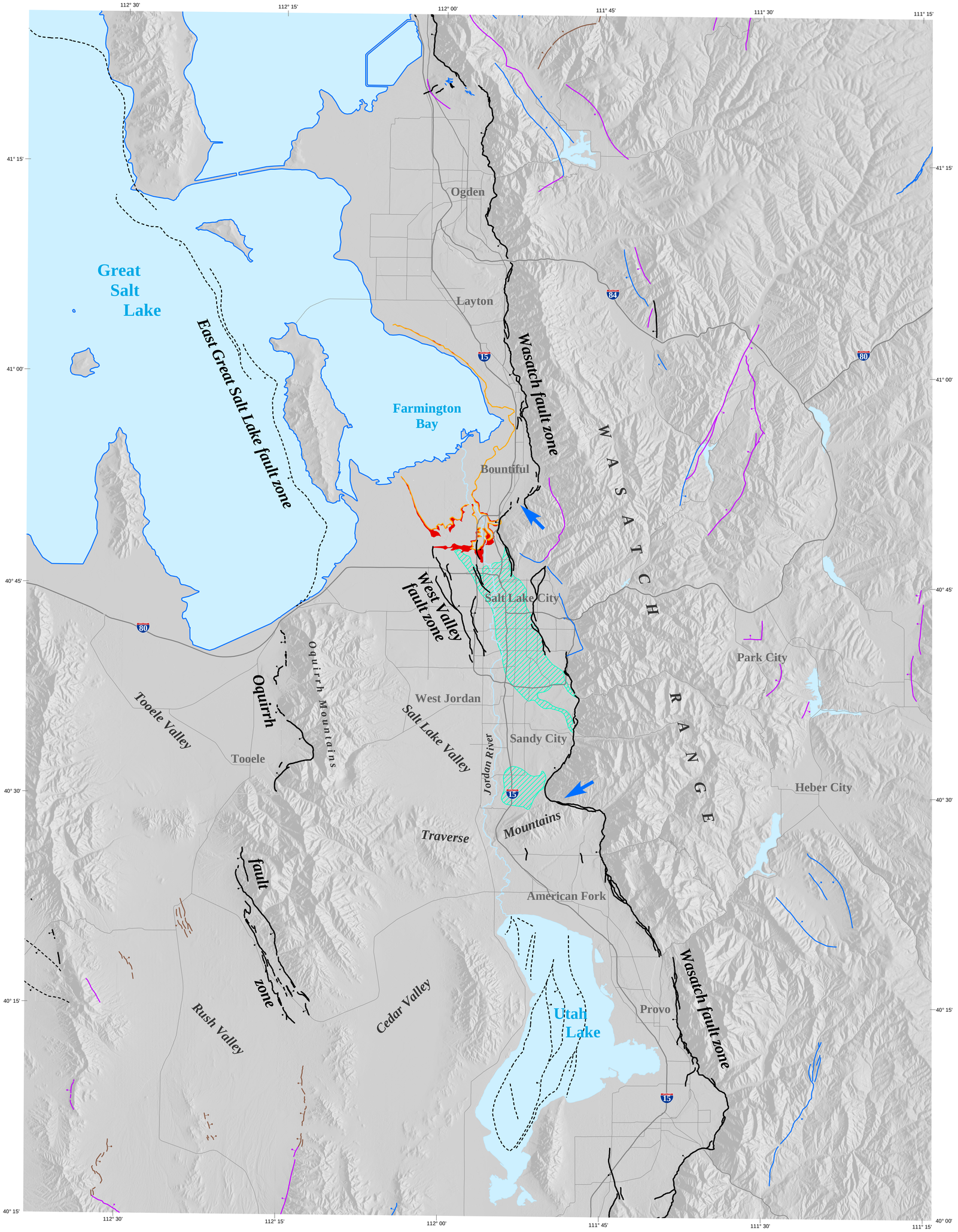

Tectonic-Subsidence Hazards

Shoreline before tilting at 4,212 feet (1,284 m).

Areas of lake-shore flooding corresponding to a lake elevation of 4,212 feet (1,284 m).

Source: Chang and Smith (1998a, figure 7a).

Areas of possible localized ponding of shallow ground water, with subsidence greater than 3 feet (1 m) and ground-water depth less than 3 feet (1 m).

Source: Keaton (1986, plate 4).

Quaternary Faults

Dashed where location is inferred

- Latest Quaternary [<15,000 years]
- Late Quaternary [<130,000 years]
- Middle to Late Quaternary [<750,000 years]
- Quaternary [<1,600,000 years]
- Bar and ball on down-thrown side

Fault data modified from Black and others (2003).

Rupture scenario (between arrows)

Explanation

This map illustrates the potential consequences of tectonic subsidence that could occur if a moment magnitude (**M**) 7.0 earthquake were to rupture the Salt Lake City segment of the Wasatch fault zone. Tectonic subsidence may tilt the valley floor toward the fault, resulting in local flooding caused by migration of the shore of Great Salt Lake. No significant flooding will occur when lake levels are at or below the historical average lake elevation of 4,200 feet (1,280 m). As the lake rises above this level to the maximum historic lake elevation of 4,212 feet (1,284 m), lake waters will increasingly flood the Jordan River Floodplain and surrounding areas. Tilting may also compromise the performance of gravity-flow structures such as wastewater-treatment plants and sewer lines. As the valley floor tilts, part of the ground surface is lowered. If this occurs in areas underlain by shallow ground water, the ground water may pond and flood basements and buried facilities.

Limitations

The earthquake described here happens every thousand years or so. Other active faults in the region may subject the study area to earthquakes, and their effects will undoubtedly differ from this scenario. Some effects may be worse than the scenario suggests and some may not be as severe. The predicted earthquake hazards are also based on specific analytical techniques. Different techniques may alter the scale and extent of mapped hazards. Because the hazards at any particular site may be different than shown, the maps should not be used for site-specific design or in place of site-specific hazard evaluations.

N
W E
S

Scale 1:250,000

10 5 0 10 Miles

10 5 0 10 Kilometers

Study Area Index Map

ISBN 1-55791-704-3

Basemap source data modified from the Utah Automated Geographic Reference Center; Utah State Geographic Information Database. Relief shading derived from 1:24,000 scale USGS Digital Elevation Models.

Universal Transverse Mercator Projection, Zone 12. 1927 North American Datum.

UTAH GEOLOGICAL SURVEY
UTAH GEOLOGICAL SURVEY
a division of
Department of Natural Resources